Polydopamine-Based Thin Film Composite Membranes for Pervaporative Concentration of Potassium Acetate Solution

by

Zhelun Li

A thesis

presented to the University of Waterloo

in fulfillment of the

thesis requirement for the degree of

Doctor of Philosophy

in

Chemical Engineering

Waterloo, Ontario, Canada, 2022

Examining Committee Membership

The following served on the Examining Committee for this thesis. The decision of the Examining Committee is by majority vote.

External Examiner	Dr. Huu Doan Professor
Supervisor	Dr. Xianshe Feng Professor
Internal Member	Dr. Eric Croiset Professor
Internal Member	Dr. Boxin Zhao Professor
Internal-external Member	Dr. Shunde Yin Associate Professor

Author's Declaration

I hereby declare that I am the sole author of this thesis. This is a true copy of the thesis, including any required final revisions, as accepted by my examiners.

I understand that my thesis may be made electronically available to the public.

Abstract

Potassium acetate (KAc) is a valuable chemical product due to its widespread application in multiple fields. During the production of KAc, the concentration of dilute KAc solution is a vital pre-treatment procedure to produce KAc powder or liquid concentrate of KAc. Several techniques have been applied to concentrate salt solutions, including evaporation, freeze crystallization and reverse osmosis (RO). However, these techniques either have high energy costs, complicated systems, or high operating pressures. Meanwhile, pervaporation is emerging as a promising technique for concentration of salt concentration, ascribing to its low energy consumption, mild working environment, and capacity to handle highly concentrated feeds. Attempts were thus made in this work to fabricate thin film composite (TFC) membranes favorable for the pervaporative concentration of KAc solutions. Among several technologies for manufacturing TFC membrane selective layer, self-polymerization of dopamine has become a promising technology for pervaporation concentration due to the ease of operation, diversity of target surface, and hydrophilicity of dopamine. However, the shortcoming is that polydopamine (PDA) is vulnerable to harsh environments, predominantly alkaline environments, ascribing to the non-covalent bonds in its structure. Besides, the polymerization of dopamine is a slow process, and the non-polar aromatic ring in the dopamine structure also limits the hydrophilicity of the coating. Therefore, a key point in this work is modifying dopamine polymerization to make it more favorable to fabricate membranes for pervaporative concentration.

In the first work, self-assembled polyethyleneimine/poly(acrylic acid) (PEI/PAA) bilayers were applied as “tape” to deposit onto the PDA coating to make a dense and stable selective layer. It was shown that the number of polyelectrolyte bilayers could be effectively reduced by using a PDA sublayer in constructing the composite membranes. The TFC membrane with a single PEI/PAA bilayer on top of the PDA sublayer was adequate for the pervaporative concentration of the salts. The mass transfer resistance

of the membranes was carried out via making membranes with different amounts of polyelectrolyte bilayers.

However, the intrinsic property of the PDA coating was not modified in the first work, and the extra deposition process complicated the fabrication. In the second work, a single-step co-deposition of dopamine and polyvinylamine (PVAm) was carried out to take advantage of the covalent bonding between PDA and PVAm and the adhesive properties of PDA oligomers. It was shown that both the hydrophilicity and stability of the membrane were improved by incorporating PVAm into the membrane during the coating/deposition process. Moreover, the deposition was significantly accelerated. It was found that a PVAm content of 20-30 wt% (solvent free basis) in the PVAm/dopamine depositing solution was appropriate for fabricating TFC pervaporation membranes for concentrating aqueous KAc concentrations.

Yet, the aforementioned fabrication processes were only conducted upon the hydrophilic surface. Applying this technique to hydrophobic surfaces, in fact, is more desired for the pervaporative concentration process from the water crossover point of view. However, the deposition of PVAm on hydrophobic surfaces is challenging because of its strong hydrophilicity nature. In the third work, the co-deposition of PVAm/dopamine was successfully applied to the hydrophobic polyvinylidene fluoride (PVDF) surface using methanol as a co-solvent with water and postponing the addition of PVAm. The investigations on how the methanol concentration and postponed time of adding PVAm affect the deposition kinetics were conducted. Moreover, the hollow fiber membranes were fabricated in this work which helps look into the perspective of this membrane in the actual industry.

In the fourth project, the reactive oxygen species (ROS) co-produced by Cu^{2+}/H_2O_2 was used alternatively as the oxidant to accelerate the co-deposition of PVAm/dopamine. A facile method was applied to lead the ROS generated around the target surface, enhancing the deposition kinetics and efficiency even further. Moreover, it was found that the facile method made the deposition solution reusable, and

incorporating Cu^{2+} in the structure further improved the coating stability.

All fabricated membranes were tested in a sweeping gas pervaporative concentration of KAc solution with a feed concentration up to 70 wt%. Comprehensive investigations on the permeate performance, including the water permeate flux, water permeance, and activation energy, were all carried out.

Acknowledgments

I would firstly like to thank my supervisor Prof. Xianshe Feng for his incredible support over the past four years. His mentorship, advice, and effort were essential to every step of the development of this work, from the title to the bibliography and everything in between. I am constantly inspired by his dedication to his students, and consider myself especially lucky to count myself amongst such a privileged group.

Thank you, as well, to my committee – Prof. Huu Doan, Prof. Eric Croiset, Prof. Boxin Zhao, Prof. Shunde Yin– for taking the time to take part in my defense of this thesis and contribute their insights to this research. I am also grateful to Prof. Tizazu Mekonnen for his input into my research as a comprehensive committee member.

I am also grateful to my wonderful lab mates Dr. Xuezhen Wang, Dr. Xiaotong Cao, Dr. Silu Chen, Dr. Elnaz Halakoo, Jinxuan Zhang, and Xiaojia Li for their thoughtful advice throughout the development, analysis, and writing of my thesis.

The research support provided to this project by the Natural Sciences and Engineering Research Council of Canada (NSERC) is gratefully acknowledged. The University of Waterloo Graduate Scholarship, the Doctoral Thesis Completion Award awarded to me during my doctoral studies are also deeply appreciated.

Last but not least, I would like to express my gratitude to my parents for their unconditional support, encouragement, and love.

Table of Contents

List of Figures

List of Tables

List of Symbols

A	Effective membrane area, m^2
C	Permeate concentration, mol/m^3
D	Diffusivity coefficient, m^2/s
E_D	Activation energy for diffusion, J/mol
E_J	'Apparent' activation energy for permeation, J/mol
E_P	'True' activation energy for permeation, J/mol
J	Permeation flux, $g/(m^2 \cdot h)$
L	Membrane thickness, m
p	Partial vapour pressure, Pa
p^p	Permeate pressure, Pa
p^{sat}	Saturated vapour pressure, Pa
P	Permeability coefficient, Barrer
Q	Weight of collected permeate during a time period, g
R	Universal gas constant, 8.314 J/(mol·K)
R_L	Resistance of each polyelectrolyte bilayer, $m^2 \cdot h \cdot kPa/mol$
R_{PDA}	Resistance of polydopamine sublayer, $m^2 \cdot h \cdot kPa/mol$
R_{PES}	Resistance of PES base membrane, $m^2 \cdot h \cdot kPa/mol$
R_{Total}	Total resistance of whole membrane, $m^2 \cdot h \cdot kPa/mol$
S	Henry's solubility coefficient, $mol/(m^3 \cdot Pa)$
T	Temperature, ℃
X	Feed molar fraction
Y	Permeate molar fraction
γ	Activity coefficient
Δt	Time interval of collecting one permeate sample, h
ΔH_V	Molar heat of vaporization, J/mol
ΔH_S	Molar heat of sorption, J/mol

Chapter 1

Introduction

1.1 Background

As a powerful and eco-friendly deicer that is considered a substitute for chloride salts, potassium acetate (KAc) has been attracting more attention over the past few decades. Moreover, KAc can also be used as a food additive and fire extinguishing agent. Therefore, there is a considerable profit behind the production of KAc. During the production of KAc, the concentration of dilute KAc solution is an important pre-treatment procedure before the drying process (e.g., spray drying) to produce KAc powder or liquid concentrate of KAc. Moreover, the concentration of wastewater containing KAc can also be used to recover this valuable salt. The concentrations of other salt solutions are also desired because of the same benefits. Several techniques have therefore been proposed to concentrate salt solutions, including evaporation, freeze crystallization and reverse osmosis (RO). However, these techniques either have high energy costs (e.g., distillation), complicated systems (e.g., freeze crystallization), or high operating pressures (e.g.,RO). Thus, membrane distillation (MD) and pervaporation, both of which have low energy consumption and mild operating environments, are proposed as alternative concentration technologies. Pervaporation is considered advantageous over MD as the membrane wetting and fouling that usually occurs in the MD process are not concerns in pervaporation processes. In most cases, the solvent of saline solutions in industry is water, and thus only the removal of water will be discussed in this study.

For pervaporation, thin film composite (TFC) membranes with thin selective layers supported on a porous membrane substrate attract more attention than homogeneous membranes and integral asymmetrical membranes. This is because the TFC membranes

have the potential to produce a higher permeation flux than homogeneous membranes and are more flexible than integral asymmetrical membranes when choosing membrane materials. Polydopamine (PDA) coating based on oxidative self-polymerization of dopamine is considered as a suitable technique to fabricate the selective thin film in the TFC membrane for pervaporative concentration, as PDA is demonstrated to be super hydrophilic and can firmly adhere to a broad range of surfaces[1,2]. However, PDA coatings are vulnerable to harsh environments, especially alkaline environments, because of the non-covalent interactions in the structures [3,4]. This limits the application of PDA coating in the concentration of KAc solution, due to the alkaline nature of KAc solutions. Furthermore, the non-polar aromatic ring in the PDA structure inhibits its hydrophilicity, limiting its application as the selective layer in pervaporative concentration [5–7]. Lastly, the deposition of PDA is a slow process, which can require up to a few days to achieve a compact coating[8–10]. Therefore, further modifications of the PDA deposition technique are desired.

Due to the active functional groups, such as catechol and amine groups existing on the PDA surface, PDA coating is widely applied as a platform for secondary modification. As a versatile and energy-saving method, layer-by-layer (LBL) self-assembly of polyelectrolytes via electrostatic force is also considered a favorable technique to fabricate membranes for the pervaporation process. However, up to hundreds of polyelectrolyte bilayers could be required to achieve high selectivity for a membrane in pervaporation [11–14], making this technique time-consuming and impractical. In the first work, PDA coating and LBL self-assembly of polyelectrolytes [polyethylenimine (PEI) as polycation and poly (acrylic acid) (PAA) as polyanion] were both applied in the fabrication of the TFC membrane. The amine groups on PEI and the catechol groups on the PDA surface are expected to react via Michael addition or Schiff base reaction[15,16], reinforcing the conjunction between PDA and PEI and enriching the loading of PEI onto the PDA surface. Moreover, the polyelectrolyte layer could also strengthen the structure of the PDA coating. On the other hand, PDA coating could, in

turn, act as an interim layer between the porous substrate and polyelectrolyte bilayers to reduce the number of polyelectrolyte bilayers required. Besides, these two deposition techniques could be carried out independently, which provides the feasibility to optimize them separately to achieve specific performance.

However, the subsequent deposition of polyelectrolyte layers did not modify the intrinsic property of the PDA, and the polymerization and deposition kinetics of the dopamine was not enhanced. Moreover, the involvement of additional deposition techniques and steps makes the overall deposition process more complicated and time-consuming. The one-step co-deposition of PDA with other materials, which was proposed by Lee's group in 2012[17], may solve these problems. As demonstrated in several works, the abundant catechol groups in dopamine could react with amino groups via Schiff-based and Michael addition reactions and form robust covalent bonds with the corresponding materials[7,18]. Based on this, several researchers co-deposited dopamine with amine-containing polymers, among which polyethyleneimine (PEI) is most extensively studied [5,7,10]. It has been widely demonstrated that co-deposition with PEI could endow the PDA coating with a significantly enhanced wettability, a more smooth surface, and more robust stability[5,7,9,19]. However, another promising polymer that can co-deposit with dopamine, polyvinylamine (PVAm), was neglected. PVAm has the highest content of primary amines of amine polymers and thus possesses excellent hydrophilicity[20]. Also, the abundant amine groups endow it with great potential to form covalent connections and co-deposit with dopamine. A single step of co-deposition of PVAm and dopamine was thus, conducted for the first time in our second work. The polymers were deposited on a microporous polyethersulfone (PES) substrate to fabricate TFC membranes. The so-formed membranes with different PVAm contents were then tested in pervaporative concentration of KAc solutions.

The hydrophilicity nature of PVAm is favorable for the pervaporative concentration of salt solutions. However, a significant concern with the super hydrophilic PVAm is that it may affect its co-deposition with dopamine on hydrophobic target surfaces. As

elucidated in several works, a thin air/vapor layer could be formed between the hydrophobic surface and the aqueous solution, limiting the deposition of the hydrophilic materials on the target surface[21–24]. On the other hand, using a hydrophobic substrate is more suitable for the pervaporative concentration since it may prevent the pore wetting and water crossover more efficiently, ascribed to the low surface energy. Therefore, a way to improve the deposition of PVAm/dopamine on a hydrophobic surface is desired. As has been demonstrated by several works, including alcohol in the solvent is an effective way to solve this problem since it is water-miscible and possesses a better wettability to the hydrophobic surface[25,26]. Moreover, the sole deposition of PDA is less affected by the hydrophobicity of the target surface, ascribed to the aromatic ring in the PDA structure, which could attach to hydrophobic surfaces through hydrophobic interaction[22,27]. Therefore, in the next step, the investigation of how the inclusion of methanol in the solvent and the postponed addition of PVAm affect the overall co-deposition performance of PVAm/dopamine on the hydrophobic surface was carried out. Also, to make our research closer to the actual industry application, TFC hollow fiber membranes were fabricated in this work step.

Applying a more active oxidant has also been demonstrated as an effective way to accelerate the self-polymerization and deposition of dopamine. In 1989, Epstein's team found that Cu^{2+} and H_2O_2 could produce reactive oxygen species (ROS), including $O_2^{\bullet-}$ and $HO_2^{\bullet}$, as well as $OH^{\bullet}$, in alkaline environments[28]. Since dopamine's oxidized self-polymerization was reported a few decades later, several works have been done regarding triggering this process using ROS co-produced by Cu^{2+}/H_2O_2[1,8]. Zhang et al. [8] found that by using ROS as the oxidant, the kinetics of dopamine polymerization were improved more than 14 times compared with that using air as the oxidant. Also, the so-formed coating was found to possess enhanced stability, which may be ascribed to the incorporation of Cu^{2+} in the coating and the smaller PDA particle size[8,29]. This technique was also utilized in our work to further enhance the co-deposition kinetics of PVAm/dopamine and the coating stability. However, all of the previous works added

the Cu^{2+} and H_2O_2 in the solution bulk before the polymerization at one time, which may make most of the dopamine polymerize in the solution instead of adhering to the target surface. In our work, a facile method was applied by adding the Cu^{2+} in the deposition solution contacting the outer surface of the hollow fiber membrane, while H_2O_2 was injected into the cavity of the membrane contacting its inner surface. Therefore, the generated ROS will be concentrated around the target surface, and the depostion kinetics were significantly improved. Also, by doing so, the waste of dopamine was avoided, and the deposition solution became reusable.

Even though the performance of pervaporation for separating mixtures of volatile components have been extensively studied over the past few decades, research on pervaporative concentration of salt solutions is relatively rare. Nearly all pervaporation experiments reported in literature are carried out using a vacuum to remove the permeate, while sweeping gas pervaporation which is also suitable for pervaporative concentration of salt solutions, is rarely used. In addition, most studies on pervaporative concentration of saline solutions only focus on the permeation flux and selectivity performance of the membranes, while the activation energy for permeation and membrane resistance are not investigated in depth. However, these parameters are important to characterize the properties of the membranes. Therefore, in our works, we applied the fabricated membranes in the sweeping gas pervaporative concentration for KAc solutions and detailly investigated the permeate performance, including the flux, permeance, and activation energy.

1.2 Research Objectives

This research aimed to fabricate suitable TFC membranes for pervaporative concentration of highly concentrated KAc solutions. The specific objectives of this project are presented below:

1. To improve the membrane fabrication efficiency and membrane stability via modifying the fabrication technique.

2. To explore a wider applied surface of the proposed co-deposition of PVAm/dopamine.
3. To investigate the pervaporative concentration performance of the fabricated membranes for salt solutions in terms of flux, permeance, activation energy, and salt rejection.
4. To make this study more integrated into the actual industry application by fabricating TFC hollow fiber membranes.

1.3 Thesis Structure

The overall thesis structure is illustrated in **Fig 1.1**. The thesis consists of 7 chapters, and they are organized as follows:

Chapter 1 presents the background and objectives of this study.

Chapter 2 presents the literature review.

In Chapter 3 to Chapter 6, a series of techniques and strategies were applied to fabricate TFC membranes for sweeping gas pervaporative concentration of KAc solution. In each chapter, comprehensive studies were carried out on membrane performance, including investigations on the water permeate flux, permeance, activation energy, and membrane stability.

Chapter 3 presents a study regarding combining self-polymerization of dopamine and layer by layer self-assembly of polyelectrolytes to fabricate the selective layer of the TFC membrane.

Chapter 4 introduces the one-step co-deposition of dopamine with PVAm on a flat-sheet PES substrate. The involvement of PVAm in dopamine polymerization enhances the deposition kinetics and the coating stability significantly.

Chapter 5 explores a broader application range of the co-deposition of dopamine/PVAm by successfully applying it on the hydrophobic hollow fiber PVDF substrate. The use of hollow fiber substrate makes the research closer to the actual industry application.

In **Chapter 6**, the co-deposition of dopamine/PVAm is further accelerated by using ROS co-produced by Cu^{2+}/H_2O_2 to oxidize the polymerization process. A facile strategy is applied in this chapter to make the deposition even more efficient and make the deposition solution reusable.

Based on the research findings, the recommended future works are presented in **Chapter 7**.

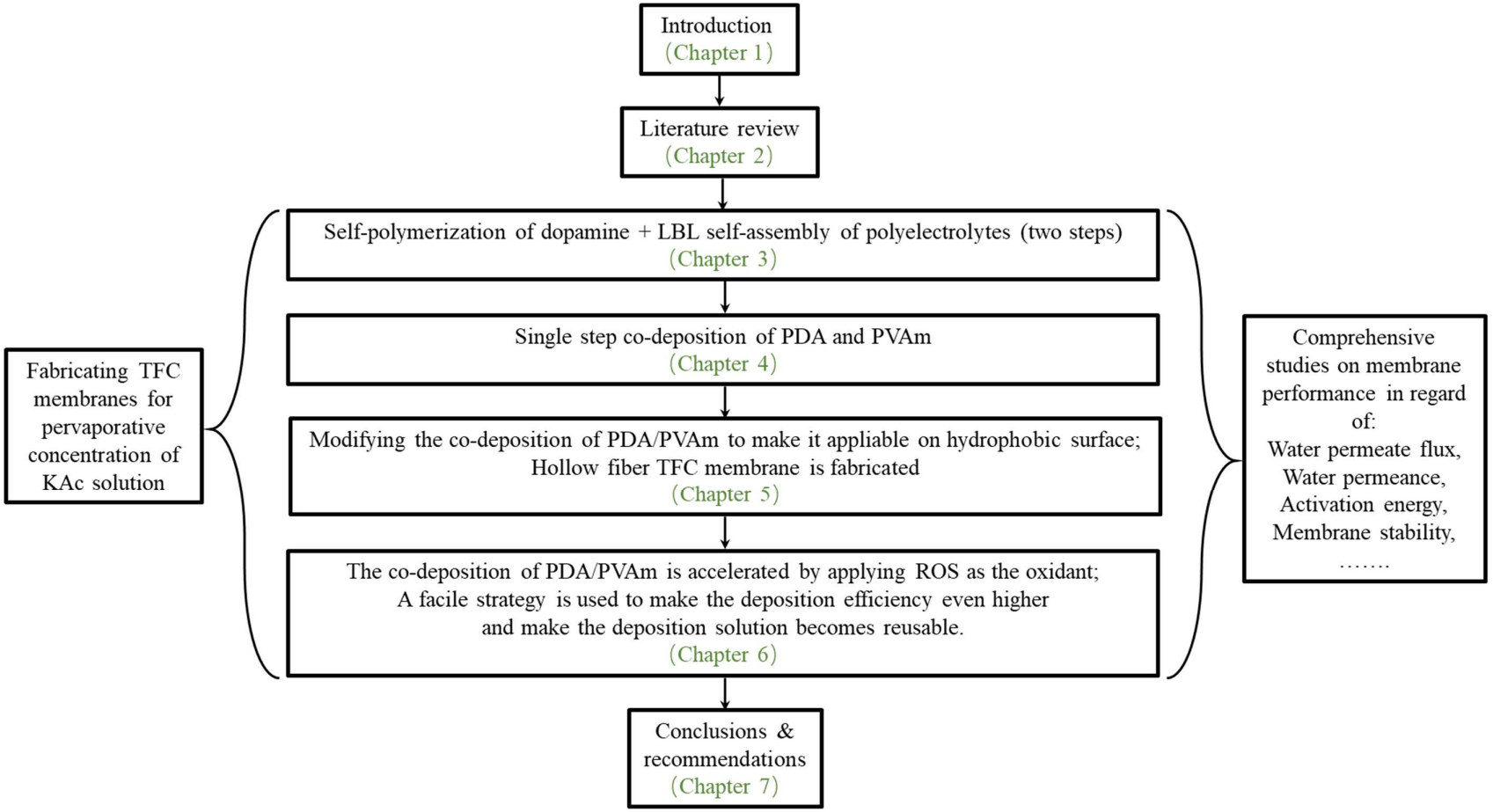

Fig.1.1 Illustration of thesis structure.

Chapter 2

Literature Review

2.1 Techniques for concentration of KAc solution

Potassium acetate (KAc) is a valuable salt because of its wide range of uses. As a deicer which has been widely used for airport runways, KAc is much less aggressive to soils and has a higher deicing efficiency than conventional chloride salt deicers such as magnesium chloride ($MgCl_2$), sodium chloride (NaCl) and potassium chloride (KCl). Thus, even KAc has a higher cost, it is still considered a potential substitute for chloride salt deicers. Moreover, similar with sodium acetate (NaAc), KAc is also widely used in food industry as acidity regulator and preservative. In industry, KAc is produced in form of saline solutions through the reaction of potassium hydroxide or potassium carbonate with acetic acid, using water as the solvent. However, in most cases, KAc is used as the form of powder (e.g., food additives or spherical solid deicer) or highly concentrated liquid concentrate (e.g., 50 wt% KAc solution as liquid deicer). Thus, the concentration of KAc solutions is usually carried out during the production of KAc salt. The concentration of KAc solutions is mainly for:

1. Pre-treatment for subsequence drying or crystallization to produce KAc powder.
2. Producing liquid concentrate product of KAc.
3. Decreasing the storage and transport cost by decreasing the volume of the solution.
4. Recovering this valuable salt from wastewater containing KAc.

Several methods such as evaporation, freeze crystallization and reverse osmosis have been employed to concentrate dilute saline solutions. Moreover, membrane distillation as an emerging technique is also proposed as an alternative method. However, some

drawbacks of these methods limit their applications. A brief introduction of the technologies for concentration of saline solution is presented in the following.

2.1.1 Evaporation

Evaporation is a simple and widely applied unit operation in industry to concentrate salt solutions. During the evaporation process, the salt solution desired to be concentrated is heated up and the water is removed through the form of gas phase. However, the energy consumption of evaporation process in industry is extremely high which limits its development[30].

2.1.2 Freeze crystallization

Concentration by freeze crystallization is a freezing process in which water is crystallized to ice and separated from saline solution. A typical freeze crystallization process includes, from beginning to end, nucleation, crystal growth and separation of formed ice[31]. In industry, all above procedures need to be conducted in different unit equipment separately, which makes the whole system complicated and results in a high investment cost.

2.1.3 Reverse osmosis

RO is a pressure-driven membrane process in which a semipermeable membrane was used to separate two aqueous streams, one rich in salt at feed side and another one poor in salt at permeate side. External pressure was applied at feed side to overcome the osmotic pressure which was induced by the concentration difference of salt between two sides, and thus the water in feed side will pass through the membrane with the salt being retained.

In RO, the pressure applied on the feed side stream is quite high, which is usually 2-17 bar for brackish water and 40-70 bar for seawater. [32] A higher pressure is required for

a higher salt concentration in the feed which limits its capacity for the concentration of high salinity solution.

2.1.4 Membrane distillation

Membrane distillation (MD) process is an emerging membrane technology, which has potential of providing high permeate flux at a low transmembrane pressure and ability to handle high concentration feed using low-grade or waste heat[9–12]. In MD process, the feed stream is allowed to contact with one side of a hydrophobic porous membrane, and vapor molecules are able to pass through the membrane while the liquid is prevented from penetrating the pores. The driving force for MD is the vapor pressure difference between the porous hydrophobic membrane surfaces. Thus, the hydrostatic pressure encountered in MD is much lower than that applied in pressure-driven membrane processes like RO, which makes it a promising technology for concentrating highly saline water[33].However, membrane wetting and membrane fouling tend to happen during MD and these problems limit the application of MD [34].

2.2 Pervaporation

As a promising concentration technology which has a low energy consumption and operation cost, pervaporation is attracting more and more attention over the past few decades[35–40].Compared with conventional concentration technology RO, pervaporation technology shows a more efficient performance and a higher capacity when treating high concentration feed streams. Unlike MD, membrane fouling and membrane wetting are not concerns in pervaporation [41,42]. Because of the high salt concentration involved in this study, pervaporative concentration will be focused and introduced in detail as follow.

2.2.1 Pervaporation configurations

Mass transport through pervaporation membrane is produced by maintaining a vapor pressure gradient across the membrane, and **Figure 2.1** illustrates two most used pervaporation configurations in the laboratory: vacuum pervaporation and sweeping gas pervaporation, to achieve the required vapor pressure gradient.

Among these two configurations, vacuum pervaporation, in which the low vapor pressure maintained on the permeate side of the membrane is produced with a vacuum pump. However, in a commercial-scale system, the vacuum pump requirement is sometimes too large to be economical and practical. In sweeping gas pervaporation, the low pressure at the permeate side is produced by sweeping the permeate side of the membrane with a flow of a carrier gas. The sweeping gas pervaporation is of interest if the permeate has little value and can thus be discharged without condensation[36].

In this work, the permeate is water and water vapor is not harmful for environment. Therefore, water vapor can be discharged without any further treatment and sweeping gas pervaporation can be applied in this case.

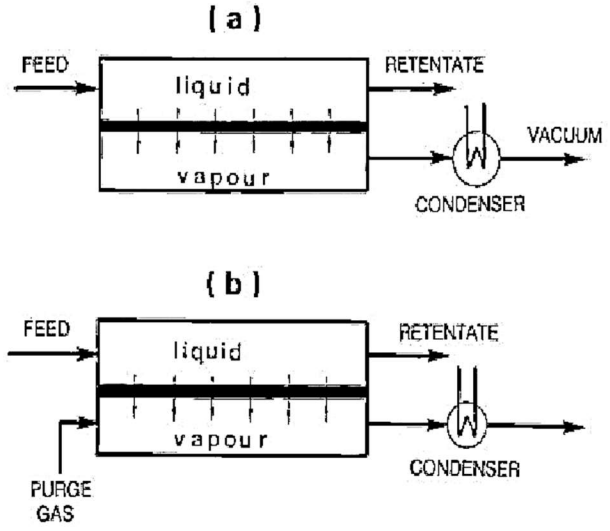

Fig.2.1 Schematic diagram of the pervaporation process

(a) vacuum pervaporation (b) sweeping gas pervaporation [36].

2.2.2 Mass transport in pervaporation membranes

To describe the mass transfer in pervaporation, several models have been proposed. The solution-diffusion model is accepted by most researchers[43–45]. According to the solution-diffusion model, pervaporation process generally involves three sequential steps as shown in **Figure 2.2**:

1. Sorption of the components on membrane surface at feed side;
2. Diffusion of the adsorbed components through the membrane;
3. Desorption of the permeating components from the downstream side of the membrane as vapor.

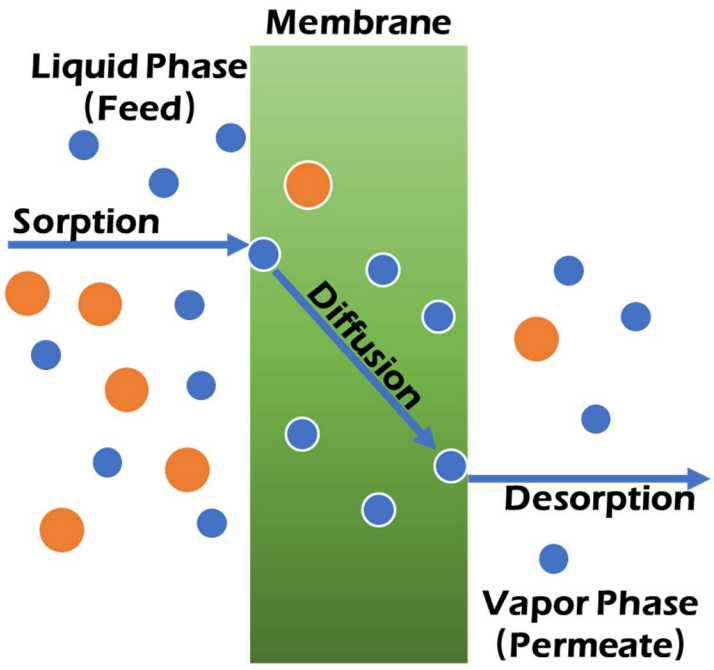

Fig.2.2 Illustration of solution diffusion model for mass transport in pervaporation.

In the solution-diffusion model, the sorption of the components can be a selective step if the components to be separated have different solubilities in the membrane and the diffusion is considered as the rate controlling step in pervaporation[45,46]. The

permeability of absorbed component in the membrane is determined by the solubility coefficient and diffusion coefficient. The desorption step is commonly thought to be fast enough so that its impact on the mass transfer in pervaporation process is negligible.

Fick's law can be applied to describe the pervaporation process:

$$J_i = -D_i \frac{dC_i}{dL} \tag{2-1}$$

where J_i represents the permeation flux of component i (i is usually water molecule when dealing with pervaporative concentration of saline solutions); D_i represents the diffusion coefficient; L represents the effective thickness of membrane and C_i represents the permeate concentration. The $"-"$ in equation (2-1) represents the molecular diffusion and concentration gradient is in opposite direction. The concentration at the membrane surface can be described using the Henry's law

$$C_i = S_i \cdot p_i \tag{2-2}$$

where S_i and p_i represent the Henry's solubility coefficient and partial vapor pressure of i in equilibrium with the feed liquid, respectively. Equation (2-1) and (2-2) can be combined to get equation (2-3) if Henry's solubility coefficient is independent of concentration.

$$J_i = -D_i \cdot S_i \frac{dp_i}{dL} \tag{2-3}$$

Defining P_i as the permeability coefficient which is expressed by

$$P_i = D_i \cdot S_i \tag{2-4}$$

and integrating equation (2.3) over L, we obtain

$$J_i = P_i \frac{p_{i,0} - p_{i,L}}{L} \tag{2-5}$$

where $p_{i,0}$ and $p_{i,L}$ represent the partial vapor pressure of component i at the feed and permeate interface of the membrane, respectively. Equation (2-5) implies that the partial pressure difference across the membrane serves as the driving force for mass transfer in pervaporation. Equation (2-5) can be further described as

$$J_i = P_i \frac{X_i \gamma_i p_i^{sat} - Y_i p^p}{L} \quad (2\text{-}6)$$

where γ_i represents the activity coefficient of component i in the feed solution, p_i^{sat} and p^p represent the feed side saturated vapor pressure of component i and permeate side pressure, respectively, X_i and Y_i represent the mole fractions of component i in the feed and permeate, respectively. However, for asymmetric and composite membranes, the effective membrane thickness is difficult to be determined and therefore permeability coefficient normalized by membrane thickness, $\frac{P_i}{L}$, was used to describe the membrane performance in pervaporation,

$$\frac{P_i}{L} = \frac{J_i}{X_i \gamma_i p_i^{sat} - Y_i p^p} \quad (2\text{-}7)$$

$\frac{P_i}{L}$ is the permeance of the membrane to component i.

2.2.3 Activation energy for pervaporation transport

In pervaporation, the temperature dependence of permeation flux generally exhibits an Arrhenius type of relation

$$J = J_0 \exp(-E_J/RT) \quad (2\text{-}8)$$

where J_0 is the pre-exponential factor for the process, R is the ideal gas constant, T is the absolute temperature and E_J is the apparent activation energy for permeation which can be obtained from the slope of $ln(J)$ vs $1/T$ plot. However, E_J characterizes the temperature dependence of not only the membrane permeability, but the driving force as well. The "true" activation energy which specifically characterizes the membrane permeability will be discussed later. The temperature dependence of diffusivity coefficient, D, and solubility coefficient, S, may be expressed by

$$D = D_0 \exp(-E_D/RT) \quad (2\text{-}9)$$

$$S = S_0 \exp(-\Delta H_S/RT) \quad (2\text{-}10)$$

and according to equation (2.4), these two equations can be combined to yield

$$P = P_0 \exp(-E_P/RT) \quad (2\text{-}11)$$

where D_0, S_0,and P_0 are the pre-exponential factors, E_P represents the "true" activation energy for permeation which specifically characterizes the temperature dependence of membrane permeability, obtained from the combination of the activation energy for diffusion, E_D, and the sorption enthalpy, ΔH_S. Rearranging equation (2-7) and (2-11), we obtain:

$$(P/L) = J/(\Delta p) = (P_0/L)\exp(-E_P/RT) \quad (2\text{-}12)$$

where Δp represents the transmembrane partial pressure difference which is calculated from $\Delta p = X\gamma p^{sat} - Yp^p$. The activation energy (E_P) that characterizes the temperature effect of the membrane permeability coefficient can be obtained from the slope of $ln\,(J/\Delta p)$ vs $1/T$ plot. Moreover, a simple rule of thumb can be applied to estimate E_P by subtracting the heat of vaporization (ΔH_V) from the E_J value, written as

$$E_P = E_J - \Delta H_V \quad (2\text{-}13)$$

This rule of thumb is quite useful as evaluating E_J from the $ln\,(J)$ vs $1/T$ data is much easier than evaluating E_P from the $ln\,(J/\Delta p)$ vs $1/T$ data. However, it should be mentioned that equation (2-13) only applies when the permeate pressure is sufficiently low compared to the partial vapor pressure at the feed side. Otherwise, equation (2-12) should be applied to evaluate E_P.

2.2.4 Performance characterization for pervaporative concentration

Generally, in pervaporative concentration process, the membrane performance is evaluated in terms of membrane productivity and membrane selectivity.

Membrane productivity is usually characterized by permeation flux J, which can be calculated by

$$J = \frac{Q}{A\Delta t} \quad (2\text{-}14)$$

where Q is the weight of permeate collected during a time period Δt, and A is the effective membrane area.

The membrane selectivity in pervaporative concentration is usually characterized by salt rejection (R):

$$\mathrm{R} = \frac{(C_f - C_p)}{C_f} \times 100\% \quad (2\text{-}15)$$

where C_f and C_p represent the salt concentrations in the feed and permeate, respectively.

2.3 Fabrication techniques of thin film composite (TFC) membrane for pervaporation

Based on membrane structure, pervaporation membranes can be generally divided into three categories: homogeneous membranes, integral asymmetric membranes and TFC membranes. As permeate flux is not only affected by the intrinsic permeability of the membrane material but also the effective thickness of the membrane[46], the integral asymmetric membranes and TFC membranes have advantages over homogenous membranes because they have thin selective layers which lead to a higher permeate flux. However, the application of integral asymmetric membrane for pervaporation is limited, as it is unlikely for a single polymer to have optimum selectivity and mechanical stability at the same time. Meanwhile, the selective layer and mechanical support of TFC membrane can be prepared from different materials, and they can thus be selected and modified separately to meet specific functions. Along this line of consideration, the TFC membrane which has a thin selective film supported on a porous substrate attracts more interest than homogenous membranes and integral asymmetric membranes.

Various techniques have been proposed to fabricate thin selective layers, such as

interfacial polymerization, electrostatic self-assembly, and oxidized self-polymerization of dopamine. A brief introduction of these techniques is given in the following.

2.3.1 Interfacial polymerization

Interfacial polymerization is one of the most widely studied techniques to prepare the dense and thin active layer for TFC membranes[47–49]. In this technology, polycondensation occurs between two monomers dissolved in immiscible solvents, forming an ultra-thin film with several nanometers to several microns at the interface, and remaining attached to the substrate. TFC membranes fabricated by this technique have also been applied to the pervaporation process. For instance, An et al.[50] successfully fabricated an ultrathin selective layer of around 50 nm on a polyacrylonitrile substrate via interfacial polymerization between 1,3-diamino-2-propanol and TMC, and applied the membrane to the pervaporative dehydration for ethanol. The prepared membrane exhibits a water flux of 0.6 kg/m^{2}h and an outstanding separation factor of 264 at 25 °C. However, the interfacial polymerization method consumes a large amount of solvent, limiting its application prospect[51].

2.3.2 Electrostatic self-assembly of polyelectrolytes

Electrostatic layer-by-layer (LBL) self-assembly, which was first introduced in 1991[52,53], has been attracting attention as an effective technique to fabricate selective layers for TFC membrane over the past few decades because of its versatility and simplicity[54]. **Fig.2.3** illustrates a typical electrostatic self-assembly deposition process on a substrate whose surface is negatively charged. Following the procedures in **Fig.2.3**, a dilute polycation solution is allowed to contact with the substrate first, during which the polycations will be adsorbed onto the negatively charged surface of the substrate due to

electrostatic attraction. However, only one layer of polycation is assumed to be adsorbed because of the growing electrostatic repulsion. It is worth to mention that, during the deposition, part of the charges on the adsorbed polycations are assumed to be neutralized by the negative charges on the substrate surface while another part of charges remain un-neutralized, and these un-neutralized polycation charges invert the substrate surface from negatively charged to positively charged, which is called charge overcompensation. Charge overcompensation is important in the formation of polyelectrolyte multilayers as it makes the electrostatic self-assembly process to be repeatable and the polyelectrolyte layers to be stackable[55–57]. To achieve a charge overcompensation, caution should be exercised during the determination of the deposition time. If the deposition time is too short, then the self-assembly of the polyelectrolyte layers might be stopped. After a certain time of deposition, the substrate is taken out from the polycation solution and rinsed thoroughly by de-ionized water to remove the excess polycation molecules that are not adsorbed by the surface. This step is aiming to prevent the reaction between the excess polycations on the base membrane and the polyanions in the dilute solution during the subsequent deposition cycle. Thereafter, the rinsed base membrane with a positively charged surface is exposed to a dilute polyanion solution. Similarly, one layer of polyanion molecules will be adsorbed onto the previously deposited polycation layer and thus form a so-called “bilayer” which contains one layer of polycation and one layer of polyanion. Then, the membrane is taken out and rinsed again using de-ionized water and the surface charge of the membrane reverts to negative. And thus, the new surface is ready for the next round of polycation deposition. By repeating the processes above, a multilayer structure of polyelectrolytes which comprises of alternating polycation-polyanion layers will be established.

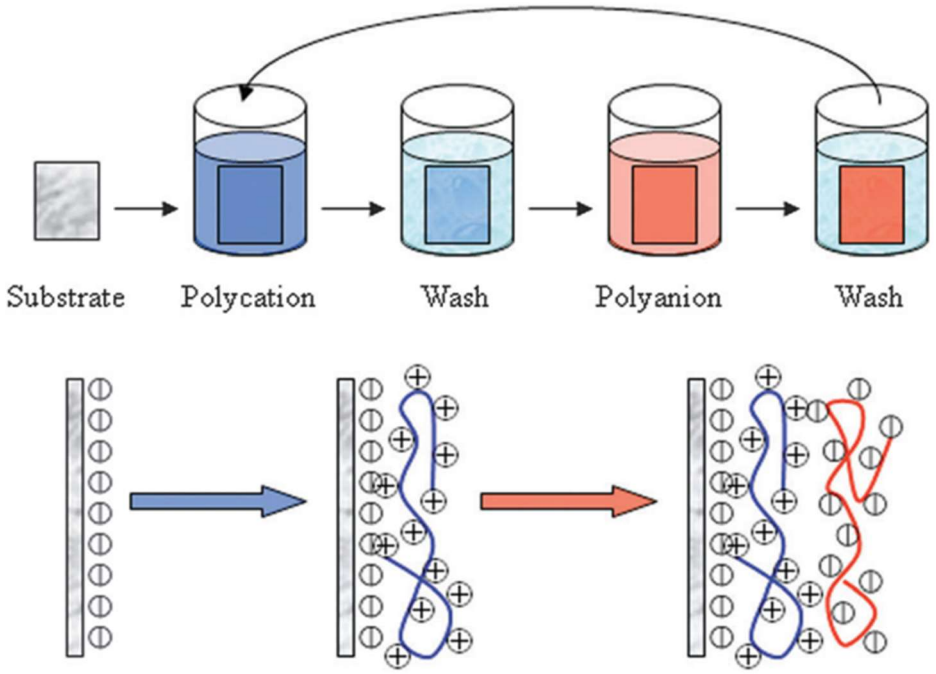

Fig.2.3 Illustration of electrostatic self-assembly process[58]

The electrostatic self-assembly technique has been widely used for the making of TFC membranes for pervaporative separation. However, the fabrication of self-assembled polyelectrolyte TFC membrane is time-consuming. As the thickness of each polyelectrolyte bilayer is only about 0.5-3nm[59,60], a large number of bilayers up to hundreds may be required to achieve a high selectivity according to early works[11–14]. To solve this problem, Zhu *et al.* developed a facile deposition strategy by using a relatively dilute polyelectrolyte solution in the first few cycles of deposition and a more concentrated polyelectrolyte solution in the subsequent depositions[60,61]. The resultant membrane with no more than 10 polyelectrolyte bilayers showed a good permeability and selectivity for dehydration of isopropanol. Moreover, applying an external electric field during the deposition has also demonstrated to be effective to reduce the number of required polyelectrolyte bilayers [62–67]. Employing a layer of PDA as binder between the porous substrate and polyelectrolyte bilayers could also be a promising strategy and was firstly

employed in our work.

2.3.3 Oxidized self-polymerization of dopamine

In 2007, Lee *et al.* reported an improved surface modification technique in which oxidative self-polymerization of dopamine produced adherent polydopamine (PDA) coatings on various surfaces[1]. Since then, the studies on PDA coating increased dramatically, as it can adhere to virtually all types of material surfaces without surface pre-treatment and can act as a versatile platform for secondary modifications. The extraordinary potential of PDA coating has been demonstrated in several areas, including biosensors and bioelectronics [68,69], tissue and pharmaceutical engineering[70], nano-technology[71,72], and membrane separation[2,73–75].

PDA layers is formed based on the oxidative polymerization of dopamine. However, the specific reaction mechanism and the structure of the PDA is still under discussion now. Some proposed structures of PDA and the underlying reaction mechanism sre shown in **Fig.2.4**. As illustrated in the figure, dopaminechrome and 5,6-dihydroxylindoles (DHI) are formed through the oxidation of dopamine before the polymerization. Then, PDA is produced after covalent oxidative polymerization of DHI[1,76]. However, according to Dreyer et al. [77], PDA is not a covalent polymer but a supramolecular aggregation of DHI bonded via π-stacking and hydrogen bonding interactions. Meanwhile, in some other work, the presence of self-assembled physical trimer during dopamine polymerization was reported[3], and a structure model of PDA consisting of hydroquinone, indolequinone and its tautomer was also proposed[78]. Thus, a widely accepted assumption for the mechanism of PDA formation is the combination of covalent bonding polymers and non-covalent interactions.

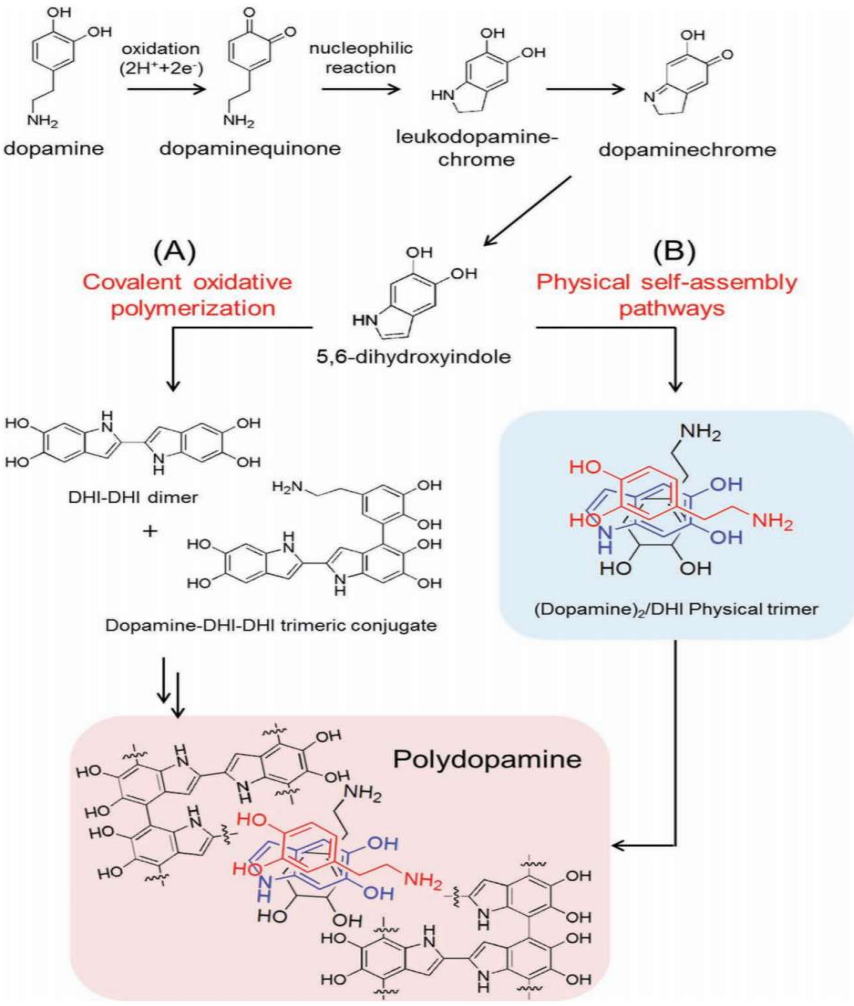

Fig.2.4 Various reaction mechanisms and structures for PDA proposed in the literature[3]

Unlike its structure and combination mechanism, the versatility of PDA as a surface coating has already been clearly demonstrated. When Lee *et al.* [1] firstly introduced the PDA coating technique, the PDA was proved to be able to firmly adhere to various material surfaces including noble metals (Au, Ag, Pt, and Pd), metals with native oxide surface (Cu, stainless steel, NiTi shape-memory alloy), oxides (TiO_2 ,SiO_2 and etc.), semiconductors (GaAs and Si_3N_4), ceramics (glass and hydroxyapatite), and synthetic polymers [polystyrene (PS), polyethylene (PE), polycarbonate (PC), polyethylene (PET)]. Moreover, polyethersulfone (PES)[18,79,80], polyvinylidene fluoride (PVDF) [81],polydimethylsiloxane (PDMS)[82] and polytetrafluoroethylene (PTFE)[83], which

are popular polymer materials for membrane fabrication, are also proved to have suitable surfaces for PDA deposition. PDA coating has been used to fabricate composite membranes for salt removal from water by nanofiltration[84], dehumidification of propylene gas[85] and separation of thiophenes from octane by pervaporation[86]. Besides, antifouling performance of the FO and RO membrane [75,87],and the permeation flux of ultrafiltration membrane[88] were demonstrated to be enhanced after PDA coating. In most cases, the PDA coating is applied to serve as a transition layer, in other words, a platform for a secondary modification[1,17].

Through Michael addition or Schiff base reaction, the large number of active catechol groups in PDA make it readily conjunct with other molecules containing primary amine or thiol groups, and therefore provide the condition for further modifications[1]. According to this, Zhang *et al.* grafted a layer of PEI onto a PDA-coated PES substrate to fabricate a novel positively charged membrane for nanofiltration, and a rejection of up to 96.5% for cationic dyes was achieved[18]. Similarly, PES-PDA- poly(ethylene glycol)(PEG) UF membranes with enhanced stability and anti-fouling performance were fabricated via grafting of PEG-NH_2 on a PDA-coated PES substrate[89]. Moreover, as the catechol groups have strong coordination capability with metal ions, the presence of abundant catechol groups in PDA also made the deposition of MOFs onto “inert” polymer surfaces possible. Zhou *et al.* [90] successfully deposited various MOFs, including HKUST-1, MOF-5, MIL-100(Fe) and ZIF-8, on chemical inert nanofibrous membrane surfaces after coating a PDA layer as nucleation center, to obtain a hierarchically structured porous films. For lithium-ion battery application, PAA was grafted on PDA-coated silicon particles[91] or MnO particles[92] via thermal crosslinking of imino on PDA and carboxyl on PAA to produce a high-performance anode.

PDA coating seems to be a useful surface modification method. However, the non-covalent interactions in PDA make it unstable, especially in strongly alkaline

environment[3,4]. As reported by Zhao et al. [82], lots of cracks could be detected on the PDA layer coated onto a PDMS membrane upon drying from the optical image, which further indicates the fragility of PDA coating. Furthermore, even though many studies have proved the PDA coating can help improve the membrane hydrophilicity[2,74,84,93], the aromatic ring in PDA limits this improvement[5–7].

Several modification strategies proposed to solve these problems are introduced in the following section.

2.4 Optimization strategies for oxidized self-polymerization of dopamine

In the previous sections, we introduced the versatility and the promising prospect of the oxidized self-polymerization of dopamine in detail. However, several problems remain with this technique, such as unsatisfied hydrophilicity, weak stability (especially in alkaline environment), prolonged reaction time, and low efficiency when depositing on hydrophobic surfaces. Therefore, many modification methods have been proposed to deal with these issues. The methods could be categorized into a few strategies based on their mechanisms, including deposition with other polymers, using more active oxidants, and changing solvents. A detailed description of these modification methods is given below.

2.4.1 Co-deposition with other materials

In 2012, Lee et al.[17] proposed a dopamine-involved one-step surface functionalization method for the first time via mixing dopamine and various other materials in the deposition solution to endow the formed coating with desired properties. Since then, the co-deposition of dopamine with other materials has received more and more attention as a promising

strategy to functionalize the material surfaces. According to mechanisms, the co-deposition process with dopamine can be summarized into two categories: non-covalent co-deposition and covalent co-deposition.

The non-covalent co-deposition of dopamine with co-components involves several interactions, such as hydrogen bond, electrostatic attraction, and hydrophobic force. For instance, Zhang et al.[94] applied poly(ethylene glycol) (PEG) and poly(vinyl alcohol) (PVA) separately in the polymerization of dopamine, and both polymers could co-deposit with dopamine through hydrogen bonds. The so-formed coating possessed enhanced wettability and was more suitable for post-modifications. However, compared to neat PDA coating, the non-covalent co-deposition involves even more nonstable interactions, which is detrimental to the stability of the formed coating[95,96].

Therefore, covalent co-deposition that could introduce more covalent interaction, which is more robust than non-covalent interaction, to the formed coating is a more promising strategy, especially for application in harsh environments.

As demonstrated in several works, the dopamine/PDA can react with amino groups via Schiff-based and Michael addition reactions and form robust covalent bonds with the corresponding materials[7,18]. Inspired by this, several researchers co-deposited dopamine with amine-containing polymers, with polyethyleneimine (PEI) being the most extensively used [5,7,10]. It was found that the coating layer formed via the co-deposition of dopamine and PEI was improved in various aspects compared with that formed with neat dopamine. Firstly, the so-formed deposition layer exhibited significantly enhanced wettability ascribed to the inherent hydrophilicity of PEI. Moreover, the co-deposition of dopamine /PEI also resulted in a more uniform and smooth coating. This is because the covalent interaction between PEI and dopamine could suppress the formation of large PDA aggregates and thus avoid their stacking on the target surface[96]. Last but not least, the incorporation of PEI greatly improves the coating stability due to the more abundant

covalent bonds in the structure. Therefore, the covalent co-deposition of PEI with dopamine was widely applied to modify the resultant coating layer.

However, the researchers neglected another promising polymer that can co-deposit with dopamine, polyvinylamine (PVAm). The comparison of the structures of PEI and PVAm is shown in **Fig.2.4**. PVAm has the highest content of primary amine groups of any polymer and thus possesses good hydrophilicity and enormous potential to cooperate with other polymers and modify different surfaces[20]. Because of its unique features, PVAm has been widely applied in membrane fabrication for plenty of applications, such as CO_2 capture[97–99], pervaporation for the separation of liquid mixture[100,101], and membrane filtration[102]. Because of the abundant amine groups in the structure, PVAm also has great potential to form covalent bonds with dopamine. Inspired by this, PVAm was applied to co-deposit with dopamine in this work in Chapter 4,5,6, and a more favorable deposition performance than that with PEI was obtained.

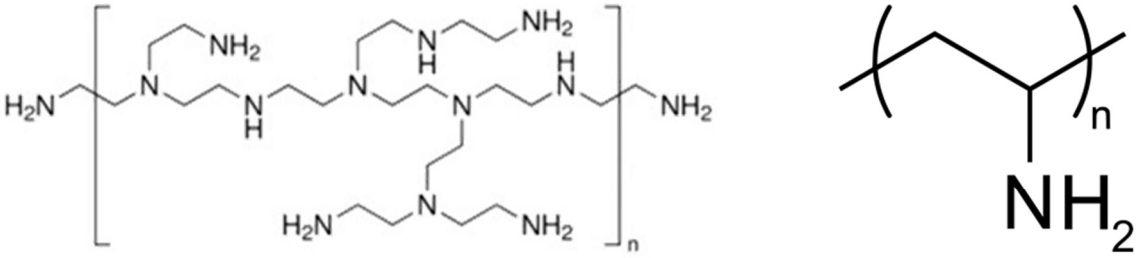

Fig.2.5 The polymer structures of PEI and PVAm.

2.4.2 Use more active oxidant

In most works, oxygen in the air was applied as the oxidant for dopamine polymerization. However, the formation rates of PDA coating in those cases are extremely low[103].

Moreover, the so-formed coating is also reported to involve plenty of large PDA aggregates, which make the coating surface uneven and influence the coating stability[8]. It was proposed that the dopamine polymerization and deposition may be enhanced by replacing the relatively weak oxidant, air, with a more potent and active oxidant. As early as 1989, Epstein's team demonstrated that Cu^{2+} and H_2O_2 could produce reactive oxygen species (ROS), including $O_2^{\bullet-}$ and $HO_2^{\bullet}$, as well as $OH^{\bullet}$, in alkaline environments[28]. Several works have applied ROS co-produced by Cu^{2+}/H_2O_2 to trigger the oxidized self-polymerization of dopamine. Xu's group found that by replacing air with ROS, the kinetics of dopamine polymerization were improved more than 14 times [8]. Moreover, the so-formed coating was also found to have a more uniform and compact structure and thus possess enhanced stability[8,29]. This technique was also used in the Chapter 6 to enhance the dopamine deposition.

Chapter 3

Concentration of potassium acetate solutions via sweeping gas pervaporation using TFC membranes comprising of a PDA sublayer and PEI/PAA bilayers[1]

3.1 Introduction

As a powerful and eco-friendly deicer, potassium acetate (KAc) is considered a substitute for chloride salts. Moreover, KAc can also be used as food additive and fire extinguishing agent. Thus, there is a considerable profit behind the production of KAc. During the production of KAc, the concentration of dilute KAc solution is an important pre-treatment procedure before the drying process (e.g., spray drying) to produce KAc powder or liquid concentrate of KAc. Moreover, concentration of wastewater containing KAc can also be used to recover this valuable salt. The concentrations of other salt solutions are also desired because of the same benefits. Several techniques have been therefore proposed to concentrate salt solutions, including evaporation, freeze crystallization and reverse osmosis (RO). However, these techniques either have high energy consumptions (e.g., distillation), complicated systems (e.g., freeze crystallization), or high operating pressures (e.g., RO) [30,31]. Thus, membrane distillation (MD) and pervaporation, both of which are known for low energy consumptions due to their moderate operating conditions, have been proposed as alternative technologies for concentrating low- and non-volatile solutes. Pervaporation is often considered to be advantageous over MD as the membrane wetting and fouling which usually occurs in MD process are not concerns in pervaporation processes [41,104,105].

[1] The work from this chapter has been published in *Sep. Purif. Technol.* 277 (2021) 119429.

For pervaporation, thin film composite (TFC) membranes comprising of a thin selective layer and a porous substrate appears to have attracted more interest than structurally homogeneous and integral asymmetric membranes. This is primarily because the TFC membranes typically have a higher permeation flux than homogeneous membranes and are more flexible than integral asymmetric membranes in selecting suitable membrane materials to finely tune membrane structures. Although TFC membranes are typically fabricated via interfacial polymerization between an amine and an acyl chloride on the surface of a porous substrate, polydopamine (PDA) coating based on oxidative self-polymerization of dopamine has been attempted to form the thin selective layer of TFC membranes for pervaporation applications. While PDA is hydrophilic and can firmly adhere to a broad range of surfaces [1,2], the stability of PDA coatings is a concern due to noncovalent interactions in the structure [3,4]. Zhao et al. [82] reported defects on the PDA layer coated onto a PDMS membrane, and more than one PDA coating is often required to form a defect-free skin layer [29]. When PDA coating alone is not satisfactory yield the desired permselectivity, an additional modification is needed [2]. In fact, because of the active functional groups (e.g., catechol and imino groups) in PDA, PDA coating is generally used as a platform for further surface modifications. For example, a PEI layer was grafted onto a PDA-coated PES substrate by Zhang et al. [18] to produce a positively charged nanofiltration membrane, and a rejection of up to 96.5% for cationic dyes was achieved. Zhou et al. [90] managed to deposit various MOFs on the surfaces of chemically inert nanofibrous membranes after coating a PDA layer to facilitate nucleation, and hierarchically structured porous films were produced.

On the other hand, layer-by-layer (LBL) self-assembly of oppositely charged polyelectrolytes is a versatile technique for fabrication of hydrophilic membranes suitable for pervaporative dehydration of aqueous solutions. However, each polyelectrolyte bilayer is only about 0.5-3 nm thick [59,60], and a large number (up to hundreds) of bilayers were

usually required to achieve a high selectivity in early studies [11–14]. The slow layer by layer growth makes the membrane fabrication time-consuming and impractical for commercial applications. To address the issue, Zhu et al. [60] developed an approach for polyelectrolyte deposition that used a varying concentration of polyelectrolytes where dilute polyelectrolyte solutions were used in the first few cycles of polyelectrolyte deposition and more concentrated polyelectrolyte solutions were used afterward. As a result, membranes with fewer than 10 polyelectrolyte bilayers displayed a good permselectivity for dehydration of isopropanol. In addition, applying an external electric field to enhance the polyelectrolyte deposition has also demonstrated to be effective to reduce the number of polyelectrolyte bilayers required [62–67].

In this work, an initial PDA coating and subsequent LBL assembly of polyelectrolytes were applied to fabrication of TFC membranes, where the PDA coating functioned as a transition layer between the porous substrate and dense polyelectrolyte bilayers to reduce the number of the polyelectrolyte bilayers required. Polyethylenimine (PEI) and poly(acrylic acid) (PAA) were used as the cationic and anionic polyelectrolyte pair. This approach has the following advantages: (1) The amine groups in PEI and the catechol groups in PDA surface are expected to react via Michael addition or Schiff base reaction [15,16], thereby reinforcing the conjunction between PDA and PEI that favors PEI loading onto the PDA surface. (2) While the deposited PDA acted as an “anchor” to facilitate the deposition of PEI, the subsequently deposited polyelectrolyte layer would in turn act as a “tape” to strengthen the PDA layer, resulting in a microscopic interlocking to augment the integrity of the thin layers. (3) These two deposition techniques could be carried out independently, which offers an opportunity to optimize them separately to achieve specific performance.

Pervaporation separation of solvent mixtures have been studied extensively over the past few decades, and there has been increased interest recently in water separation from

high-salinity salt solutions. The majority of pervaporation research reported in literature uses vacuum-mode operation to remove the permeate, while sweeping gas pervaporation which appears to be particularly suitable for the purpose of concentration of aqueous salt solutions is not well studied. In the present work, sweeping gas pervaporation was utilized for concentration of KAc solutions. In addition to water permeation flux and salt rejection, the activation energy for water permeation and mass transfer characteristics of the membranes were also investigated. In an attempt to look into how the solute in the feed impact the membrane performance, the pervaporation behavior of aqueous solution containing other select salts (KCl, NaAc, NaCl and $MgCl_2$) was also determined.

3.2 Experimental

3.2.1 Materials

Microporous polyethersulfone (PES) membrane (Sepro Membranes, MWCO rating 10k) was used as the substrate for membrane fabrication. Dopamine hydrochloride and tris(hydroxylmethyl) aminomethane (Tris) were purchased from Sigma-Aldrich. Polyethyleneimine (PEI) (branched, Mw 25,000)) and poly(acrylic acid) (PAA) (Mw 450,000) were supplied by Sigma-Aldrich and Polysciences, respectively. KAc and KCl (Sigma-Aldrich), NaAc (BDH Inc.), NaCl (EMD Chemicals Inc.) and $MgCl_2$ (Acros Organics) were used as model solutes to prepare feed solutions, and they were all used as received. De-ionized water was used in preparing aqueous solutions for membrane fabrication and pervaporation tests.

3.2.2 Membrane preparation

The TFC composite membranes prepared in this work was comprised of a PDA sublayer

and polyelectrolyte bilayers. A dopamine solution at a concentration of 1 g/L was prepared by dissolving dopamine in a 15 mM Tris buffer solution, and the solution pH was adjusted to 8.5-8.8 using hydrochloric acid. Freshly prepared dopamine solution was allowed to contact the surface of the substrate membrane using the single-sided deposition technique [60,61]. The dopamine solution was exposed to air during dopamine deposition to facilitate oxidative self-polymerization of dopamine. The possible mechanism for dopamine polymerization has been described elsewhere [84,88]. A deposition time of 24 h was used to make sure a sufficient deposition, and the membrane was then rinsed with de-ionized water before subsequent depositions of polyelectrolytes.

The polycation and polyanion solutions used for LBL buildup were prepared by dissolving the PEI and PAA in de-ionized water, respectively, at a concentration of 0.02 monomol/L. The pH of the prepared PEI and PAA solutions were measured to be 7.9 and 3.5, respectively. In consideration that the PDA surface was negatively charged at a pH over 3 [106], the membrane coated with PDA was allowed to contact with the PEI solution first so that the cationic PEI would be readily adsorbed onto the PDA sublayer via electrostatic forces. During this process, the PEI macromolecules were also expected to graft onto the PDA layer firmly through the Michael addition or Schiff base reaction between the catechol groups on PDA surface and the amine groups of PEI polymer [1]. After PEI deposition, the membrane was rinsed gently with de-ionized water, followed by deposition with the anionic PAA, resulting a self-assembled polyelectrolyte bilayer. Both PEI and PAA deposition was achieved by contacting their respective solutions for 30 min. The membrane was gently rinsed with de-ionized water, and the alternative depositions of polycations and polyanions were repeated to yield multiple polyelectrolyte bilayers. The above procedure is depicted in **Fig.3.1**. In this work, composite membranes with up to 9 polyelectrolyte bilayers were fabricated, and for convenience they were designated as PDA-$(PEI/PAA)_n$, where subscript n represents the number of PEI/PAA bilayers deposited

onto the PDA sublayer.

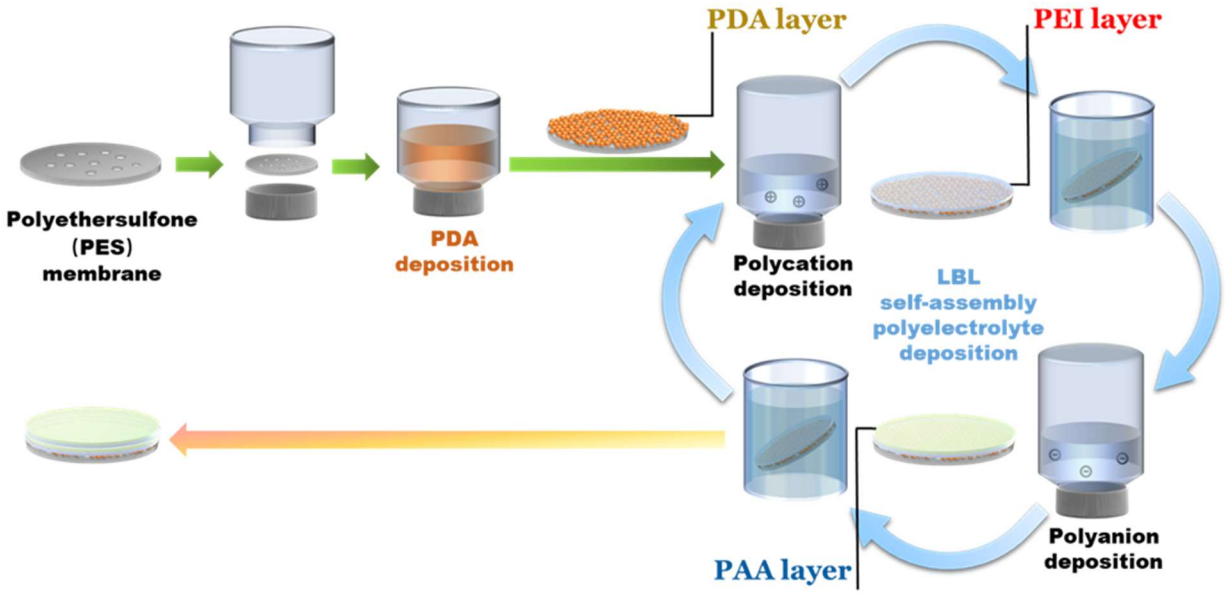

Fig.3.1 Fabrication of TFC membranes comprising of a PDA sublayer and PEI/PAA bilayers.

3.2.3 Pervaporation

The sweeping-gas pervaporation experiments were conducted with a setup shown in **Fig.3.2**. The membrane was mounted in a stainless steel membrane cell with an effective area for permeation of 21.2 cm^2. The feed solution was pumped from a thermostatted solution tank to the permeation cell, and the residue stream was circulated back to the feed tank. The heat loss at the feed side was alleviated since a circulation system was applied and the tube length was designed to be as short as possible. The permeate side of the membrane was purged with a dry air stream to remove the permeated water vapor, and a cold trap was used to condense and collect the permeate. To confirm that the cold trap could collect all permeate, another cold trap was installed following the existing one temporarily,

and the collected vapor in the secondary cold trap was measured to be negligible. The uncondensed gas was released to the atmosphere after measurement of gas flow rate using a bubble flowmeter. The permeation flux (J) was evaluated from:

$$J = Q/A\Delta t \quad (3\text{-}1)$$

where Q is the weight of collected permeate over a period Δt, and A is the effective membrane area. A conductivity meter (WTW inoLab Cond Level 2) was used to determine the salt concentration of permeate (C_p). The salt rejection (R) of the membrane was evaluated by:

$$R = (C_f - C_p)/C_f \times 100\% \quad (3\text{-}2)$$

where C_f is the salt concentration in the feed solution.

The effects of operating temperature (30-70℃), salt type and concentration in the feed (KAc 1-50 wt%; NaAc 10-40 wt%; KCl, NaCl and $MgCl_2$ 5-20 wt%) on the pervaporation performance of the membranes were investigated. For a given pervaporation run, the quantity of permeate water was less than 1% of the feed water so as to maintain a largely constant feed concentration. During the pervaporation experiments, water was gradually removed from the feed due to permeation, and thus water in the same amount as collected in the permeate was added to the feed after each pervaporation run. In addition, any residue salt on the membrane was flushed away after each pervaporation experiment by circulating de-ionized water for at least 15 min. Under a given operating condition, the pervaporation experiment was repeated at least twice, and the average data were reported.

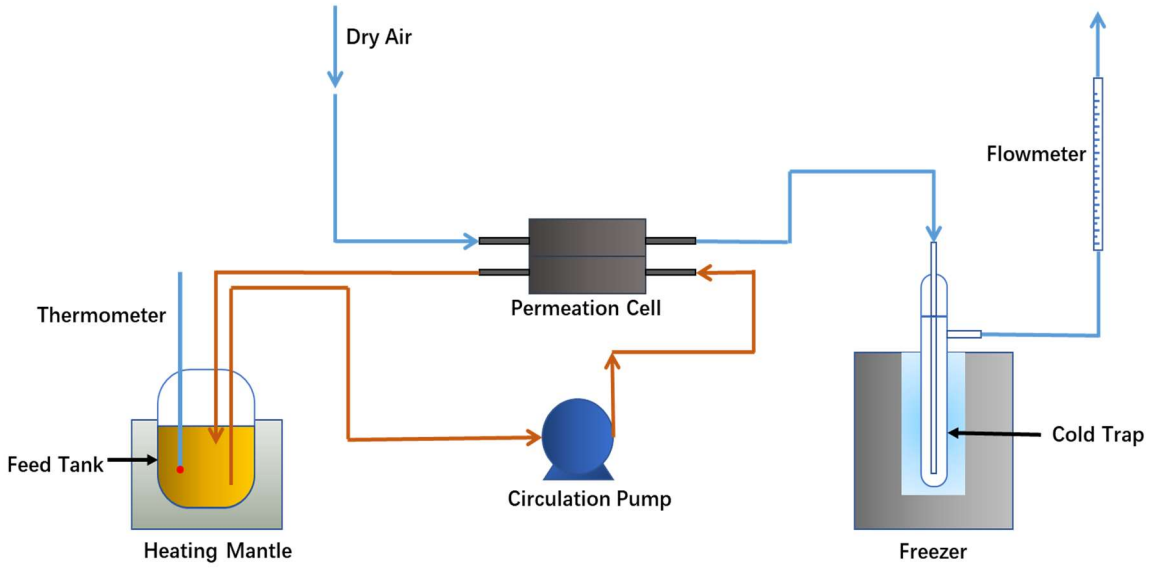

Fig.3.2 Schematic diagram of the experimental setup for pervaporation.

3.3 Results and discussion

3.3.1 Effects of feed concentration and temperature on pervaporative concentration

It was demonstrated in this study that with a PDA sublayer, the TFC membrane with a single PEI/PAA bilayer would be sufficient to handle the pervaporative concentration of salt solutions. **Fig.3.3** shows the water permeation flux of PDA-$(PEI/PAA)_1$ membrane at various feed KAc concentrations and temperatures. As expected, with an increase in feed salt concentration, the water permeation flux decreased. For a feed solution containing 50 wt% of KAc, the water flux was only approximately a quarter of pure water flux. This is because a higher salt concentration imposes a more severe osmotic deswelling of the membrane [107], resulting in a decrease in water solubility in the membrane at the liquid/membrane surface and a decrease in the diffusivity of water molecules in the membrane In addition, a higher salt concentration in the feed stands for a reduction in water concentration, thus decreasing the transmembrane driving force for water permeation. All

these negative effects explain the decline in water flux with an increase in feed salt concentration. It can be anticipated that the water flux decline would be further augmented if concentration polarization would occur adjacent to the membrane surface at feed side[108,109].

Fig.3.3 also illustrates the positive effect of operating temperature on water permeation. The pure water permeation flux increased from 556 to 2661 g/(m^2h) with an increase in temperature from 30 to 70℃. Such a significant flux increase is mainly attributed to the following factors. On the one hand, the vapor pressure of water in the feed increases almost exponentially with temperature, thus a drastic increase in the driving across for water transport in the membrane. On the other hand, at a higher temperature, the water molecules become more energized for diffusive migration in the membrane, while the thermal motion of polymer chains of the membrane is intensified, thereby leading to a higher diffusivity of water molecules across the membrane. The temperature effects on the membrane permeability will be analyzed in more details later.

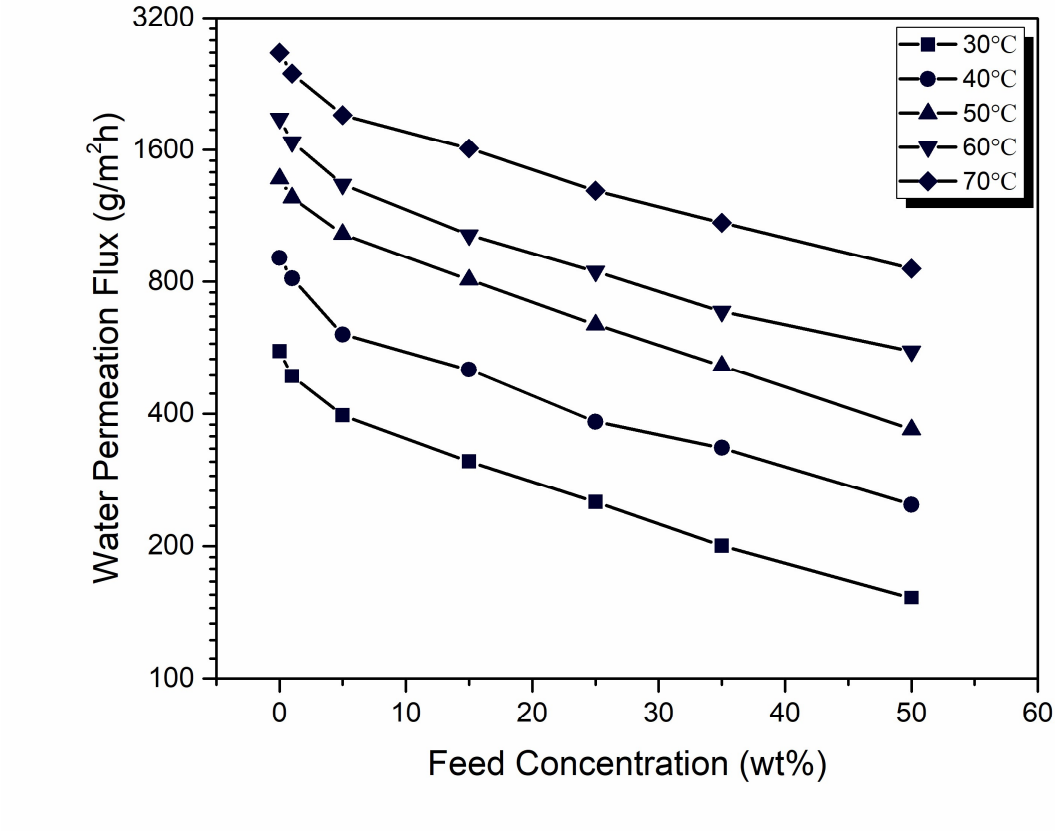

Fig.3.3 Effects of KAc concentration in feed on water flux at different temperatures. Membrane: PDA-$(PEI/PAA)_1$.

3.3.2 Effects of feed salt types on pervaporative concentration

From a solution thermodynamics point of view, the saturated vapor pressure of water will be reduced by the addition of a nonvolatile solute. The saturated vapor pressure in equilibrium with the feed solution determines the driving force for pervaporative mass transfer. To look into the effects of the nature of the salts on water permeation flux, pervaporation experiments with aqueous solutions of different salts (i.e., KCl, NaAc, NaCl

and $MgCl_2$) were carried out as well, and the water permeation flux as a function of feed salt concentration for the different types of salt is presented in **Fig. 3.4** at a temperature of 50℃. Note that the feed salt concentration was expressed in molarity for convenience of comparation. As expected, the water flux decreased with an increase in the feed salt concentration for all the salts tested, and the most drastic decrease in water flux was observed for salt $MgCl_2$. This is understandable because the van't Hoff factor for $MgCl_2$ is the highest among the salts studied here, which means the water vapor pressure of the feed solution is affected most significantly by $MgCl_2$ concentration. Therefore, as far as the salt concentration dependence of water flux is concerned, $MgCl_2$ solute will affect the water permeation more significantly than other salts. The data in the figure also showed that the salt concentration dependencies of water flux for NaCl and KCl were similar, while the same trend was observed for KAc and NaAc at low concentrations. It is also worth mention that, for all the feed situations studied, the salt concentrations of permeate are lower than 0.005 wt%, indicating an essentially complete salt rejection of the prepared membrane in pervaporative concentration.

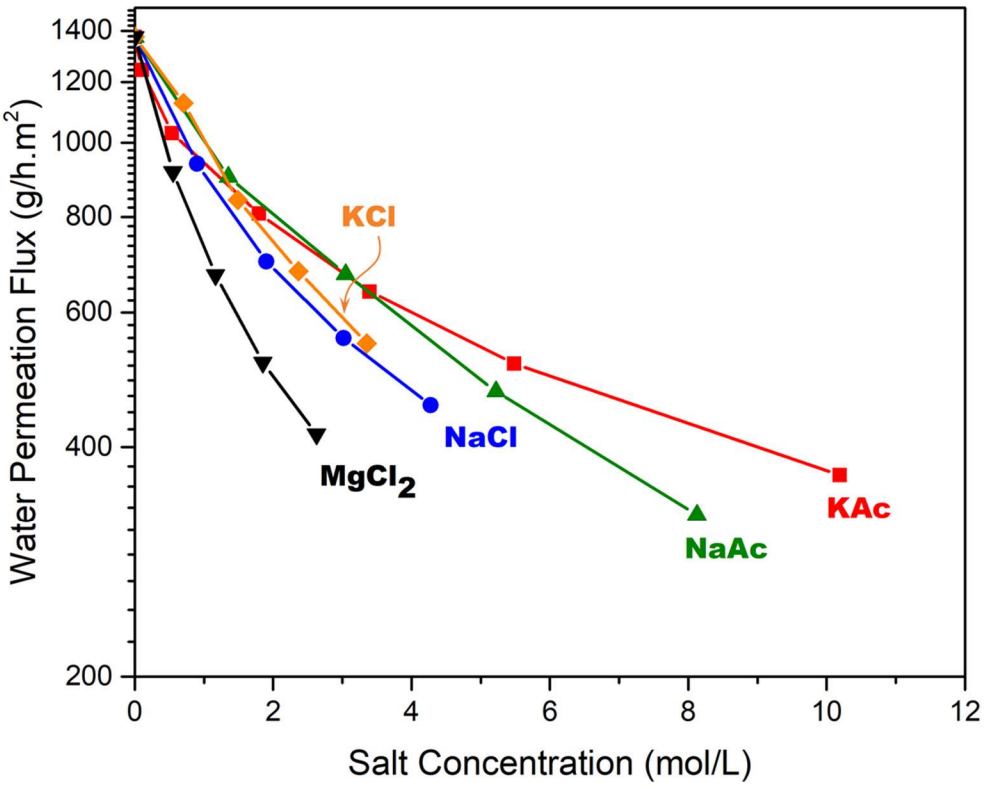

Fig.3.4 Water permeation flux at different feed salt concentrations. Temperature, 50℃; Membrane, PDA-(PEI/PAA)$_1$.

3.3.3 Activation energy of permeation

The experimental results of the water permeation through the PDA-$(PEI/PAA)_1$ membrane for different salts in the feed at different concentrations and temperatures are presented in **Fig.3.5**, where a linear relationship between logarithmic water flux and reciprocal temperature was displayed for a given salt in the feed at a given salt concentration. The activation energy for permeation can be evaluated by fitting the data in Figure 5 to an Arrhenius-type equation:

$$J = J_0 \exp(-E_J/RT) \quad (3\text{-}3)$$

where J_0 is the pre-exponential factor for the process, R is the ideal gas constant, T is the absolute temperature, and E_J is the activation energy for water permeation. It may be mentioned that the activation energy so determined characterizes the overall temperature dependence of water permeation flux that have accounted for effects of temperature on the membrane permeability and the mass transfer driving force. Thus, E_J is essentially an apparent activation energy, and it is shown to consist of the intrinsic activation energy (E_p) for water permeation measuring temperature dependence of membrane permeance and the heat of evaporation (ΔH_V) of water [36].

In a TFC composite membrane, the effective thickness of the active skin layer can hardly be determined accurately, and thus the permeance of the membrane is often used to characterize the membrane permeability. The membrane permeance to water can be calculated from water permeation flux (J) normalized by the mass transfer driving force:

$$(P/l) = J/\Delta P = J/(X\gamma p^{sat} - Yp^{p}) \quad (3\text{-}4)$$

where p^{sat} and p^{p} are the saturated water vapor pressure on feed side and the permeate side pressure, respectively, X and Y are mole fractions of water in the feed solution and permeate vapor, respectively, and γ is the activity coefficient of water in the feed solution. The membrane permeance at different temperatures is plotted in **Fig. 3.6**. The intrinsic

activation energy (E_p) that characterizes the temperature dependence of membrane permeability or permeance can be evaluated from the slope of the straight line based on the following equation:

$$(P/l) = (P_0/l)\exp(-E_P/RT) \quad (3\text{-}5)$$

The calculated apparent and intrinsic activation energies (E_J and E_p) for water permeation are presented in **Fig.3.7**. In general, an increase in feed salt concentration leads to an increase in both E_J and E_p for all tested salt solutions, and feed concentration of $MgCl_2$ showed the most significant effect on the activation energy of water permeation. This is in agreement with physical reasoning. As an approximation, E_p is a combination of the activation energy for diffusion (E_D) and the enthalpy change of sorption (ΔH_S). The former can be considered as an energy barrier that needs to be overcome by the permeating molecules (i.e., water in this study) for diffusive migration in the membrane. The membrane swelling tends to be lessened when the salt concentration in the feed is increased, which results in a relatively rigid membrane structure that imparts to a greater energy barrier for water molecules to diffuse. This will contribute to an increase in E_p and E_J. As explained before, $MgCl_2$ has a van't Hoff factor greater than other salts studied here, and thus a stronger osmotic de-swelling of the membrane by $MgCl_2$ is expected as well. It is thus not surprising to note the strong impacts of $MgCl_2$ content in feed on the activation energy for water permeation.

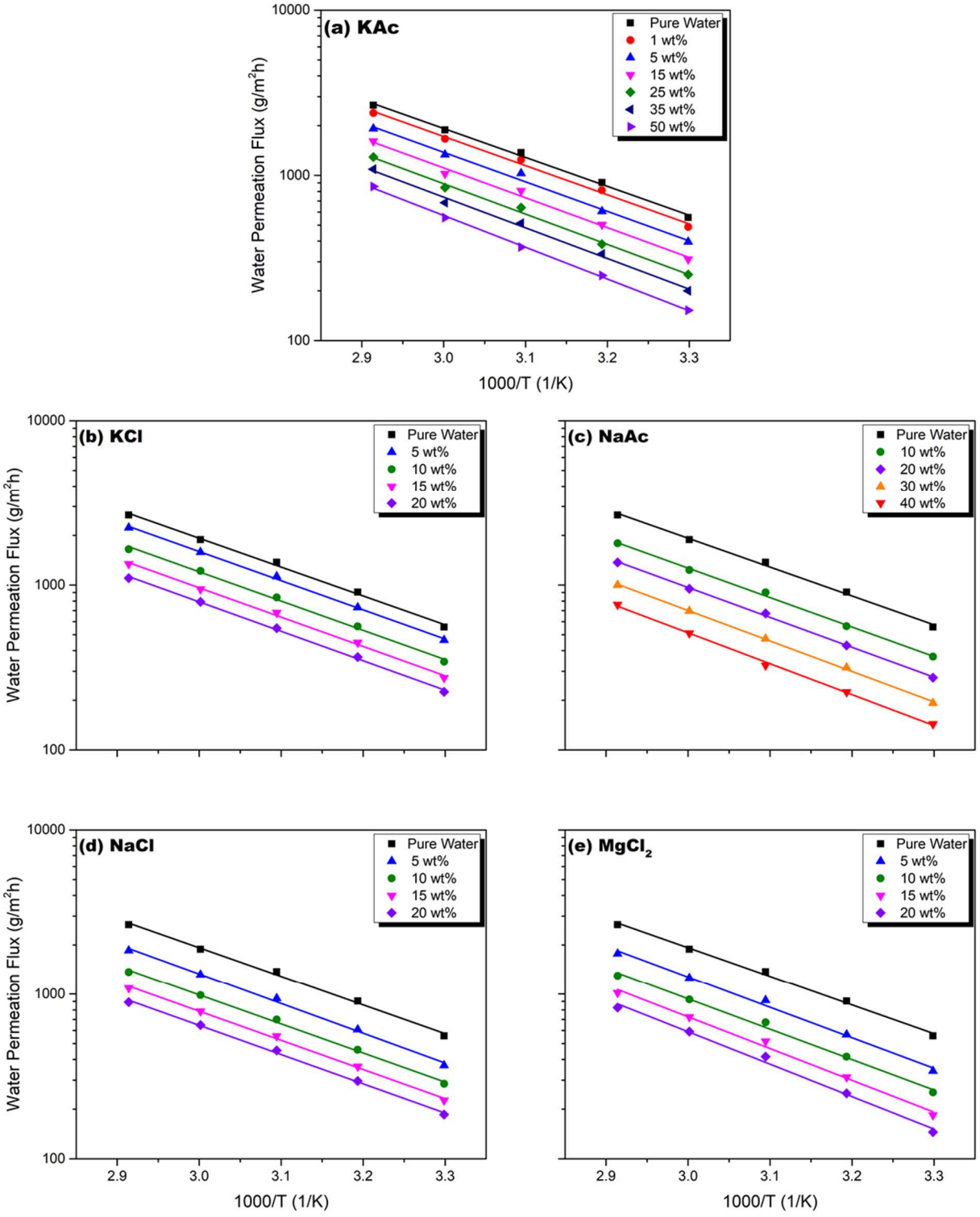

Fig.3.5 Effects of temperature on water flux at different feed concentrations. Salt in feed solution: (a) KAc, (b) KCl, (c) NaAc, (d) NaCl, (e) $MgCl_2$. Membrane, PDA-$(PEI/PAA)_1$.

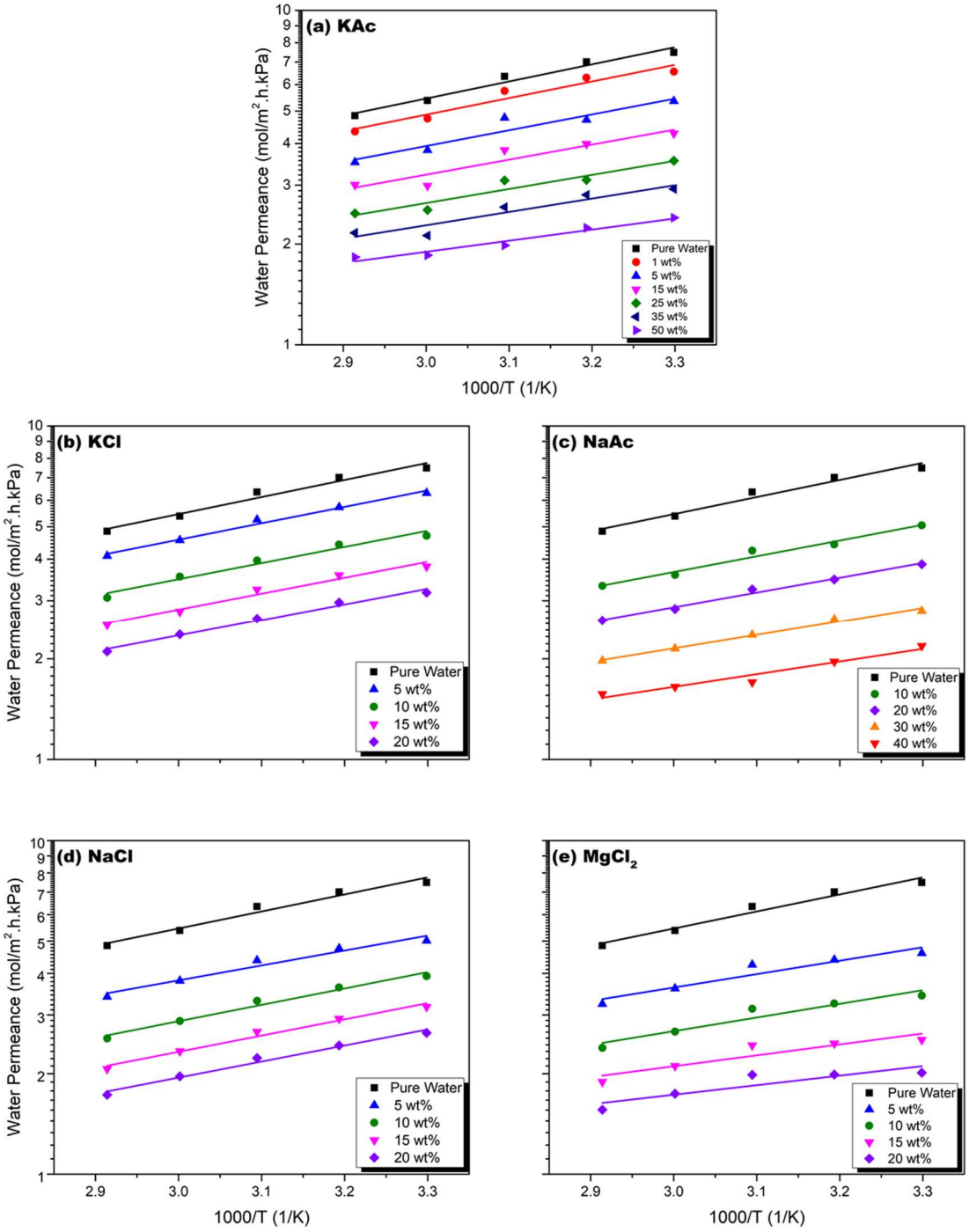

Fig.3.6 Effects of temperature on water permeance in PDA-$(PEI/PAA)_1$ membrane at different feed concentrations. Salt in feed solution: (a) KAc, (b) KCl, (c) NaAc, (d) NaCl, (e) $MgCl_2$.

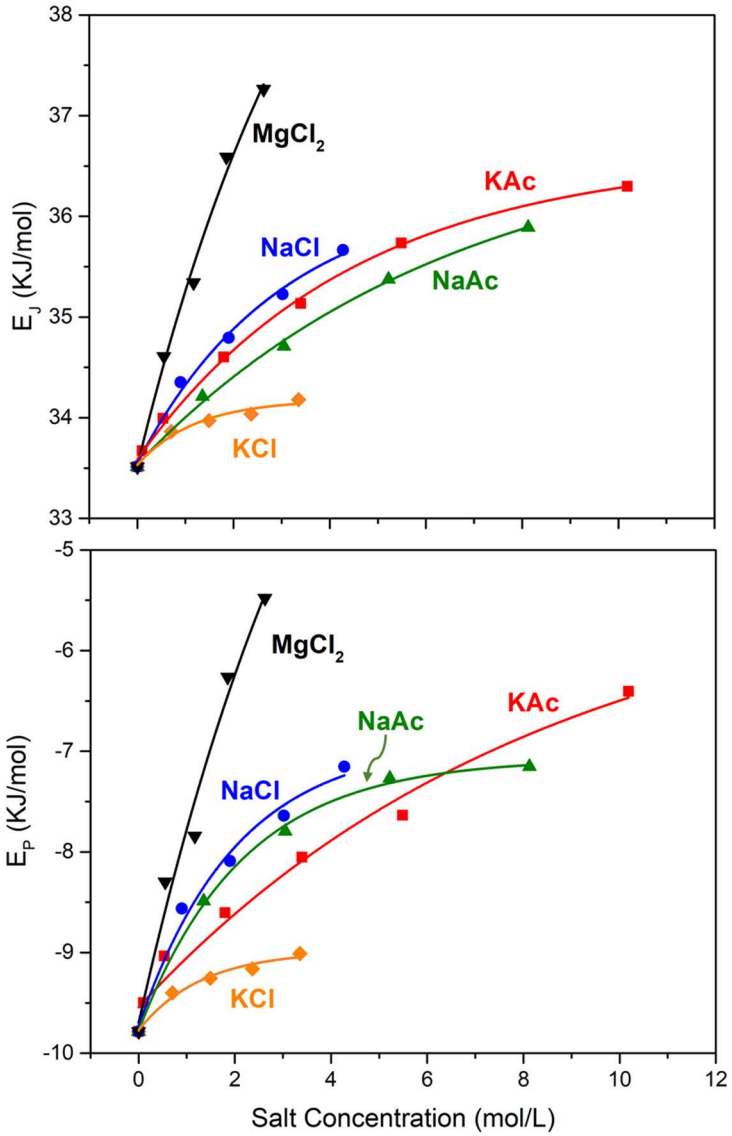

Fig.3.7 Effects of feed concentration on E_J and E_P for water permeation from feed solutions containing different salts. Membrane, PDA-$(PEI/PAA)_1$.

To have a closer look into the pervaporation characteristics of the polyelectrolyte bilayer deposited on a PDA intermediate layer, membranes with different numbers of polyelectrolyte bilayers were also fabricated and tested for water permeation from aqueous KAc solutions. The water flux and membrane permeance are plotted in **Figs. 3.8** and **3.9**, respectively. The activation energies E_J and E_p for water permeation at different KAc concentrations in the feed are shown in **Fig.3.10**, where both E_J and E_p values increased with an increase in the number of deposited bilayers. That is, the water flux and permeance of the membrane with more PEI/PAA layers tend to be more sensitive to a change in temperature. However, at high salt concentrations in the feed solutions, the increase in the activation energy is less significant and tends to be level off for membranes with relatively large numbers of polyelectrolyte bilayers. A possible explanation for this phenomenon is that increasing the number of the PEI/PAA bilayers enhances the overall hydrophilicity of PDA-(PEI/PAA) TFC membrane, which helps the membrane to retain water strongly and alleviates the deswelling effect imposed by the high salinity of the feed solution. In addition, it is worth to mention that the E_p values are negative in all cases. As mentioned above, E_p is a combination of the activation energy for diffusion (E_D) and the sorption enthalpy (ΔH_S) based on a consideration of solution-diffusion in mass transport across the membrane. The diffusion is an activated process where the penetrant molecules need to be energized enough to migrate, and increasing temperature will thus facilitate the diffusion rate, resulting in positive E_D values. On the other hand, at a higher temperature, water molecules have a greater tendency to escape the retention by the membrane, and thus the ΔH_S is usually negative. Obviously, when the negative ΔH_S dominates over the positive E_D, a negative E_P will result. Similar observations can be made with many other membranes for pervaporative dehydration of saline solutions[41,110–113]

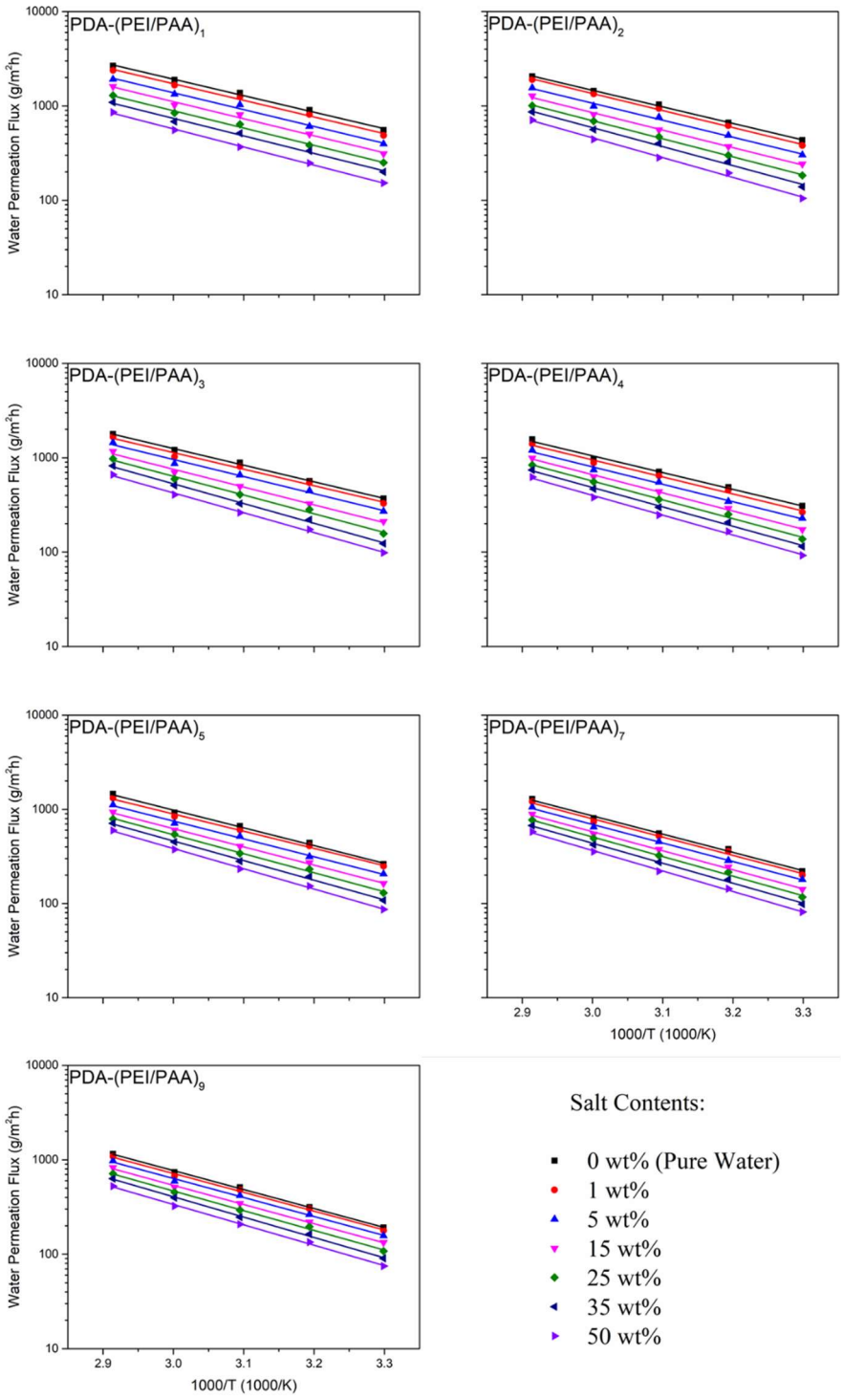

Fig.3.8 Effects of temperature on water permeation from aqueous KAc solutions at various concentrations through membranes having different numbers of PEI/PAA bilayers.

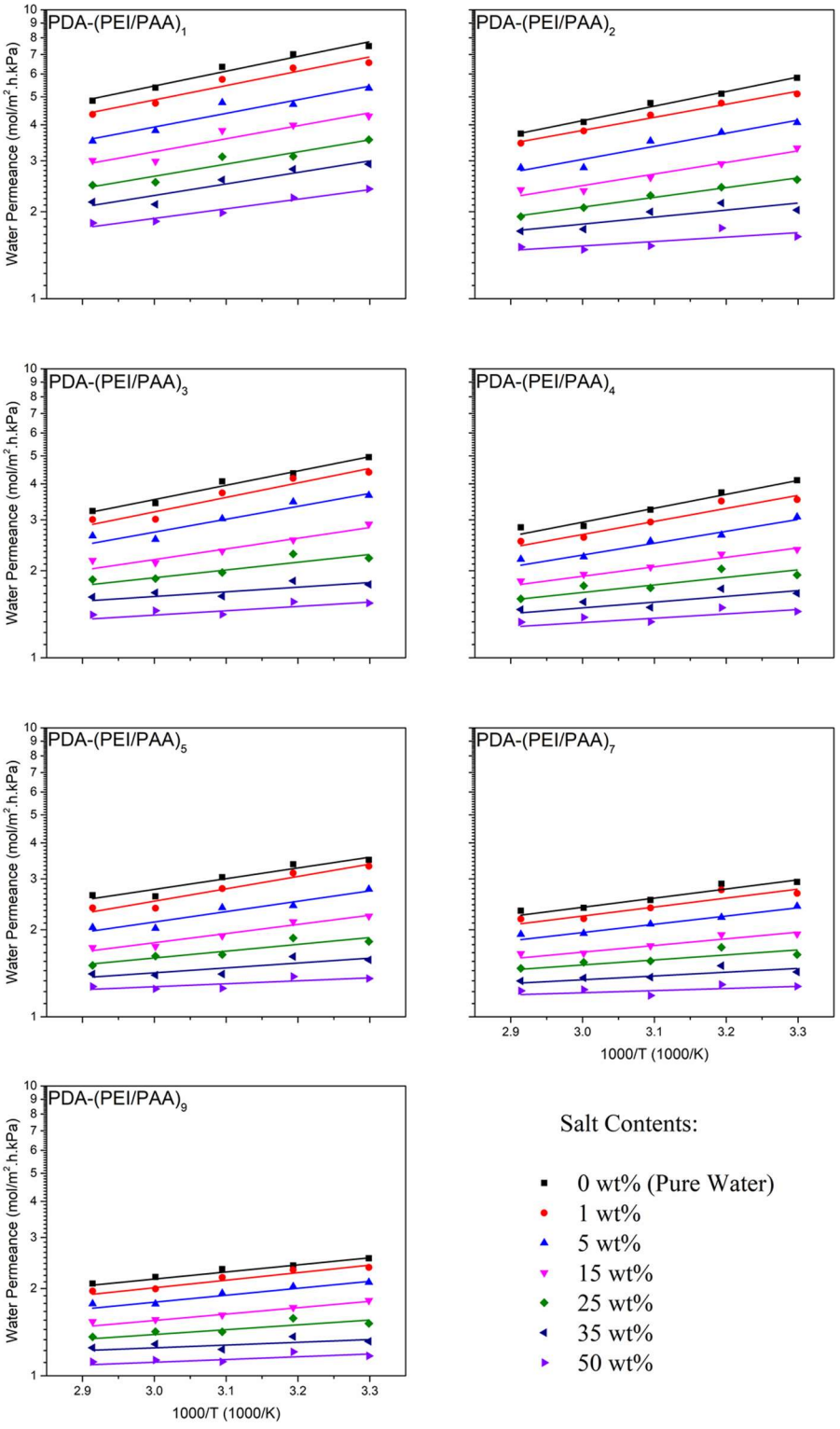

Fig.3.9 Effects of temperature on water permeance of the membranes having different numbers of PEI/PAA bilayers.

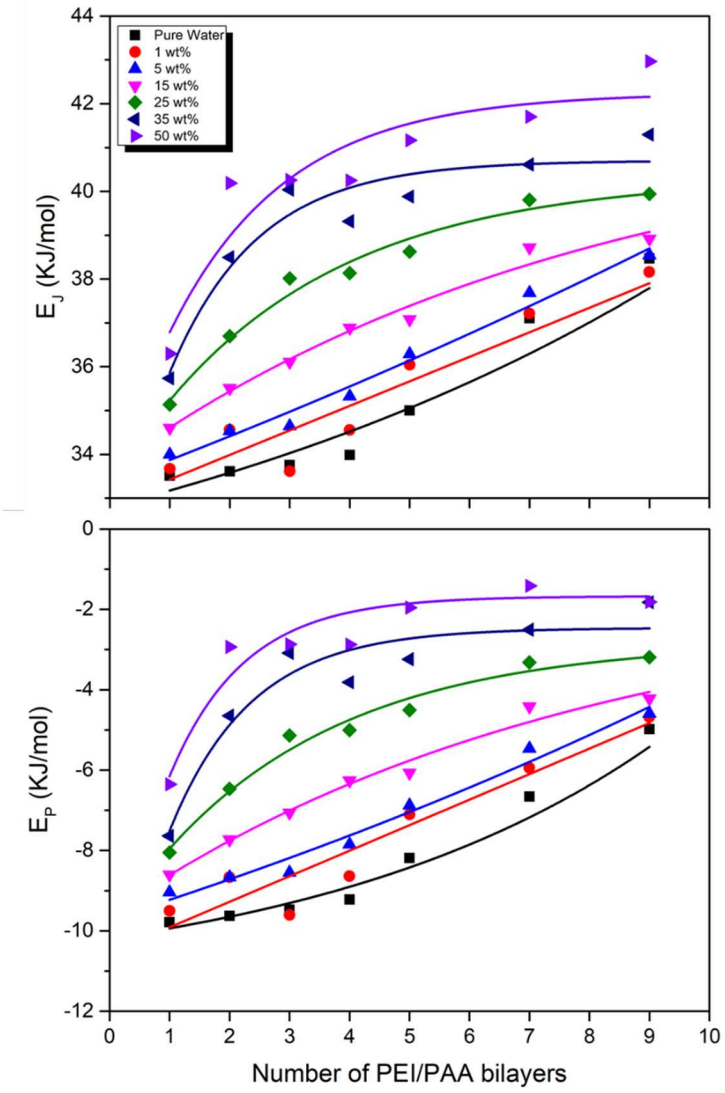

Fig.3.10 E_J and E_P for water permeation in pervaporative concentration of KAc solutions using membranes with different numbers of PEI/PAA bilayers.

3.3.4 Analysis of membrane resistance to water permeation

Considering Equation (3-3) for water flux, the reciprocal permeance (l/P) can be considered as the overall resistance of the membrane to water permeation. Assuming that

the mass transfer resistance of each electrolyte bilayer is the same, the total resistance of the TFC membrane R_t can then be described as

$$R_t = R_{PES} + R_{PDA} + nR_L \quad (3\text{-}6)$$

where R_{PES}, R_{PDA} and R_L represent the resistances of the PES substrate, the PDA sublayer and a single electrolyte bilayer, respectively, and n is the number of polyelectrolyte bilayers in the composite membrane.

Fig.3.11 shows the total membrane resistances of the TFC membrane to water permeation for pervaporative concentration of KAc solutions. A linear relationship ship between the membrane resistance and the number of polyelectrolyte layers in the membrane was observed except for membranes having 1 or 2 polyelectrolyte bilayers. This implies that the above assumption of constant resistance contribution from a single polyelectrolyte bilayer is largely valid after the deposition of the initial two polyelectrolyte bilayers during the layer-by-layer growth. This may be attributed to two factors. On the one hand, the coating of a PDA intermediate layer onto the PES substrate did not completely cover or block all the large pores on the surface, as shown by the water leakage across the membrane observed when the PDA-coated PES membrane was subjected to a pervaporation test. The initial depositions of polyelectrolyte on the on the PDA-coated PES substrate served to fill and block the pores, and as such the formation of the first few polyelectrolyte bilayers was expected not only to contribute to mass transfer resistance due to addition of the bilayer but also to increase the resistance of the interior porous layer due to penetration to the pores. Consequently, the total resistance of the TFC membrane increased more than proportionally with the deposition of the first few bilayers. In addition, the possible conjunctions via Michael addition and Schiff base reaction between the PDA and the first PEI layer would also lead to a large loading of the polyelectrolyte, making the first bilayer more resistant to water permeation than polyelectrolyte layers formed subsequently. In light of these, membranes with three or more electrolyte bilayers that

displayed a linear trend in **Fig.3.11** were considered, and the resistance of a single polyelectrolyte bilayer (R_L) was evaluated from the slope of the straight line. the tangent that represents the resistance of the bilayers for the initial few points are larger. The resistance so determined for each bilayer is presented in **Fig.3.12**. It is shown that the salt concentration in the feed did not have a significant effect on the mass transfer resistance of a single PEI/PAA bilayer, at least in the concentration range investigated, and this was an indication that the membranes were stable in concentrating the salt solutions. On the other hand, the PEI/PAA bilayer resistance decreased only slightly from an average of 0.031 $m^2 \cdot h \cdot kPa/mol$ to 0.028 $m^2 \cdot h \cdot kPa/mol$ with an increase in temperature from 30℃ to 70℃, suggesting a weak positive effect of temperature on the permeance of an individual PEI/PAA bilayer. This is in agreement with the increased E_p values of the TFC membranes as the number of the bilayers increased (**Fig.3.10**).

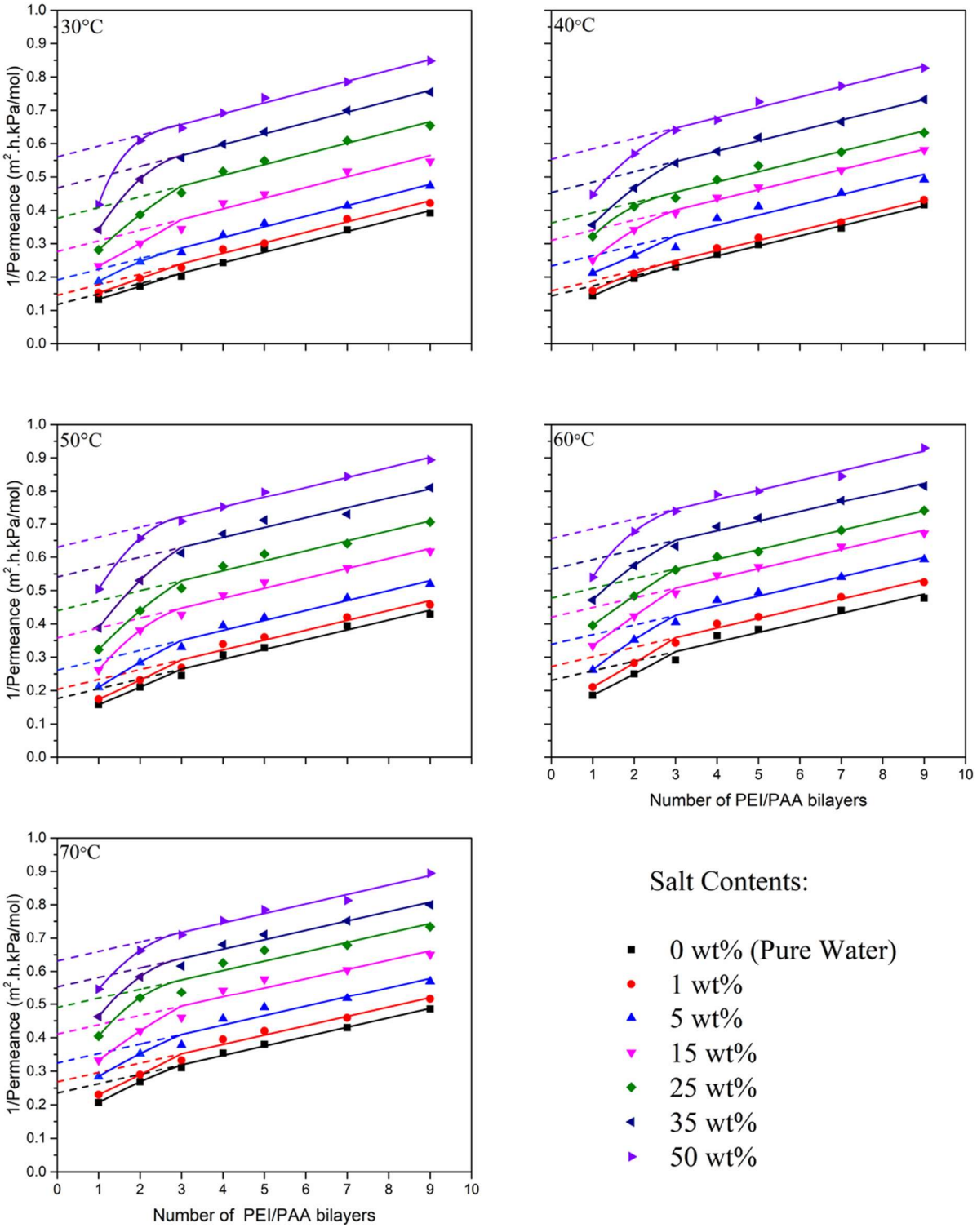

Fig.3.11 Membrane resistance to water permeation versus number of PEI/PAA bilayers.

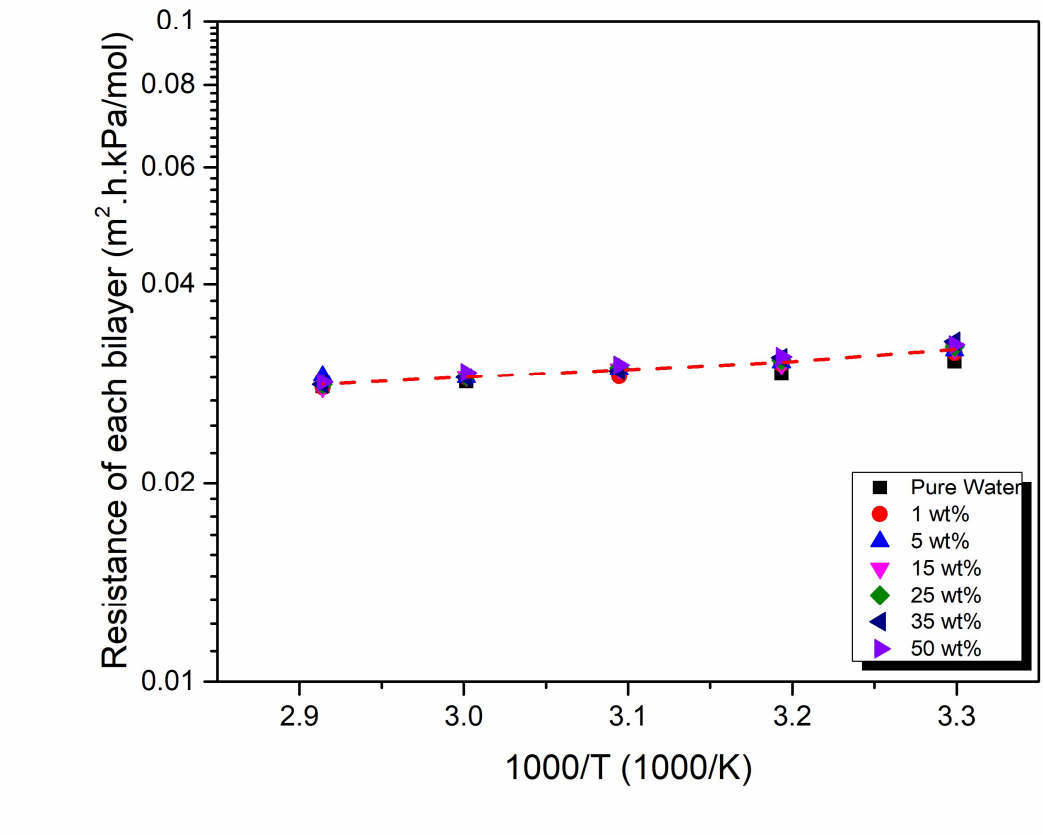

Fig.3.12 Effects of temperature on mass transfer resistance of each PEI/PAA bilayer.

3.4 Conclusions

Pervaporation performance of the prepared TFC membranes comprising of a PDA sublayer and PEI/PAA bilayers for concentration of saline solutions was studied. The effects of temperature, feed salt type and concentration on water permeability through the membranes were investigated. It has been demonstrated that the TFC membrane with only one PEI/PAA bilayer on top of the PDA sublayer was effective for pervaporative concentration of the salts, and essentially complete salt rejections were achieved for all tested situations. The feed salt type was found to have a significant impact on the membrane

permeability to water, and it seemed that anions of the salts affected the membrane permeability to water more significantly than the cations. The activation energy for water permeation increased with an increase in the PEI/PAA bilayer numbers. The PEI/PAA polyelectrolyte bilayer resulted in a TFC membrane which is more sensitive to the change of feed temperature. Moreover, the negative value of activation energy for water permeation based on membrane permeability showed that the water solubility dominated over the water diffusivity in pervaporative transport. The resistance of PEI/PAA bilayer was found to be largely the same when the number of the bilayers was sufficiently large, which indicated the bilayers were stable in the salt solutions at the different feed salt concentrations and temperatures.

Chapter 4

Co-depositing polyvinylamine and dopamine to enhance membrane performance for concentration of KAc solutions via sweeping air pervaporation[2]

4.1 Introduction

Potassium acetate (KAc) is a chemical of high commercial value widely used as a food additive, fire extinguishing agent and eco-friendly deicer, as well as precursor for production catalysts and nanomaterials. In the production of KAc, the concentration of aqueous KAc solutions is an important step. At present, evaporation and reverse osmosis are mainly used for concentrating saline solutions. However, the thermal process of evaporation is energy intensive to operate, while the nonthermal reverse osmosis is disadvantageous when treating high salinity feed because of the high osmotic pressure [30]. As such, pervaporation has been proposed to remove water from saline solutions. While there is a geat deal work on pervaporation for solvent dehydration and organic compound removal from water, its application in concentrating high salinity solutions is not well investigated [107,110]. In pervaporation, the mass transport through the membrane is induced by maintaining a vapor pressure of the solvent at the downstream side lower than the saturated vapor pressure of the solvent in the feed solution. Instead of applying vacuum

[2] The work from this chapter has been published in *J. Memb. Sci*. 656 (2022) 120664.

to reduce the permeate pressure, which is the conventional operating mode of pervaporation, sweeping air pervaporation appears to be particularly suitable for concentrating saline solutions from an application point of view because (1) the low pressure of water vapor at the permeate side is created by gas purging, (2) only water permeates through the membrane and the vaporous permeate water can be discharged directly, (3) instead of heating the whole feed liquid, the latent heat required for phase change of water (liquid in the feed and vapor in the permeate) can be provided by the sweeping gas. This is especially advantageous when low-grade or waste heat is available to heat up the sweeping gas.

With regard to separation membranes, thin film composite (TFC) design is preferred due to its low mass transfer resistance derived from the thin skin layer and the high mechanical strength provided by the substrate [114–116]. Many materials and methods have been proposed to fabricate the thin selective layer of the TFC membrane, among which polydopamine (PDA) formed by oxidative self-polymerization of dopamine has recently attracted considerable attention because of its unique capability of adhering to a variety of surfaces and functionalities to interact with many other polymers [17,93,96]. However, there are few potential issues in applying PDA as the thin selective film in TFC membranes for pervaporative concentration of KAc solutions: (1) KAc solution is basic, and PDA has been found not stable under alkaline environment [3,4,8,82,89]. (2) Membranes for pervaporative concentration of saline solutions should be hydrophilic in order to permeate water effectively. Although PDA is often categorized as a hydrophilic polymer, its hydrophilicity is rather limited because of the non-polar aromatic ring in the structure [5,88]. These potential drawbacks also restrict the use of PDA in some other

applications.

Various attempts have been made on improving formation and properties of PDA. For instance, Zhang et al. [8,29] used $CuSO_4/H_2O_2$ as the oxidant to enhance the oxidation conditions for self-polymerization of dopamine, and the resultant PDA layer showed improved structural stability endowed by smaller and uniform PDA particles. To minimize defects in the thin layer, a variety of polymers (e.g., poly(ethylene glycol) (PEG) [89], polyethylenimine (PEI) [18], and poly(vinyl alcohol) (PVA) [117]) have been used for grafting onto the PDA layer. Simultaneous deposition of dopamine along with a second component PEI has been attempted by Yang et al. [5,7], who developed a copolymer film with improved stability and hydrophilicity for oil/water separation as compared to the pure PDA film. Additional research has been carried out on co-deposition of dopamine-PEI for different applications [9,10,80,118]. It is believed that PEI and dopamine polymers are connected through covalent bonds between the primary amines on PEI and the catechol groups on PDA via Michael addition or Schiff base reaction.

On the other hand, polyvinylamine (PVAm) has the highest content of primary amines of amine polymers and thus possesses excellent hydrophilicity. It has been used to produce pervaporation membranes for dehydration of ethylene glycol/water and azeotropic isopropanol/epichlorohydrin/water mixtures [100,101]. The unique characteristics PVAm for surface engineering has been reviewed by Pelton [20]. PVAm has also been used to fabricate membranes for CO_2 capture via facilitated transport [97–99] and nanofiltration membranes by interfacial polymerization with isophthaloyl chloride [102].

In the present work, we report on thin film composite membranes fabricated by a single step of co-depositing a blend of polyvinylamine and dopamine onto a microporous

substrate to enhance the membrane performance for concentration of KAc solutions via sweeping air pervaporation. The effects of the blend composition on the performance of the resulting TFC membranes were investigated, and it was shown that enhanced stability and hydrophilicity were achieved by incorporating PVAm into PDA as compared to membranes comprising of PDA layer only. The membranes showed stable performance for removing water from KAc solutions with essentially complete rejection to KAc. Water permeation behavior in the membrane at different feed concentrations and temperatures was also studied. For purpose of comparison, water removal from aqueous NaCl solutions by the membrane was also carried out. In addition, to provide an insight into the PVAm/dopamine codeposition, the growth rate of the membrane skin layer during membrane formation was determined as well, and the kinetics information is not only important to membrane fabrication but also useful to better understand the general behavior of dopamine adhesion and polymerization in surface engineering. To our knowledge, no such work has been reported previously.

4.2 Experimental

4.2.1 Materials

A microporous polyethersulfone (PES) membrane supported on a non-woven fabric (molecular weight cut-off 10,000, supplied by Sepro Membranes) was used as the substrate for membrane fabrication. Dopamine hydrochloride and polyethylenimine (PEI) (branched, Mw 25,000) was purchased from Sigma-Aldrich, and polyvinylamine (PVAm) (Lupamin

1595, Mw 10,000) was generously provided by BASF. Tris(hydroxylmethyl)aminomethane (Tris) was purchased from Sigma-Aldrich and was used as the pH buffer to prepare the depositing solutions. KAc (Sigma-Aldrich) and NaCl (EMD Chemicals) were dissolved in de-ionized water to prepare the saline feed solutions.

4.2.2 Preparation of TFC membranes

A pre-determined amount of PVAm (or PEI) was dissolved in de-ionized water containing Tris (15 mM), and the pH of the solution was adjusted to 8.5-8.8 using hydrochloric acid. The PES microporous substrate membrane was rinsed with de-ionized water to remove any preservatives and then mounted in the cap of a wide-mouth bottle that had the bottom cut off. The assembly was placed upside down, and the substrate membrane was allowed to contact with a freshly mixed solution of the PVAm (or PEI) and dopamine hydrochloride at a predetermined ratio, thereby initiating deposition of the polyamine and dopamine onto the surface of the substrate membrane. The total content of the polyamine (PVAm or PEI) and dopamine hydrochloride in the depositing solution was fixed at 2 g/L, while the relative amount of polyamine and dopamine was varied to determine how the composition of the depositing solution affected the membrane properties. For convenience, a deposition solution containing 0.6 g/L of PVAm and 1.4 g/L of dopamine hydrochloride concentration was referenced to have a PVAm content of 30 wt% (on a solvent free basis) in the depositant. The depositing solution was kept at room temperature and open to the air during membrane formation. The membrane formed was then washed thoroughly with de-ionized water.

4.2.3 Characterization of the membrane

The contact angle (WCA) of water on the membrane surface was determined using a contact angle goniometer (Tantec Inc.). For each membrane sample, the contact angles at 10 randomly selected spots were measured and the averaged data were reported. The surface morphologies of the membranes were characterized using a scanning electron microscopy (SEM, Quanta FEG 250, FEI Company).

4.2.4 Separation performance

The experimental setup for sweeping gas pervaporation has been described elsewhere [119]. The effective membrane area for permeation was 21.2 cm^2. After the membrane was mounted into the permeation cell, the feed solution was circulated using a pump, and dry air at a flow rate of 7 L/min was admitted to the permeate side to purge the permeated water vapor. The feed temperature was controlled by a thermoregulator control system. The gas stream was allowed to pass a cold trap, where water vapor was condensed and collected; For practical applications, the sweeping air stream could be reused.

The permeation flux (J) of water was calculated by:

$$J = \frac{Q}{A\Delta t} \quad (4\text{-}1)$$

where Q is the weight of water collected in the permeate over a period of Δt, and A is the membrane area. The salt retention performance of the membrane was evaluated using

$$R = \left(1 - \frac{C_P}{C_F}\right) \times 100\% \quad (4\text{-}2)$$

where C_P and C_F are salt concentration in the feed and permeate, respectively. As the salts were involatile, the permeate was essentially salt free (unless the membrane was defective),

and this was confirmed experimentally with a conductivity measurement of the water samples collected from the swept permeate.

Since water was continuously withdrawn from the feed solution, the same amount of water was added to the feed tank to maintain a constant salt concentration during a pervaporation run. In addition, the feed side of the pervaporation system was thoroughly flushed with de-ionized water using the feed pump for at least 15 min to remove any residual salt prior to each new experiment at a different salt concentration. This could also prevent any depositant not firmly adhered to the substrate from getting stripped off by the flowing feed during the experiment (in case they were not thoroughly removed after the rinsing during the fabrication) and contaminating the product. All the measurements were repeated at least three times, and the average water flux data were reported.

4.3 Results and discussion

4.3.1 Rate of deposition in membrane formation

During the deposition of polyamine and dopamine onto the substrate membrane for TFC formation, the following was observed about the depositing solution. **Fig.4.1** shows the solutions with different compositions after standing still for 24 h; all solutions were clear and homogeneous at the beginning. Without co-existing polyamine, small aggregates were formed in the dopamine solution, and similar results were also reported [7,80]. The aggregates were believed to be the self-polymerized dopamine (i.e., PDA) that were not adhered to the substrate membrane. By blending PEI with dopamine, the aggregates precipitated from the solution were more significant, while the solution became more

transparent. This appeared to suggest that the PEI-dopamine interactions facilitated conversation of dopamine to PDA and PDA-PEI copolymer, but their adhesion to the substrate surface was compromised. Interestingly, by replacing PEI with PVAm, the depositing solution became darker and showed no visible aggregates. Such solution characteristics was expected to affect the resulting TFC membranes so formed, which motivated us to look into how much and how fact the (co)polymer was actually adhered to the substrate as the skin layer for the TFC membrane.

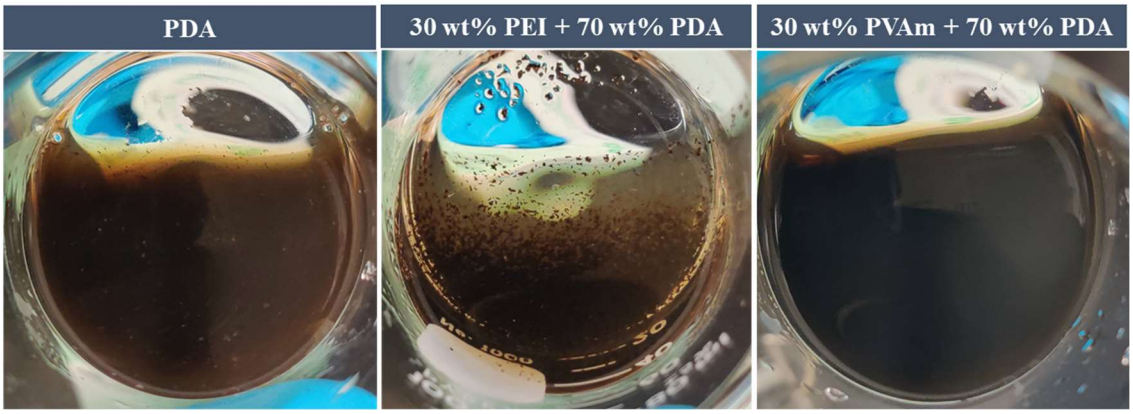

Fig.4.1 Images of the depositing solutions with different compositions after 24 h.

Fig.4.2 shows the mass gains on the substrate on a dry basis as a function of deposition time. The experiments were conducted by determining the dry weight of the membrane relative to the dry weight of the substrate. For all the three deposition solutions containing the same mass concentration (2 g/L) of the depositing macromolecules with different content of the co-existing polyamines (i.e., dopamine only (0 % polyamine), 30 wt% PVAm, and 30 wt% PEI), the amounts of the macromolecules deposited onto the substrate increased with time and then began to level off when the deposition time was sufficiently long. This was not unexpected because as the deposition continued, the concentration of

unreacted dopamine in the solution decreased due to consumption in self-polymerization (and copolymerization with polyamine, if present), resulting in a decrease in the rate of mass deposition on the substrate. In addition, the self-polymerized or co-polymerized dopamine was not completely adhered to the substrate surface, and these macromolecules (some of which were in the form of aggregates as shown above). This also contributed to the decreased film growth rate on the membrane substrate. Among the three deposition solutions, the deposition solution having a dopamine/PEI mass ratio of 70/30 showed the lowest rate of mass deposition on the membrane substrate, whereas the maximum deposition rate and maximum amount of the deposits on the substrate surface were observed when the PEI was replaced with PVAm. This means the use of PVAm as a coexisting polyamine was favorable for constructing the TFC membranes. The data in **Fig.4.2** show at a deposition time of 24 h, over 97% of the maximum deposition amount was obtained, and a deposition time of 24 h was used in subsequent membrane fabrications.

The deposition solutions were visually inspected over time as well. **Fig.4.3** shows how the depositing solutions changed appearance. In the presence of PEI, aggregates started to form in 6 h, and afterwards they gradually precipitated out of the solution. These observations matched well with the mass deposition rate shown in **Fig.4.2** where the deposition rate exhibited a dramatic reduction at around 6 h. In the case of depositing solution containing dopamine only, small particles suspended in the solution were visible at 6 h, and the particles continued to grow and the solution became darker. Eventually, the particles settled down at the bottom. Unlike the above two solutions, the dopamine/PVAm solution did not separate into layers even after 36 h. This further demonstrated that using PVAm as a coexisting polyamine for dopamine was advantageous over PEI from a

membrane fabrication point of view.

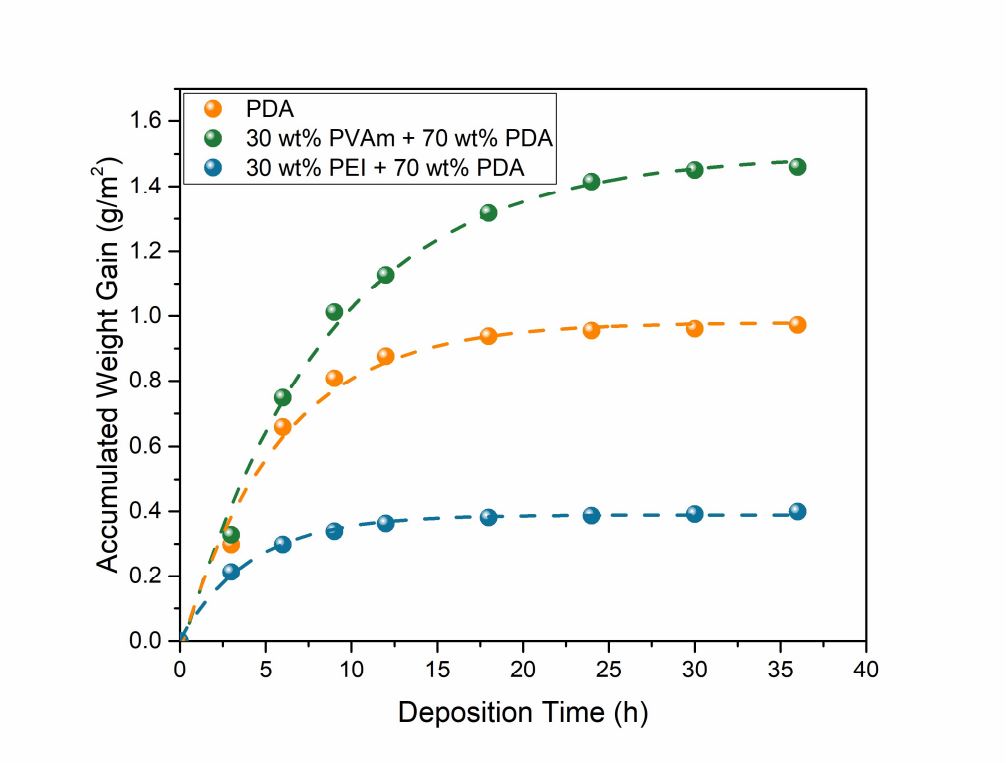

Fig.4.2 The accumulated weight gain of the membrane versus deposition time.

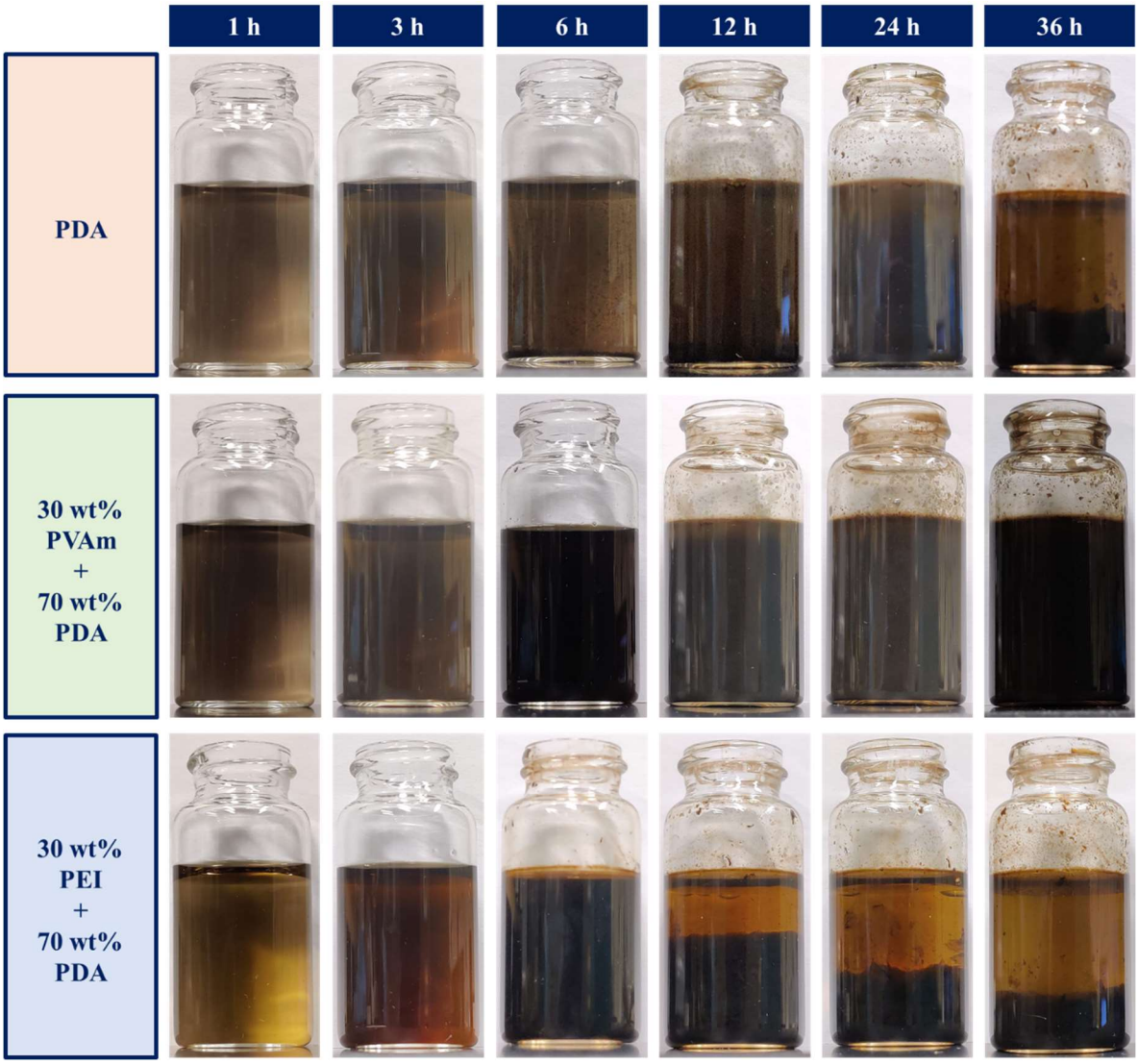

Fig.4.3 The changes in appearance of the deposition solutions over time.

A possible rationalization for this phenomenon is illustrated in **Fig.4.4**. In the dopamine solution, the dopamine molecules self-polymerize to form aggregates. While some of the aggregates near the substrate surface will adhere to the substrate, others far away from a solid surface will keep growing. Consequently, the suspended large PDA aggregates cannot be attached readily and securely to the substrate [8,27,29], and they ultimately precipitate out of the solution. In the presence of branched PEI as a co-depositant,

the primary amine groups on PEI may form covalent bonds with the catechol groups on PDA through Michael addition or Schiff base reaction [7,9,15,16]. However, the content of primary amine groups on PEI (which are at the end of the branches) is rather low, and thus there are only a limited number of dopamine that can directly link with PEI, and a large portion of the active dopamine monomers remain in the solution. Thus, the PDA unit directly attached to PEI through the covalent bond will be able to aggregate with surrounding PDA self polymerized from the active dopamine monomers in the solution. Because of the sparsely populated PDA-PEI bonds at the end of the PEI branches, there is little hindrance effect for PDA aggregation. As a result, precipitation occurs if the aggregates become large enough, which adversely affect their adhesion onto the membrane substrate surface. The situation will be different when PVAm is used as a co-depositant. Due to the enormous primary amine content of PVAm, under the influence of steric hindrance, the PDA attached to a given amine site on PVAm will not aggregate readily, resulting in a largely even arrangement of PDA on PVAm. As such, there are no large PDA aggregates precipitating out of the solution. This is helpful to adhesion to the substrate surface in membrane fabrication, as shown by the favorable mass deposition rate. In addition, after initial attachment to the substrate membrane, the PVAm/PDA tend to flatten on the surface because of the linear structure of PVAm, yielding a thin deposit layer.

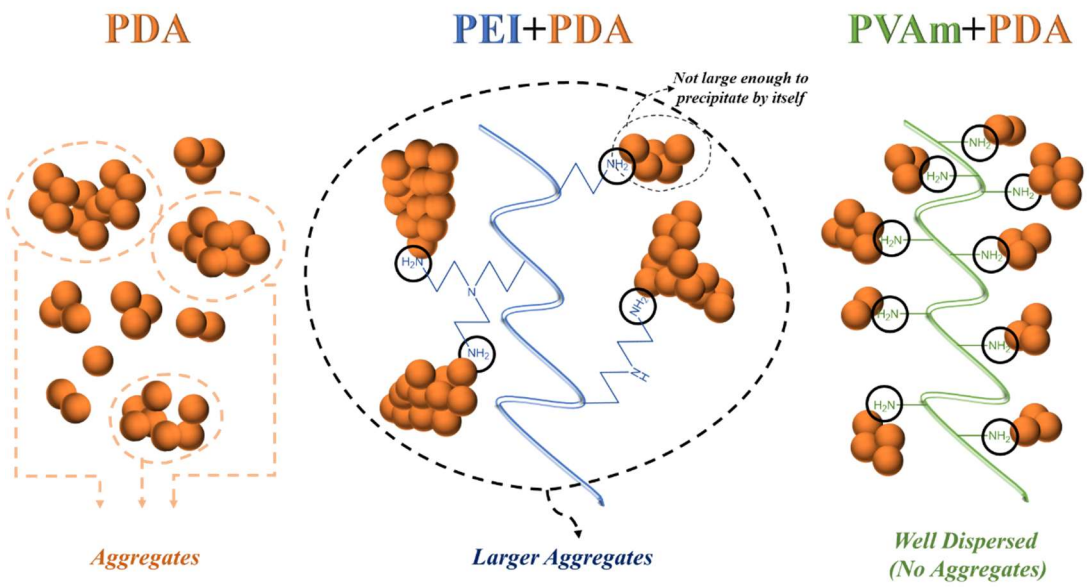

Fig.4.4 Illustration of PDA deposition with and without co-depositant PEI and PVAm.

In view of the above, if a single coating of PDA (plus PEI or PVAm) was not enough to form a defect free skin layer of the TFC membrane, additional depositions would be needed. It was thus of interest to investigate whether the layer by layer buildup would be affected by the prior surface on which coating/deposition was to occur. **Fig. 4.5** shows the mass gains (on a dry basis) on the membrane as a function of the number of depositions. For a given depositing solution, all depositions were conducted using freshly prepared solutions under the same conditions (total depositant content (dopamine + polyamine), 2 wt%; deposition time, 24 h). It was shown that the weight gains of the membrane increased linearly with an increase in the number of depositions, indicating that the amount of the depositant securely attached to the membrane was largely the same. That is, the amount of the PDA or PDA/polyamine macromolecules adhered to the membrane was determined primarily by the depositing solution, regardless of whether the coating surface was the

membrane substrate or a polymer layer (PDA or PDA/polyamine) formed prior. These data again showed that PVAm was advantageous over PEI as a co-depositant for the membrane formation.

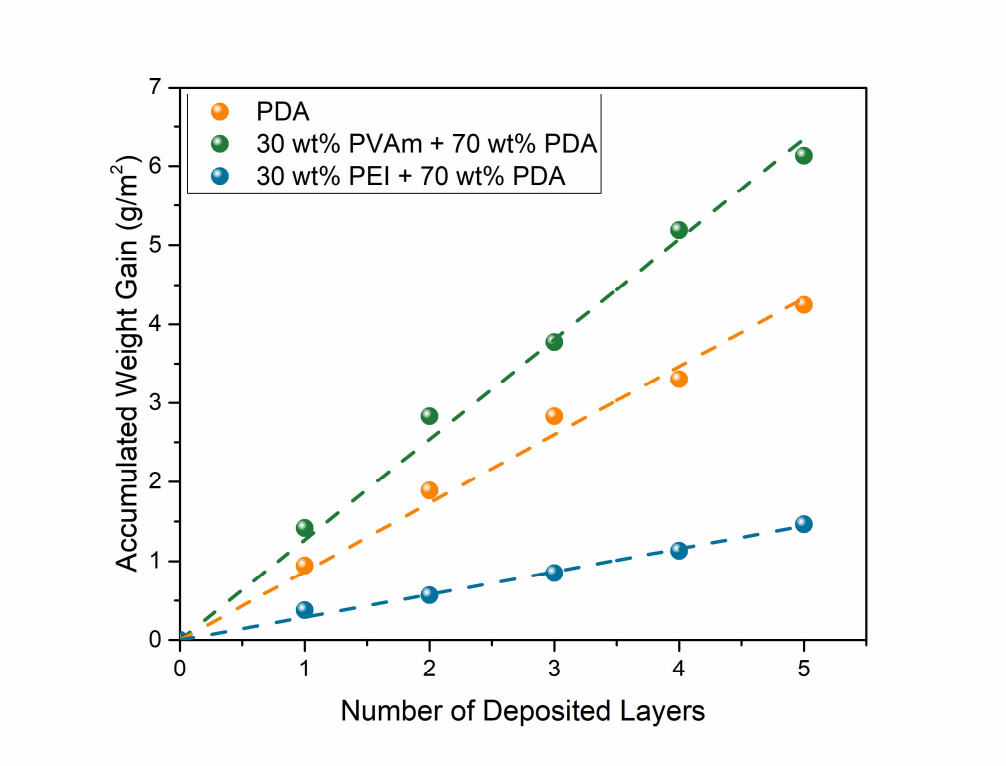

Fig.4.5 Accumulated weight gains of the membrane vs number of depositions.

4.3.2 Membrane characterization

Fig.4.6 shows the contact angle of water on the membrane surface. The contact angle decreased drastically from ~80° of the pristine PES substrate to 56° after deposition with PDA in the absence of polyamine. When PVAm was added as a co-depositant, a further decrease in the water contact angle was observed as long as the PVAm/dopamine mass ratio was sufficiently low. This is easy to understand because the attachment of PVAm onto

the membrane along with PDA would enhance the hydrophilicity of the membrane surface. However, if the PVAm/dopamine mass ratio was high enough, the relatively low PDA content would not be able to glue PVAm/PDA onto the substrate effectively. PVAm was water soluble, and it was thus no surprise that without PDA, PVAm could barely adhere to the substrate securely, resulting in a contact angle (77°) close to that of the pristine substrate. It appeared that a PVAm content of 30-50 wt% in the depositant (solvent-free basis) was appropriate for enhanced surface hydrophilicity of TFC membranes.

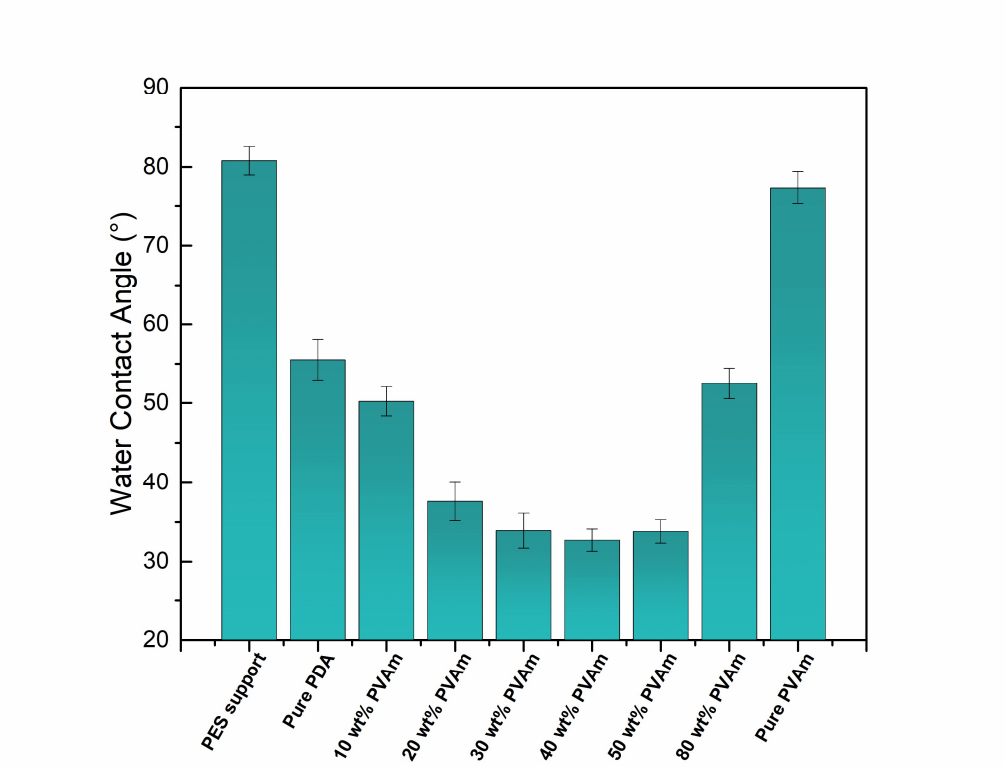

Fig.4.6 Water contact angles of membranes formed using different compositions of dopamine/PVAm depositant. For comparison, the contact angle of pristine substrate membrane was also shown.

Fig.4.7 shows the pure water flux of the TFC membranes measured with de-ionized water at an operating pressure of 1.6 bar after membrane conditioning at 2 bar for 1 h. It was shown that coating the PES substrate with PDA (in the absence of a polyamine) decreased the water flux significantly from 122 to 9.9 L/m^2h. When PVAm was used as a co-depositant, the membrane showed a further slight decrease in the pure water flux with an increase in the PVAm content and then the water flux began to increase when PVAm content was high enough. A minimum water flux was observed at a PVAm content of around 22 wt% (solvent free basis) in the depositing solution (i.e. PVAm/dopamine mass ratio 22/78 by mass). This trend matched with the results of the contact angle measurements. Unlike PVAm, when PEI was used as a co-depositing polyamine, the pure water flux increased continually with an increase in the PEI content in the depositing solution, indicating the adding of PEI to dopamine caused a decreased deposition amount, which is in agreement with the results of the mass gains on the membrane and the appearance of the deposition solutions.

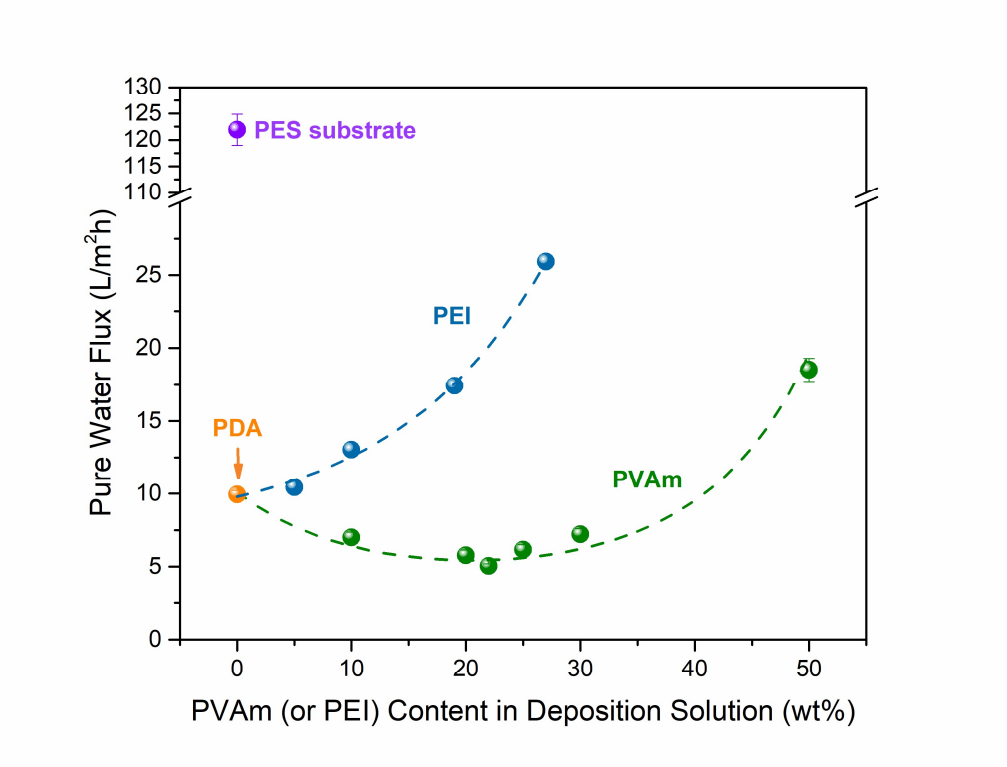

Fig.4.7 Pure water fluxes of the membranes. Polyamine content shown was on solvent free basis.

Fig.4.8 shows the surface morphology of the membranes. Surface pores were visible on the surface of the PES substrate (**Fig.4.8A**). After deposition with PDA, the pores on the substrate were largely covered, but the deposition layer attached to the membrane substrate was not uniform and there were a mass of large aggregates (**Fig. 4.8B**). This was a direct confirmation of the PDA aggregation during the deposition process. These large aggregates on the membrane surface are a potential problem to membrane stability, as they tended to be stripped off more readily by the flowing feed solution. For the surface layer formed by codepositing dopamine and PEI (PEI/dopamine mass ratio 30/70), the deposition was found insufficient to form a uniform coating (**Fig.4.8C**). **Figs.4.8 D, E, F** show the surface morphologies of the deposition layers formed by codepositing dopamine

and PVAm at a PVAm/dopamine mass ratio of 10/90, 30/70 and 50/50, respectively. There were some large aggregates on the membrane surface when the PVAm content was relatively low, and a largely uniform surface coating was formed at a higher PVAm content (i.e., PVAm/dopamine ratio 30/70). If the PVAm content in the co-depositing solution was too high, the amount of the macromolecules deposited and glued to the substrate surface would be compromised due to the small amount of dopamine available, resulting in some substrate pores remain uncovered. These results support the deposition mechanism hypothesized in **Fig.4.4**.

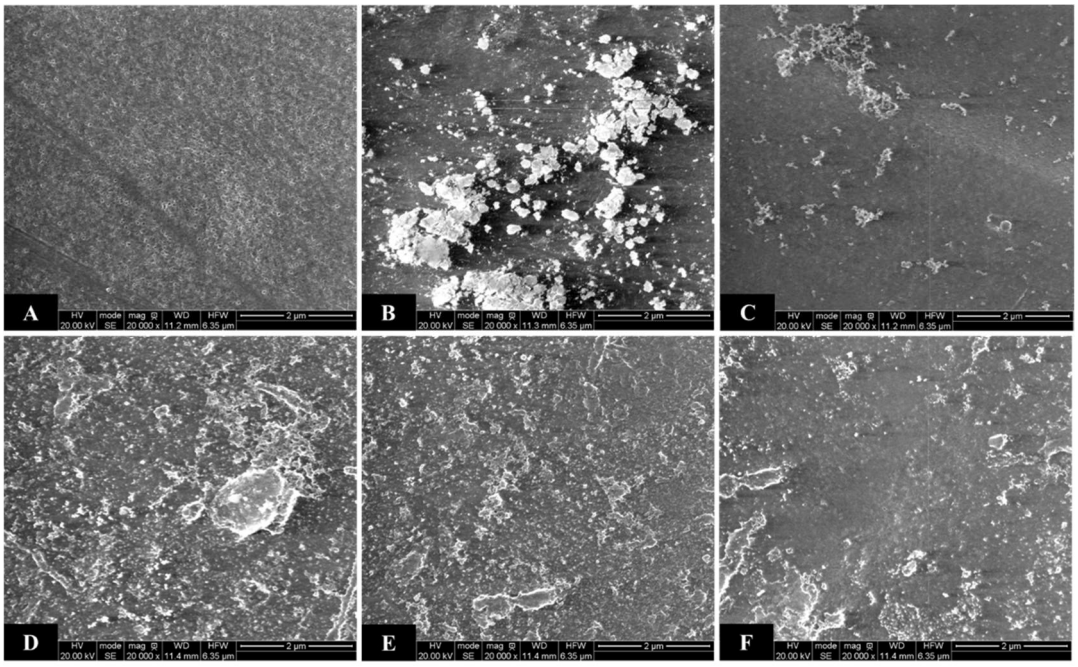

Fig.4.8 SEM images of membrane surfaces. (A) pristine PES substrate, (B) deposition with dopamine, (C) deposition with PEI/dopamine (30/70 mass ratio), and (D-F) deposition with PVAm/dopamine at a mass ratio 10/90, 30/70 and 50/50, respectively.

4.3.3 Pervaporation performance

It should be pointed out that water breakthrough across the membrane was always observed during tests with membranes having a deposited surface layer of PDA or PDA/PEI for pervaporative concentration of the salt solutions, in spite of the zero transmembrane pressure difference. That is, liquid saline water entered the permeate side, presumably driven by the capillary force as a result of the unplugged open pores on the hydrophilic surface. Thus, such membranes were not dense enough to prevent convective flow across the membrane. On the other hand, the TFC membranes consisting of a surface layer formed by co-depositing dopamine/PVAm at appropriate composition were shown to work well for the pervaporation process. **Fig.4.9** shows the water fluxes of the membranes with different contents of PVAm in the co-depositing solution for sweeping gas induced dehydration of a 70wt% KAc solution at 30, 50 and 70°C. Such a high salinity feed was selected to ensure it was below the solubility limit at the temperatures of interest (e.g., 74 wt% at 30°C). At a given temperature, the water permeation flux increased gradually with an increase in PVAm content of the membrane over the range tested (i.e., PVAm/dopamine mass ratio 16/84 to 32/68). This could be attributed, at least in part, to the increased hydrophilicity of the surface layer brought by the PVAm glued to the substrate.

However, it was found that the TFC membranes formed with a PVAm/dopamine mass ratio of 16/84 and 32/68 experienced an increase in water flux as pervaporation proceeded with time at a temperature of 70℃, as shown by the open symbols in **Fig.4.9**. These two membranes showed a 33% and 13% increase in water flux after 18 and 30 h of pervaporation runs, respectively, and liquid feed breakthrough began to occur eventually over a prolonged period. On the other hand, the TFC membranes deposited with a

PVAm/dopamine mass ratio in the range of 20/80 to 30/70 showed no issues about the membrane stability. These results are not unexpected in view of the following: (1) If the PVAm content in the deposition solution relative to dopamine content is too low, the membrane skin layer will be dominated by PDA, and a uniform coating layer can hardly be formed. More importantly, PDA-coated membranes are vulnerable to an alkaline environment (pH 9.8 for aqueous KAc at 70 wt% [120]), and this aspect will be further addressed later. (2) the water-soluble PVAm itself cannot adhere securely to the substrate without dopamine, and dopamine acts to bond PVAm and "glue" it to the substrate surface. If there is too much PVAm in the deposition solution with insufficient dopamine, there will be no adequate "glue" to fix PVAm on the substrate. Further, the PVAm macromolecules that are weakly glued to the substrate are subjected to potential leaching in aqueous solutions at high temperatures. These considerations are consistent with earlier observations that sufficient PDA is needed in the codepositing solution in order to form a membrane dense enough for pervaporation (see **Fig. 4.8F)**. Thus, there appears to exist an appropriate range of dopamine/PVAm mass ratio that is suitable to membrane formation.

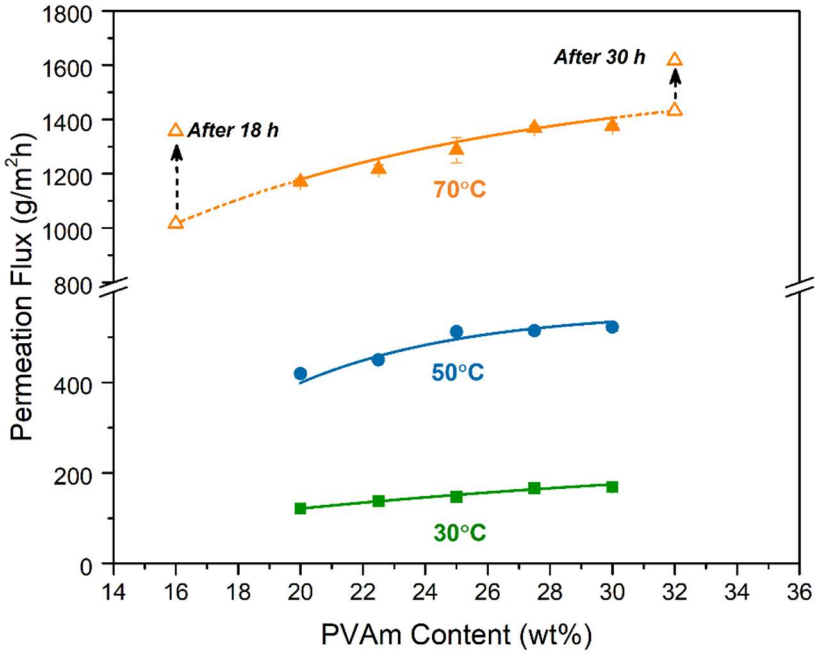

Fig.4.9 Effects of PVAm content in co-depositing solution on water flux of the resulting membranes at different operating temperatures. Feed: 70 wt% KAc solution.

In light of the alkaline characteristics of aqueous KAc solution, it is suspected that membranes with certain relatively high dopamine/PVAm ratios that are unstable for pervaporative concentration of high-salinity KAc solutions at a high temperature may not be unsuitable for processing salt solutions with neutral pHs (e.g., NaCl, LiCl, $LiNO_3$). To validate this hypothesis, TFC membranes were fabricated with a broader range of PVAm/dopamine ratios (6/94 to 35/65) and tested for treating NaCl solutions. The results were presented in **Fig.4.10** for an aqueous solution containing 23.5 wt% of NaCl. It was found that the TFC membranes with a dopamine/PVAm ratio ranging from 10/90 to 32/68 were stable in the pervaporative removal of water from such a highly concentrated NaCl

solution (~90% of the solubility limit). Clearly, the TFC membranes at certain PVAm/dopamine ratios that were too low or too high for use in concentrating basic KAc solutions performed well for concentrating NaCl solutions having a neutral pH. However, outside the range of PVAm content (i.e., 10 – 32 wt% on solvent free basis) mentioned above, the membrane stability would become an issue for use over a prolonged period. For instance, membranes fabricated with a PVAm/dopamine ratio ≤ 6/94 or ≥ 35/65 began to exhibit a gradual increase in water flux over time.

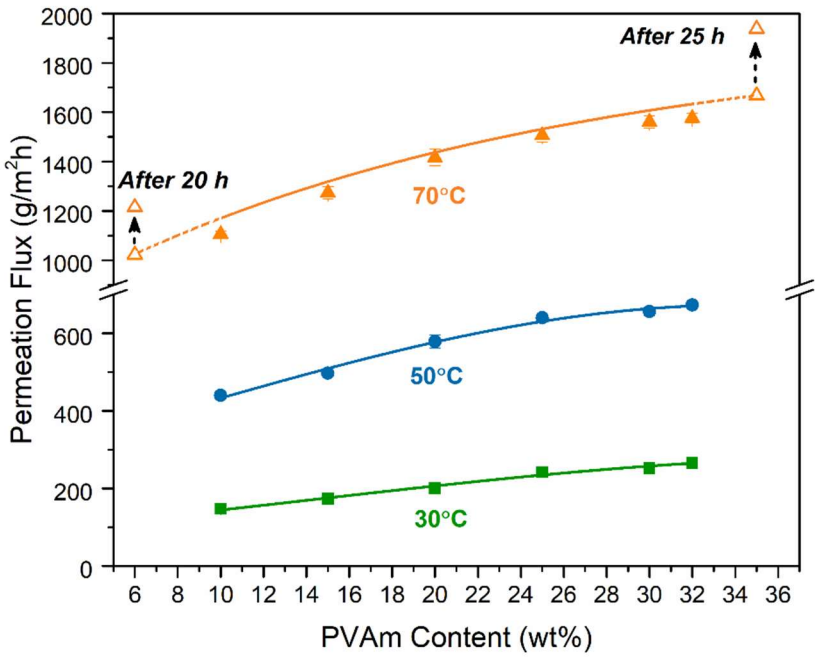

Fig.4.10 Effects of PVAm content in deposition solution on water flux of the resulting membranes. Feed: 23.5 wt% NaCl solution.

4.3.4 Activation energy of permeation

The effects of temperature on the performance of the TFC membranes for concentrating KAc and NaCl solutions at different feed concentrations are illustrated in **Figs.4.11A** and **B**, respectively. The water permeation flux increases with an increase in temperature. As the permeation flux was determined by both the transmembrane driving force for mass transfer and the membrane permeability, it was of interest to evaluate how the temperature influenced the membrane permeability. For TFC membranes where the thin skin layer thicknesses are difficult to determine accurately, permeance is often preferred to characterize the membrane permeability. There is a phase change involved in pervaporation (i.e., liquid feed and permeate vapor). In the case of water permeation, the permeance (P/l) of the membrane to water is customarily evaluated from water permeation flux (J) [110,121,122]:

$$(P/l) = \frac{J}{X\gamma p_w^{sat} - Yp^p} \quad (4\text{-}3)$$

where γ is the activity coefficient of water in the feed solution, p_w^{sat} is the saturated vapor pressure of pure water, X and Y are mole fractions of water in the liquid feed and the gas stream on the permeate side, respectively, and p^p is the pressure on the permeate side.

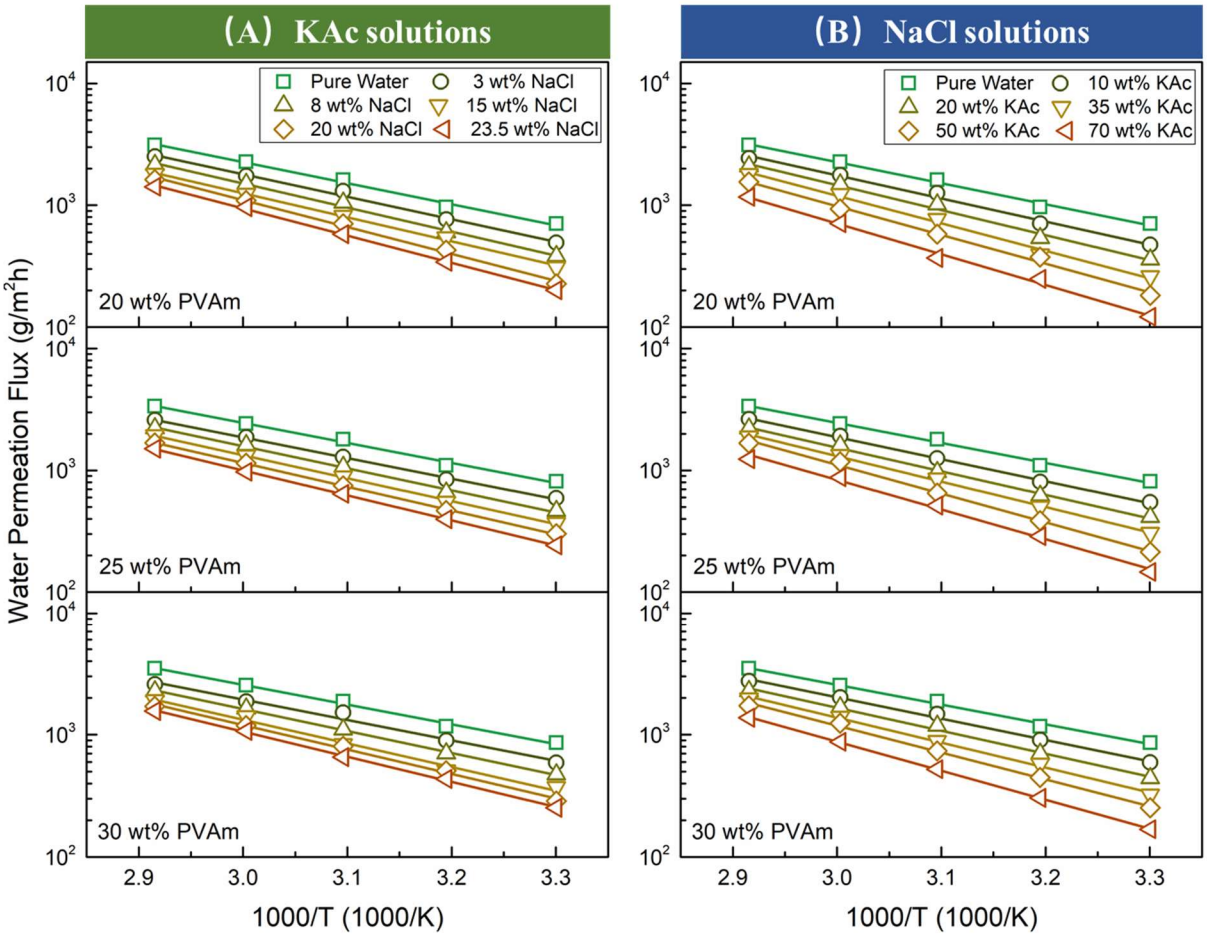

Fig.4.11 Effects of temperature on water flux at different feed salt concentrations for membranes fabricated via co-deposition of PVAm and dopamine at PVAm contents of 20, 25 and 30 wt%. Over the temperature range of interest, the solubility limits of KAc and NaCl in water were 74.7wt%[123] and 26.6 wt% [124], respectively.

Fig.4.12 shows the effects of temperature on the permeance of the TFC membranes to water permeation in concentrating the KAc and NaCl solutions. Clearly, the temperature dependencies of both flux and permeance followed an Arrhenius-type relationship. Thus, the effects of temperature on pervaporation performance can be characterized conveniently in terms of activation energy for permeation, which is usually determined from temperature dependence of permeation flux and/or temperature dependence of membrane permeance

based on the following equations:

$$J = J_0 exp\left(-\frac{E_J}{RT}\right) \quad (4\text{-}4)$$

$$\left(\frac{P}{l}\right) = \left(\frac{P_0}{l}\right) exp\left(-\frac{E_P}{RT}\right) \quad (4\text{-}5)$$

where E_J and E_P are the activation energies for water permeation based on temperature dependencies of water flux and membrane permeance, respectively. The different slopes of the straight lines in **Figs.4.11-12** suggest that the activation energies vary with membranes and feed concentrations. This is understandable when one considers such aspects as the extent of membrane swelling and the thermodynamic behavior of membrane/feed solution systems, which influence water permeation directly. For a given membrane, increasing salt concentration in the feed will reduce membrane swelling, which will affect not only the membrane permeability due to decreased flexibility of the membrane structure but also the heat effects of water sorption into the membrane. By way of illustration, **Fig.4.13** shows the activation energies E_J and E_P as a function of feed salt concentration for the TFC membrane with 30 wt% of PVAm. For purposes of comparison, the salt concentration was expressed in the units of molality in consideration that ionic molality is appropriate for activity and other thermodynamic properties of strong electrolyte solutions. Both E_J and E_P increased with an increase in the feed concentrations (**Fig.4.13A**). This was in agreement with physical reasoning that the membrane became less swollen and more rigid at a higher salt concentration, and the energy barrier to water permeation was consequently higher. Interestingly, the activation energies for pervaporative concentration of KAc and NaCl solutions were very close at a given salt molality of the feed solutions (i.e., at the same mean ionic molality for these two salts). This indicated that water permeation in

response to a temperature variation was not significantly different for these two salt solutions, but it was sensitive to the feed molality.

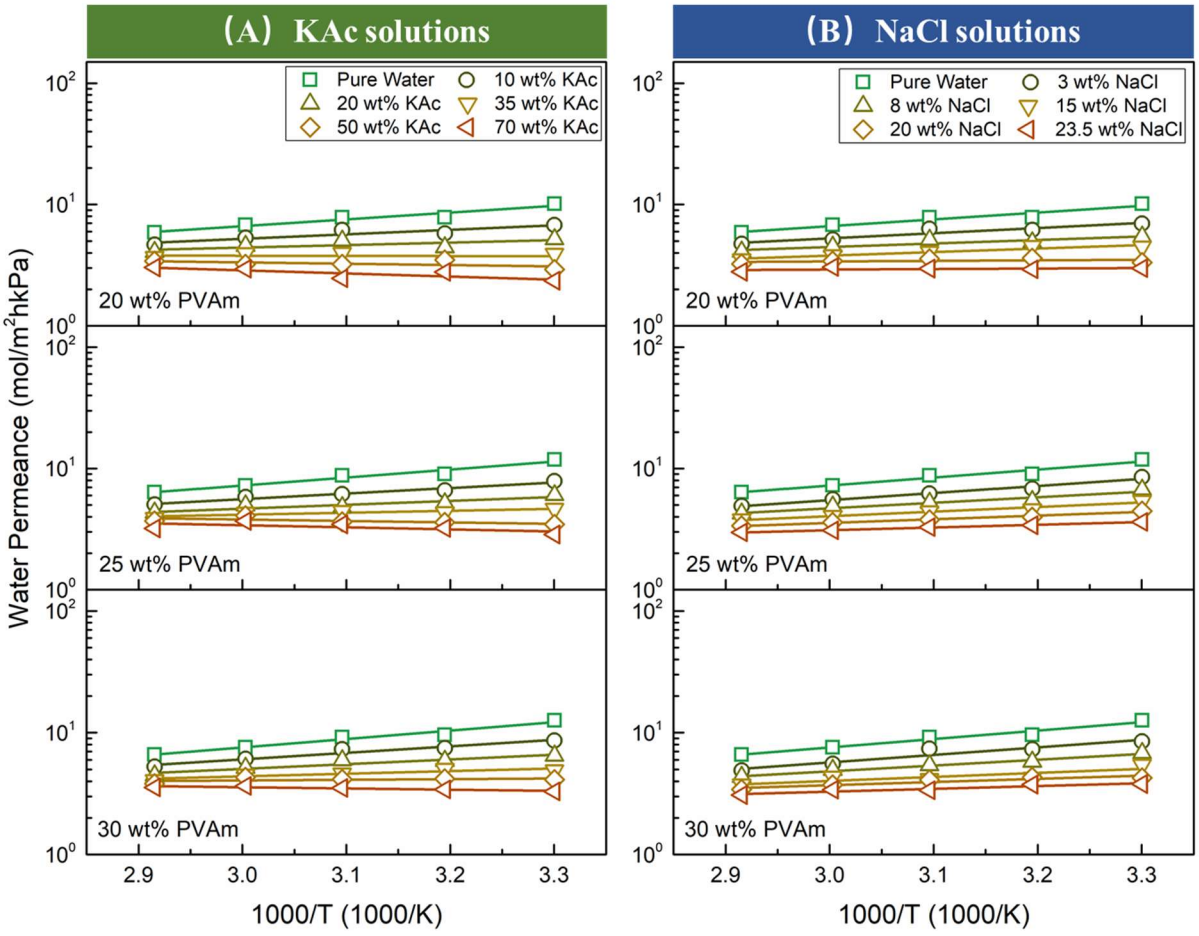

Fig.4.12 Effects of temperature on water permeance at different feed salt concentrations. Other conditions same as in Fig.4.11.

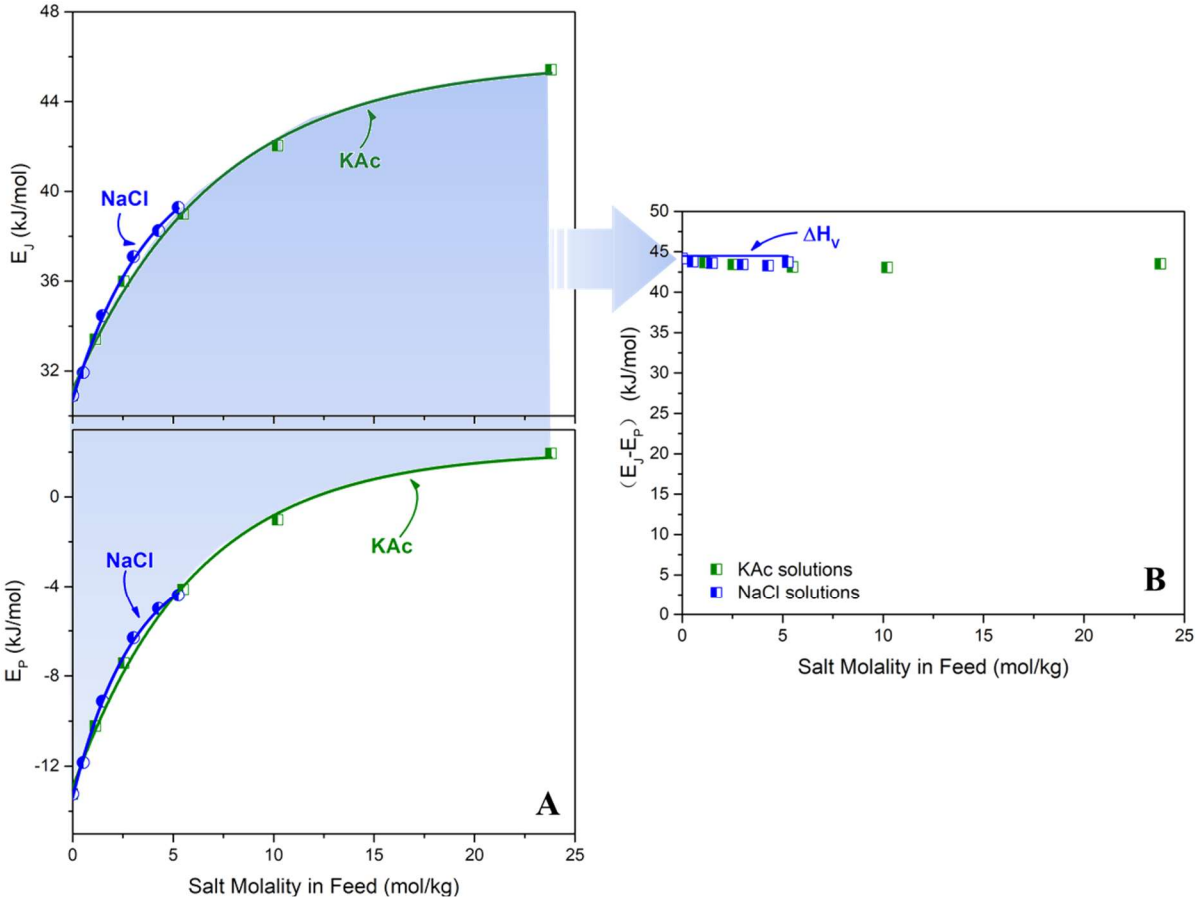

Fig.4.13 E_J and E_P for water permeation vs salt concentration (molal) in feed. Membrane depositing solution contained 30 wt% PVAm. ΔHv is the heat of evaporation of water from NaCl solutions.

While E_J is typically positive, E_P may be positive or negative depending on whether water sorption into the membrane is strongly exothermic. As a matter of fact, E_P is not really an energy quantity, rather it is a combination of the activation energy for diffusion and the enthalpy change due to sorption; the latter is a thermodynamic property determined by the membrane/feed solution system. Thus, a negative E_P will result when an exothermic sorption is affected by temperature more significantly than the diffusivity [125]. From a thermodynamic point of view, it is not unexpected to see a variation in E_P values with the

compositions of the membrane (i.e., PVAm/PDA ratio) and the feed solution. Nonetheless, as rationalized elsewhere [126], the difference between E_J and E_P is often close to the enthalpy change of evaporation of the permeant, i.e., $E_J - E_P \approx \Delta H_v$. This was found to be indeed the case for the pervaporative concentration of NaCl solutions, as shown in **Fig.4.13B**, where the latent heat of evaporation of water from the saline solution was largely constant [127,128]. However, it is not yet clear how well the above relationship applies to pervaporation of KAc solutions since the latent heat of evaporation of water from KAc solutions is not readily available and can hardly be estimated because reliable thermodynamic models for the system are lacking. This is presumably due to the complicated salt-in-water to water-in-salt transition caused by its large compositional range (i.e., high solubility of KAc in water).

Fig.4.14 illustrates how the activation energy for water permeation varies with PVAm content in the depositant used in membrane fabrication. Both E_J and E_P decreased with an increase in the PVAm content. A possible explanation was that increasing the PVAm content increased the hydrophilicity of the membrane, enhancing membrane swelling by the feed solution. As long as the skin layer of the membrane was securely attached to the membrane substrate, the enhanced hydrophilicity of the skin layer also helped to resist the de-swelling effect caused by the salts in the feed. As a result, water permeation was expedited and the energy barrier for water permeation was lowered.

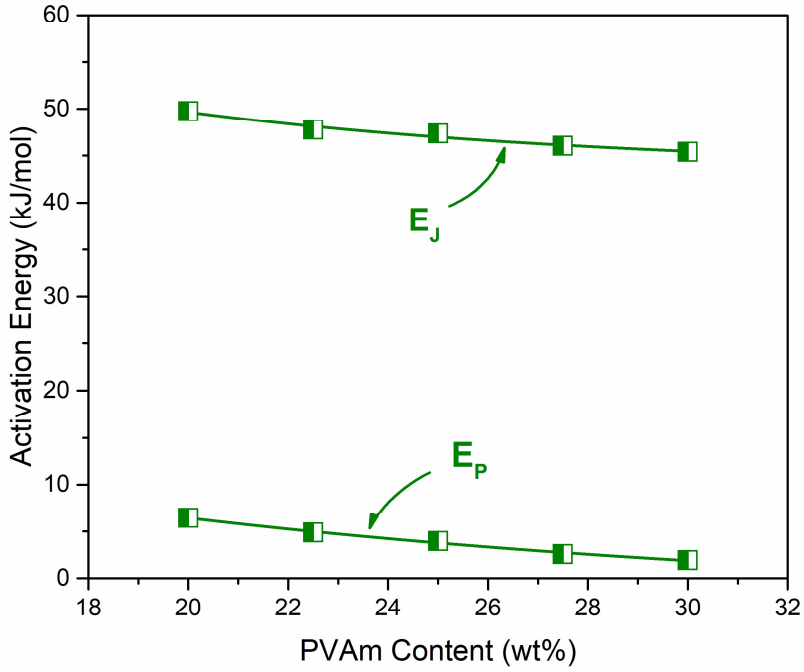

Fig.4.14 E_J and E_P for water permeation through membranes containing different amount of PVAm. Feed: 70 wt% KAc solution.

4.3.5 Membrane stability

To look into how the membrane stability was affected in an alkaline environment, the membranes fabricated with different PVAm contents were exposed to a 0.1 M NaOH solution (pH 13) for different durations. After drying, the water contact angle on the skin layer of the TFC membrane was measured, and the results were presented in **Fig. 4.15**. In the absence of PVAm, the water contact angle of the membrane (i.e., active layer PDA only) increased by 19.2° after 6 h of alkaline treatment, indicating again the instability of PDA in an alkaline environment due to the non-covalent bonds in the PDA structure [77,78]. By co-depositing a proper amount of PVAm, the membrane became more resistant to alkaline attack. For instance, there was only a slight increase in the contact angle (<3.8°) after 6 h

of alkaline treatment when the depositing solution contained 20-30 wt% of PVAm. This may be explained as follows. Due to weak non-covalent bonds among PDA oligomers[7,77,78], they will be negatively charged in an alkaline environment because of the catechol groups. Each catechol group may potentially produce two units of negative charges, and thus the repulsive force tends to break down the weak non-covalent bonds. When PVAm is present in the depositing solution, covalent bonds form between the PDA oligomers and PVAm macromolecules via the Michael addition and Schiff base reaction, the stronger covalent bonding helps retain the PDA/PVAm copolymers. As discussed before, the relative amounts of dopamine and PVAm should be balanced, because a sufficient amount of dopamine is required to glue the copolymer onto the substrate securely. A PVAm/dopamine mass ratio in the range of 20/80 to 30/70 appeared to be appropriate.

The stabilities of the membranes consisting 20 and 30 wt% of PVAm were evaluated for pervaporative concentration of highly concentrated (70 wt%) KAc solution at a temperature of 70℃ over a period of 200 h, and the results were shown in **Fig.4.16**. Both membranes demonstrated good stability for concentrating KAc solutions via sweeping air pervaporation, with essentially a complete rejection of the salts by the membrane even at such a high salt concentration in the feed, as indicated by the low conductivity (<20 μS/cm) of the liquid water collected from the air-swept permeate stream.

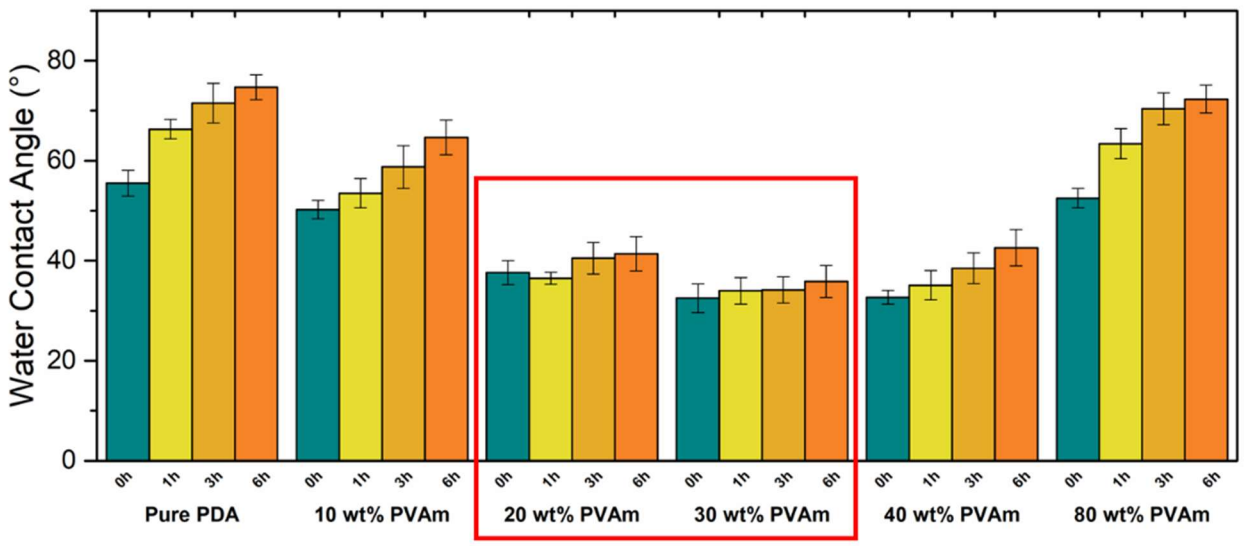

Fig.4.15 Water contact angle on membranes with different PVAm contents in dopamine/PVAm co-depositing solutions after alkaline treatment with 0.1 M NaOH solution for different durations.

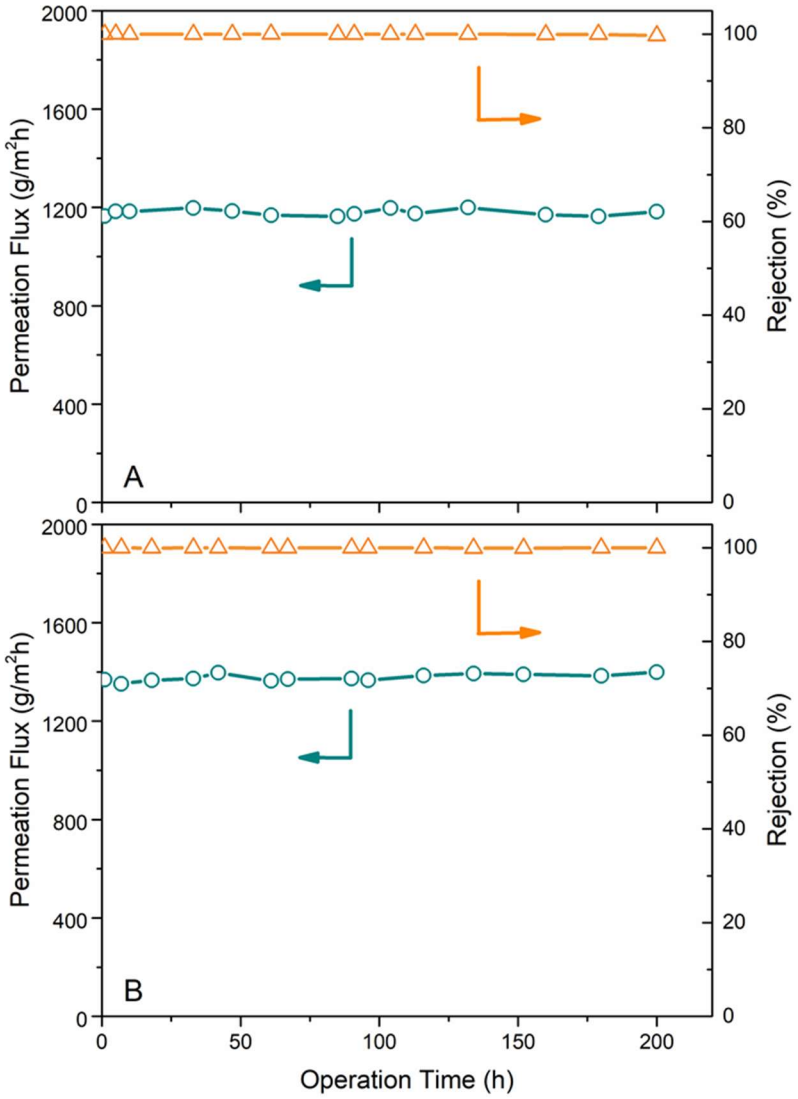

Fig.4.16 Demonstration of membrane stability for pervaporative removal of water from 70 wt% KAc solution at 70°C. Membranes

(A) PVAm/dopamine mass ratio 20/80; (B) 30/70.

4.4 Conclusions

In this work, we proposed to use PVAm as a co-depositant with dopamine to fabricate TFC membranes to take advantage of the covalent bonding between polydopamine and PVAm and the adhesive properties of PDA oligomers. The membranes were investigated for concentrating KAc solutions via sweep air pervaporation. Incorporating an appropriate amount of PVAm into the membrane was found to improve both the hydrophilicity and stability of the membrane. For pervaporative concentration of KAc solutions, a PVAm content of 20-30 wt% (solvent free basis) in the depositing solution was found to be optimal, and the membrane showed a water flux of 1.2 – 1.4 $kg/m^2.h$ at a high salt concentration of 70 wt% in the feed solution, with essentially a complete retention of the salt. In addition, the mass growth rate of the membrane skin layer during membrane formation via codeposition of the PVAm/dopamine onto a substrate membrane was determined as well; not only was such information important to membrane fabrication, it also helped provide an insight into the general behavior of dopamine adhesion and polymerization in surface engineering.

Chapter 5

Pervaporative concentration of KAc solution using a TFC hollow fiber membrane fabricated via the co-deposition of polyvinylamine/polydopamine

5.1 Introduction

Dopamine is a versatile and bio-glue that can be readily coated on virtually all surfaces through oxidative polymerization, and it has gained increasing attention for surface modifications over the past few years [1,2,85,121,129]. It has recently been found that surface deposition of dopamine along with a second polymer can be advantageous to the surface properties of the coating layer formed (e.g., enhanced hydrophilicity, stability in alkaline environment) [96]. The co-deposition approach has also been applied to membrane fabrication and modification [5,7]. By co-depositing polyvinylamine (PVAm) and dopamine on a flat sheet polyethersulfone (PES) substrate, a composite thin film composite membrane was prepared for concentrating KAc solutions via air-sweep pervaporation, and essentially a complete solute rejection was achieved even at high feed concentrations [130]. The membrane displayed a significantly improved stability in alkaline environment compared to membranes formed with dopamine only. However, it was noticed that for sweeping gas pervaporation, water crossover through the membrane

could gradually occur after system shutdown as a result of capillary condensation and pore wetting in hydrophilic microporous substrate. Once the substrate pores are filled with liquid water, salt diffusion to the permeate side will occur, causing salt crossover. This is apparently detrimental to pervaporation performance when pervaporation is resumed. The salt residue on the walls of the substrate pores will further facilitate capillary condensation and pore wetting, making liquid crossover more significant. Using a hydrophobic substrate appears to be appropriate from a standpoint of minimizing liquid crossover.

However, from a membrane formation point of view, depositing a hydrophilic polymer (e.g., PVAm) onto a hydrophobic surface is challenging because a thin layer of air/vapor (the so-called "depletion layer") may form between the hydrophobic surface and the aqueous depositing solution, impacting the binding of the hydrophilic depositant with the surface [21–24]. As one may expect, adding a water-miscible organic solvent that has a good wettability on the hydrophobic surface to the depositing solution will help overcome this problem. Indeed, Sundaram et al. [26] used methanol as a co-solvent in coating highly hydrophilic poly(carboxybetaine methacrylate) onto Teflon and other hydrophobic surfaces. Yue et al. [25] used ethanol/water mixtures as a solvent for self-polymerization of dopamine to improve the coating of polydopamine on superhydrophobic carbon nanotubes, which resulted in enhanced dispersion of the modified CNTs in aqueous solutions. However, too high a content of alcohol in the dopamine solution may suppress

its polymerization [131–134]. Therefore, the alcohol content in the solution is important and should be properly controlled.

In the present work, methanol/water mixtures were used as solvent for co-deposition of PVAm with dopamine onto a poly(vinylidene fluoride) (PVDF) hollow fiber substrate, where methanol was used to improve deposition of hydrophilic solutions on the PVDF substrate and dopamine was used to retain PVAm in place. The resulting hollow fiber membranes with a hydrophilic skin layer and a hydrophobic substrate was used for pervaporative concentration of KAc solutions. The water contact angle (WCA) on PVDF surface is normally higher than 95° [27,88,135]. Methanol was chosen as a cosolvent in preference over ethanol due to its higher polarity. In addition, according to some previous works, deposition of PDA is less affected by the hydrophobicity of the target surface, ascribed to the aromatic ring in PDA structure which could attach to hydrophobic surfaces through hydrophobic interaction [22,27]. Therefore, the effect of postponed adding of PVAm on the overall deposition density was also investigated in this work, considering the initial coated PDA could create a hydrophilized surface with abundant functional groups for the subsequent co-deposition of PVAm and dopamine. The resulting TFC hollow fiber membranes were applied to the sweeping gas pervaporative concentration of highly concentrated salt (KAc and NaCl) solutions. The membrane performance in terms of flux, permeance, and activation energy were reported. In addition, investigations on how the

methanol content and postponed time of adding PVAm affect the co-deposition of PVAm and dopamine were also conducted. To elucidate the advantages of using methanol cosolvent for codeposition of PVAm/dopamine in fabrication of a hydrophilic active layer on a hydrophobic hollow fiber substrate, membranes were also fabricated using water alone as the solvent for PVAm/dopamine codeposition. In addition, a pre-coating of dopamine to hydrophilize the surface of the substrate prior to codepositing PVAm/dopamine was also attempted to improve the membrane performance.

It may be mentioned that such hollow fiber membranes offer many advantages in membrane formation and application: (1) The deposition of the active skin layer on the hollow fiber substrate surface can be carried out in bundles, which is easily upscalable. (2) Instead of the conventional shell-and-tube configuration, a shell-less module design may be used where the hollow fiber bundle is submerged in the feed solution while the sweeping gas flow through the fiber lumina via tubesheets, which helps minimize module fabrication cost. The latter design is also convenient for membrane cleaning if needed. (3) The tubesheets may be formed on the hollow fiber substrate prior for easy handleability, followed by deposition of the active surface layer, thereby completing membrane formation. In view that the majority of pervaporation membranes are flat sheets, which require external supporting spacers in module assembly, the present study is expected to provide an insight into hollow fiber membranes for pervaporative concentration of KAc solutions.

5.2. Experimental

5.2.1. Materials

Microporous hollow fiber PVDF membrane (nominal pore size 0.3 μm, inner and outer diameters 0.7 and 1.3 mm, respectively) provided by Zhaojin Motian Membrane Company was used as the substrate. Dopamine hydrochloride, tris(hydroxylmethyl) aminomethane (Tris) and methanol were supplied by Sigma-Aldrich, and PVAm (Lupamin 1595, Mw 10,000) was kindly supplied by BASF. De-ionized water was used in preparing all aqueous solutions. For comparison purposes, both KAc (supplied by Sigma-Aldrich) and NaCl (purchased from EMD Chemicals) solutions were tested for pervaporation concentration of high salinity solutions.

5.2.2. Preparation of TFC hollow fiber membranes

The hollow fiber substrate membranes were made into small elements by bundling hollow fibers together and potted with epoxy at the ends. The PVAm/PDA composite membranes were prepared under four protocols, as listed in **Table 5.1**, to illustrate the advantage of co-depositing PVAm/PDA using cosolvent water/methanol with a dopamine pre-coating.

Table 5.1. Membrane fabrication protocols.

Protocol	Solvent for co-depositing dopamine/PVAm	Pre-coating of dopamine

W	Water	No
WM	Water + methanol	No
Wp	Water	Yes
WMp	Water + methanol	Yes

Note: To avoid unnecessary rinse, solvent for dopamine pre-coating was the same as solvent for subsequent co-deposition of dopamine/PVAm.

Under protocol W, membranes were prepared by co-deposition of PVAm and dopamine dissolved in water. A pre-determined amount of PVAm was dissolved in a Tris buffer solution (15 mM). After the solution pH was adjusted to 8.5 - 8.8 with hydrochloric acid, dopamine hydrochloride was added to the solution under agitation, followed by immediately submerging the hollow fiber substrate element into the solution to initiate codeposition of PVAm/PDA. Care was exercised such that only the outer surfaces of the hollow fibers were exposed to the solution. The total concentration of the depositant in the solution was kept at 2 g/L (1.4 g/L of dopamine and 0.6 g/L of PVAm, unless specified otherwise). After a deposition time of 12 h, the membrane element was removed from the depositing solution and rinsed thoroughly with de-ionized water.

To demonstrate the advantage of using methanol as a cosolvent in membrane formation, Protocol WM was used in membrane fabrication, which was the same as Protocol W except that mixed solvents of water and methanol at different ratios were used. To further facilitate membrane formation, a pre-coating of dopamine was used as well prior

to dopamine/PVAm disposition with and without using methanol as a cosolvent (Protocols WMp and Wp, respectively). In all cases, the dopamine solution (concentration 1.4 g/L) for pre-coating and the dopamine/PVAm solution for subsequent co-deposition were prepared by dissolving the depositant in a 15 mM Tris solution, with the solution pH being adjusted to 8.5 - 8.8 using hydrochloric acid. For easy comparison, the overall deposition time was kept at 12 h and the volume of the disposition solution was ~5 mL per cm^2 of substrate area in membrane fabrication.

5.2.3. Characterization of the deposition solutions using UV-Vis spectrophotometry

The kinetics of the dopamine polymerization in the different solutions were investigated using a UV-Vis spectrophotometer (Shimadzu UV-1900i). The variations in the UV-Vis spectra of the dopamine solutions, which were exposed to the air, was monitored over a period of 24 h. A syringe fitted with an in-line filter was used for sampling in the spectrophotometric analysis, and the absorbance at a wavelength of 420 nm was used as an indicator of PDA content formed in the solution [8,103].

5.2.4. Weight gain on membrane surface

The rate of growth of the active layer on the substrate surface was evaluated

gravimetrically. The amounts of the depositant attached to the substrate at different deposition times were determined from the difference between the weight of the membrane after drying in a vacuum oven at 70℃ for 20 min and the weight of the substrate used in the membrane formation, and the weight gain per unit outer surface area of the substrate was used as a measure of the amount of the active membrane layer formed on the substrate.

5.2.5. Membrane performance

Sweeping gas pervaporation tests were carried out to evaluate the performance of the hollow fiber membranes. As illustrated in **Fig.5.1**, the feed solution was stocked in a tank that was thermostatted using a heating mantle and a thermo-regulator. The hollow fiber membrane bundle, with tubesheets cut open at both ends, was gently bent in a U-shape and submerged in the feed solution. The effective area of the membrane for permeation was 46.5 cm^2. Dry air at a flow rate of 7 L/min was continuously admitted to the lumen side of the hollow fibers to sweep the permeated water vapor and carry it into a cold trap, where water vapor was condensed and collected. The feed water removed due to permeation was compensated after each run by adding an equal amount of de-ionized water to the feed tank.

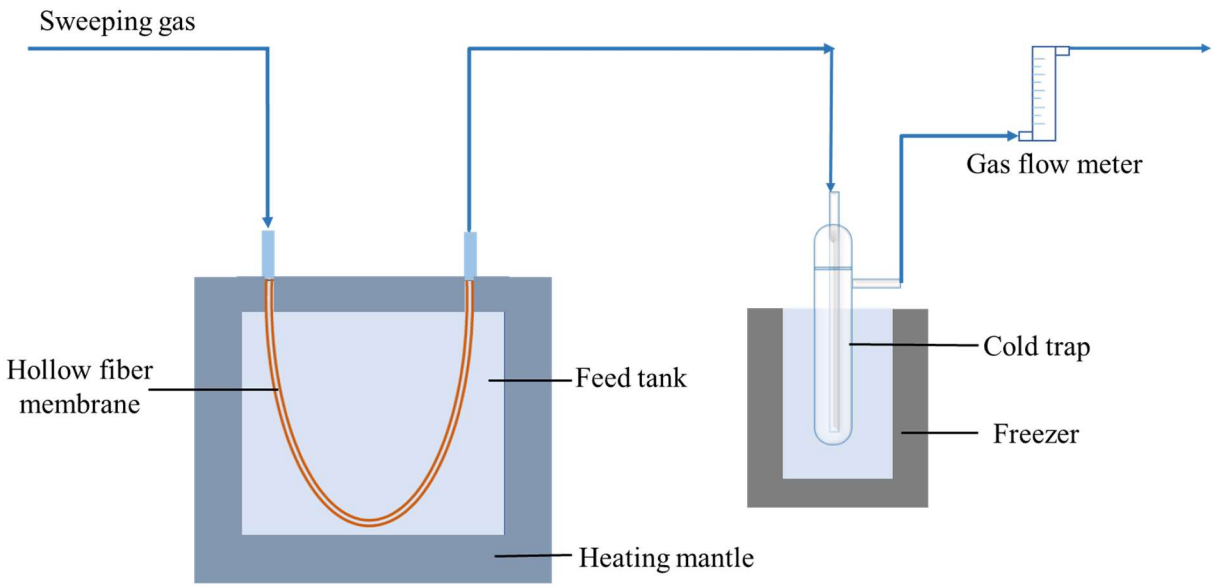

Fig.5.1. Schematic of pervaporation experiments with hollow fiber membranes.

The permeation flux (J) was calculated from the weight of water collected over a given period of time:

$$J = Q/A\Delta t \quad (1)$$

where Q is the weight of water collected from the permeate over a period Δt, and A is the effective membrane area for permeation. The salt concentration in the permeate water (C_p) was measured a conductivity meter (WTW inoLab Cond Level 2), and the salt rejection (R) was evaluated from

$$R = (C_f - C_p)/C_f \times 100\% \quad (2)$$

where C_f is the salt concentration in the feed solution. All pervaporation experiments were repeated at least three times, and the average data was reported.

5.3. Results and Discussion

5.3.1. Use of methanol as a cosolvent for dopamine/PVAm polymerization

Co-depositing PVAm and dopamine to facilitate attachment of PVAm on a hydrophilic surface by taking advantage of adhesive characteristics of dopamine was found to be effective in building up the active membrane layer [9]. We attempted to apply the same approach to fabricating a thin selective layer on a porous PVDF hollow fiber substrate. However, it was found that the surface layer growth on the hydrophobic substrate was compromised in terms of the growth rate and the amount eventually attached, in spite of the surface binding capability of dopamine on all surfaces. This was not surprising in view of the hydrophilic nature of PVAm. Thus, methanol was used as a co-solvent along with water for the depositing solutions to enhance surface wetting with the solution. In view that too much alcohol in the solution might suppress self-polymerization of dopamine[25,131], the appropriate amount of methanol in the solvent was determined. This was done by looking into the weight gains on the substrate at different methanol contents in the deposition solutions, and the results were presented in **Fig. 5.2**. The deposition time was kept at 12 h in all conditions unless otherwise indicated. The weight gains due to deposition of the macromolecules increased initially with an increase in methanol content in the solvent and then it started to drop when the methanol content was high enough, resulting in a maximum weigh gain at a methanol content of around 10 vol% (i.e., methanol/water

volume ratio 1:9).

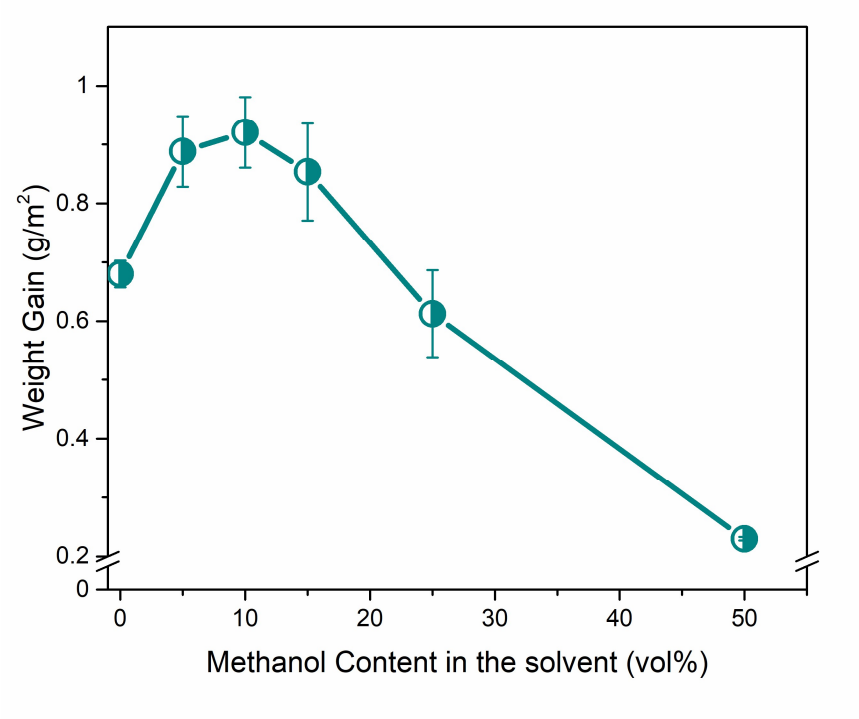

Fig. 5.2. The weight gain of the membrane vs methanol content in the solvent.

It was interesting to observe that when the methanol content in the solvent was relatively high, aggregates were gradually formed in the depositing solution, whereas the solution remained homogenous in the absence of methanol. This is illustrated in **Fig. 5.3**, where the appearances of the dopamine/PVAm solutions with different methanol contents over time were shown. Similar to the dopamine/PVAm/water mixture (**Fig. 5.3A**), the solution containing 10 vol% methanol was also homogenous over a time window of 24 h (**Fig. 5.3B**) though it became darker a little bit slower. However, at a methanol content to

25 vol%, the aggregate formation was visible at 6 h and the aggregates eventually settled at the bottom (**Fig. 5.3C**). The aggregates formation and precipitation were more pronounced in the dopamine/PVAm solution at 50 vol% methanol (**Fig. 5.3D**). The effects of alcohols on the self-polymerization of dopamine have been reported [25,131,132], and it is commonly considered that the alcohol can trap radicals and hence inhibit dopamine conversion to quinone, a key step in dopamine polymerization [25,136]. When aggregates are formed in the deposition solution prior to adhesion to the membrane substrate securely, the membrane skin layer formation as reflected by the weight gains will be compromised. Our previous study showed that the presence of PVAm helped reduce the aggregate formation in aqueous dopamine solution as a result of the large quantity of amines in PVAm [130]. However, with the addition of methanol, the polarity of the solvent was reduced, thereby affecting PVAm solubility in the solution negatively. Moreover, the solvent with a lower polarity will affect chain stretching of PVAm macromolecules due to restricted dispersion of the polar amine groups. The results shown in **Figs. 5.2** and 5.**3** suggested that a methanol content of 10 vol% was appropriate for membrane formation when a mixed water/methanol solvent was used in dopamine/PVAm deposition.

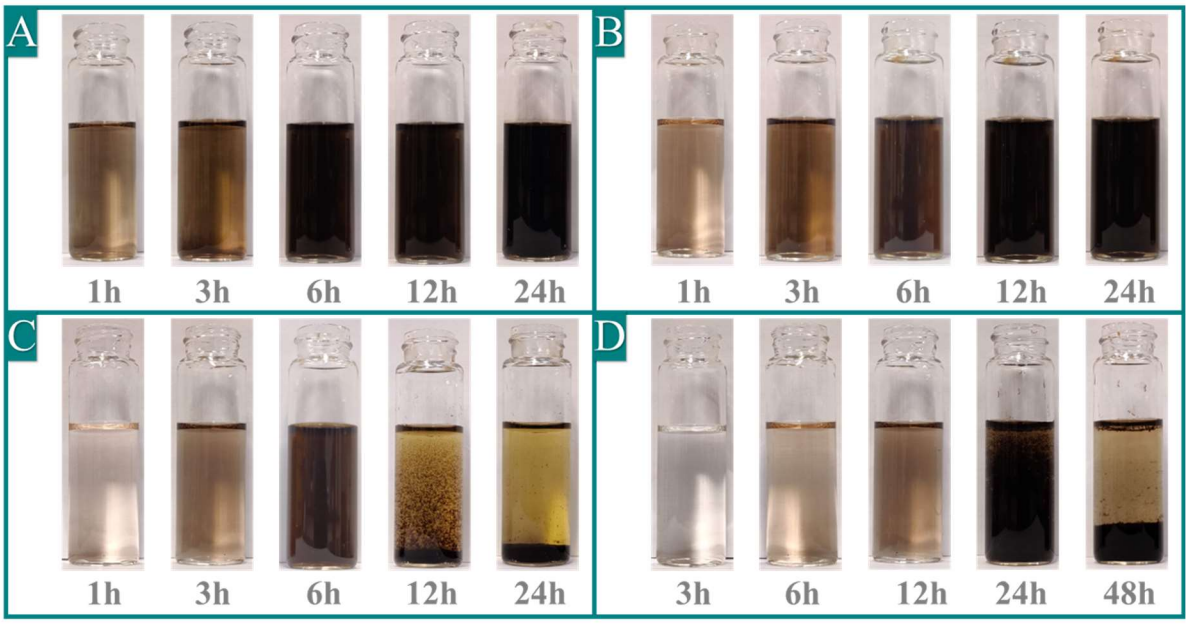

Fig. 5.3. The appearance of dopamine/PVAm solution over time with different methanol content in the solvent(vol%). (A) 0 (pure water), (B) 10, (C) 25, (D) 50.

The dopamine/PVAm solutions were also characterized using UV-Vis spectrophotometry, and the results were presented in **Fig. 5.4**. Note that an in-line filter was used in the sample analysis to remove any aggregates formed in the solution. It was shown that PDA formation in the solution was suppressed by the presence of methanol, and the membrane formation would be compromised if methanol content was sufficiently high. In general, the absorbance data were consistent with the aforementioned weight gains on membrane substrate and changes in appearance of the solution. While a small amount of methanol helps with deposition of dopamine/PVAm onto a hydrophobic surface, its

negative effects on dopamine polymerization and accompanying aggregates formation are unfavorable to bond PVAm macromolecules to the substrate by means of adhesive polydopamine. A cosolvent of water/methanol with 10 vol% methanol was used subsequently in fabricating membranes, which was shown to be advantageous to membrane formation in comparison with using water only as the solvent.

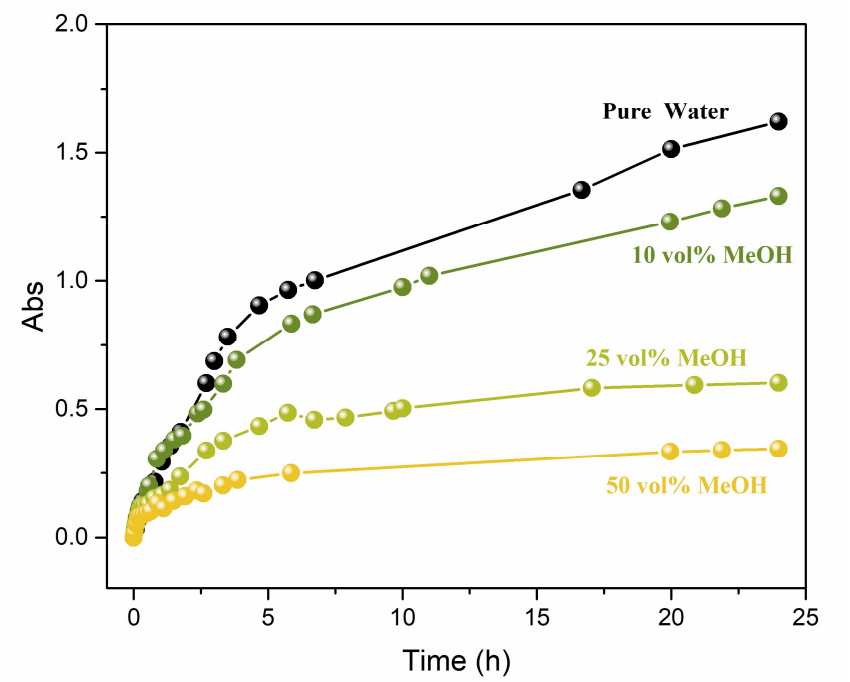

Fig. 5.4. UV-Vis absorbance of dopamine/PVAm solutions at different methanol contents. Wavelength 420 nm.

5.3.2. Pre-coating with dopamine

It has been reported that although dopamine is hydrophilic, its deposition on

hydrophobic surfaces is rather unaffected [22,27]. Therefore, it was proposed to pre-coat dopamine as a primer to form a hydrophilic binding layer that would be better prepared for PVAm/dopamine deposition. This is illustrated in **Fig. 5.5**; the prime coat of PDA is expected to yield a hydrophilic surface with functional groups that help anchor PVAm macromolecules along with dopamine in the dopamine/PVAm solution. This is supported by the weight gains shown in **Fig. 5.6**, where the total deposition time (pre-coating with dopamine and subsequent co-deposition of dopamine/PVAm) was kept constant (12 h) for easy comparisons. Clearly, in comparison with membrane preparation Protocol WM involving co-deposition of dopamine/PVAm only (denoted by * in **Fig. 5.6**), pre-coating of dopamine (Protocol WMp) was effective to facilitate membrane formation. A maximum deposition amount was observed with a dopamine pre-coating of 3 h, and membranes were thus prepared under such conditions (denoted by ** in **Fig. 5.6**) in subsequent studies for further evaluation of separation performance. **Fig. 5.7** shows a comparison of the effectiveness of the four protocols for surface layer growth during membrane formation. With Protocol WMp, the weight gain on the substrate surface was more than twice that with Protocol W. Clearly, precoating of dopamine and using cosolvent in the membrane fabrication were effective for membrane buildup on the hydrophobic substrate.

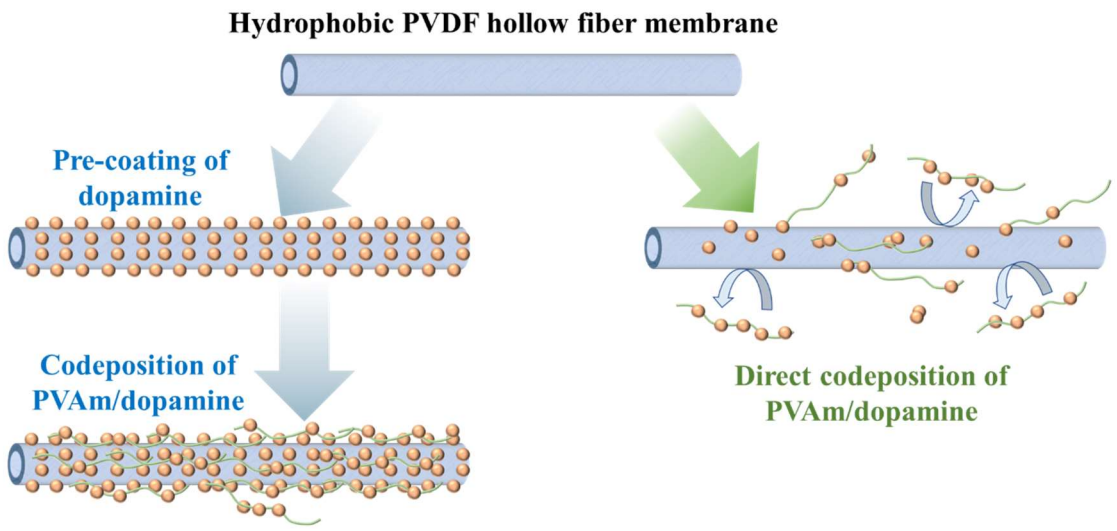

Fig. 5.5. Illustration of how precoating dopamine helps subsequent co-deposition of dopamine/PVAm.

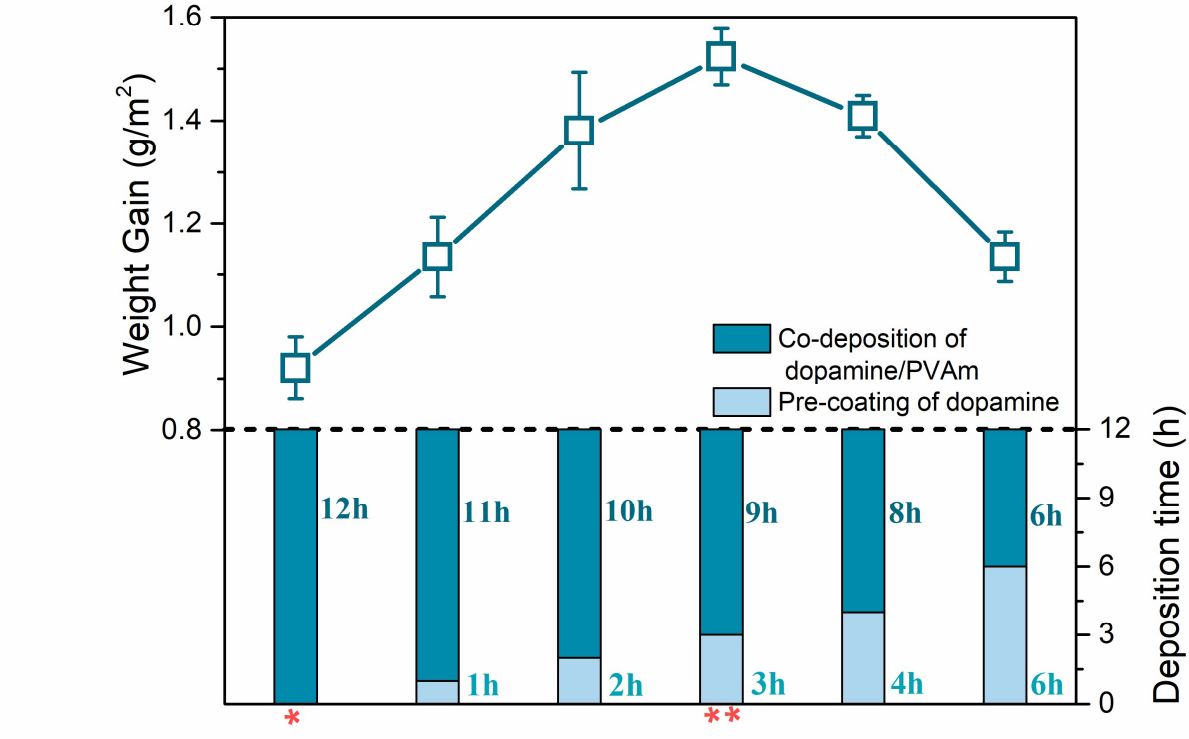

Fig.5.6. Surface layer formation as represented by weight gains in the membrane to

illustrate the advantage of dopamine pre-coating prior to co-deposition with dopamine/PVAm. Solvent, water/methanol (90/10 in vol).

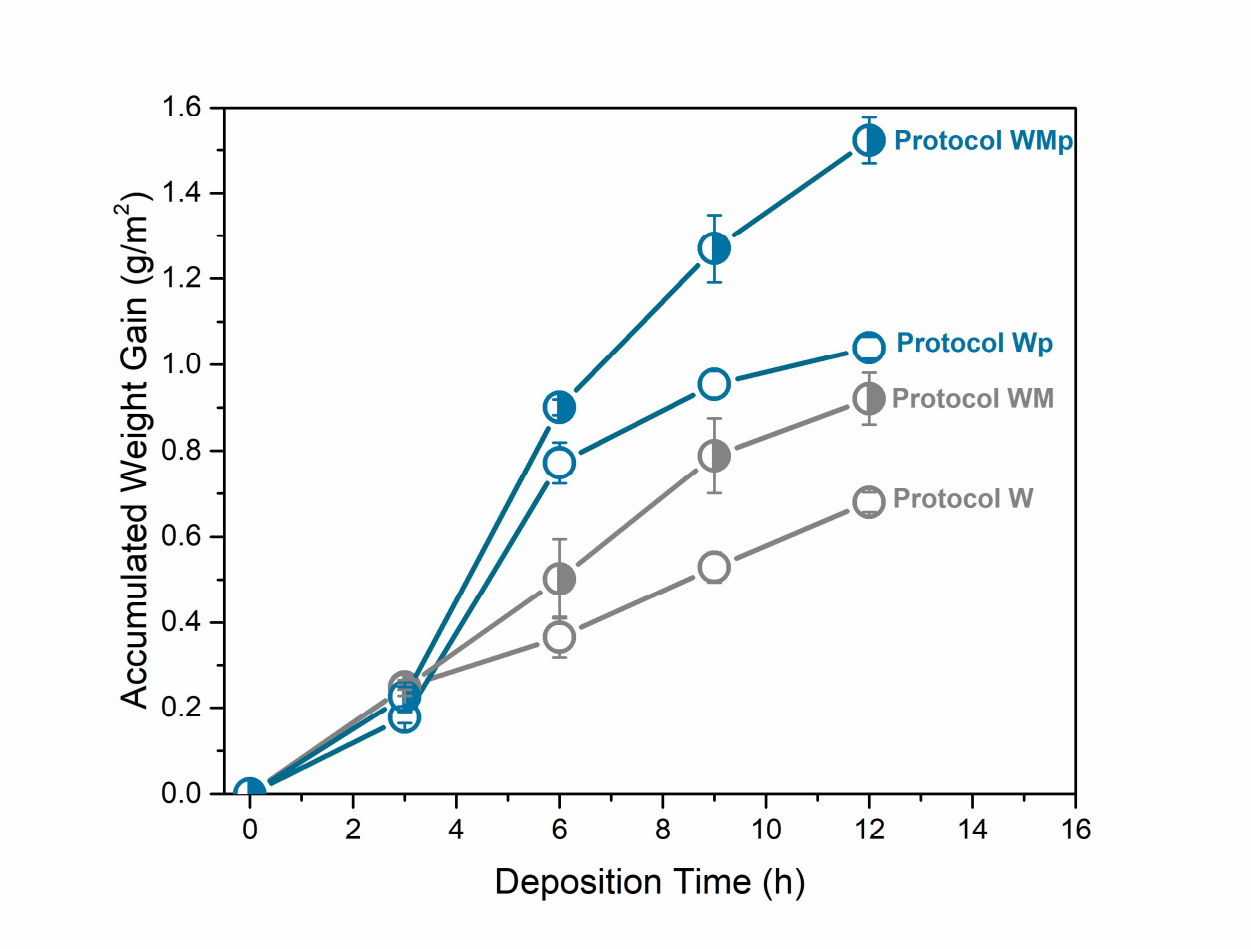

Fig.5.7. Accumulated weight gains during membrane formation. The deposition time includes dopamine pre-coating (3 h) if relevant. The PVAm/dopamine mass ratio was 30/70 in co-deposition solution, and water/methanol composition was 90/10 (in vol) when cosolvent was used.

5.3.3. Pervaporative concentration performance

Fig. 5.8 illustrates the temperature dependence of water permeation flux in concentrating KAc and NaCl solutions at different feed concentrations. In all cases, an essentially complete salt retention was achieved with the membrane, as shown by the low conductivity (<50 μS/cm) of the liquid water collected from the air swept permeate stream, even at high salt concentrations (70 wt% KAc, and 23.5 wt% NaCl) that were close to their solubility limits in the feed. Here, the concentration of NaCl solutions was also carried out to see how the membrane performed for neutral pH solutions in comparison to weakly alkaline KAc solutions. In addition, the PVAm/dopamine ratio in co-deposition solution was varied from 20/80 to 30/70 (in wt) to illustrate that Protocol WMp also worked well at lower PVAm/dopamine ratios. However, in the latter cases, the water flux tended to be lower. As one may expect, increasing dopamine content and/or decreasing PVAm content in the co-deposition solution will lead to a less amount of PVAm macromolecules securely attached to the membrane substrate by the increased amount of adhesive dopamine, making the membrane less permeable. In general, the water flux increased with an increase in the operating temperature, attributing to the increased driving force for mass transfer and enhanced thermal motion of the polymer chains. The temperature dependences of water was fit to an Arrhenius-type relation:

$$J = J_0 \exp\left(-E_J/RT\right) \quad (5.1)$$

where J is water flux, J_0 is the pre-exponential factor for the process, E_J is the apparent activation energy for water permeation that has accounted for temperature influence on transmembrane driving force for water permeation, R is the ideal gas constant, and T is the absolute temperature. To look into how the temperature affected the membrane permeability, the permeance (*P/l*) of the membrane, which was equal to water flux normalized by the mass transfer driving force, was evaluated:

$$(P/l) = J/\Delta P = J/(X\gamma p^{sat} - Yp^{p}) \quad (5.2)$$

where γ is the activity coefficient of water in the feed solution, X and Y are mole fractions of water in the feed solution and permeate vapor, respectively, and p^{sat} and p^{p} are the saturated water vapor pressure on the feed side and the permeate pressure, respectively. As shown in **Fig. 5.9**, the temperature dependence of the membrane permeance also followed an Arrhenius type of correlation:

$$(P/l) = (P_0/l)\exp(-E_P/RT) \quad (5.3)$$

where the intrinsic activation energy (E_P) for permeation can be obtained. As an illustration, **Fig. 5.10** shows the E_J and E_P values as a function of feed salt content for KAc and NaCl concentrations; for ease of comparison, the feed concentration was expressed in terms of molarity. Both E_J and E_P increased with an increase in salt concentration in the feed, which may be attributed to deswelling of the membrane caused by the salts that results in a more rigid membrane structure. Consequently, the activation energy, which is a

representation of the energy barrier to water permeation in the membrane, increased.

Based on the solution-diffusion model, E_P is mainly determined by the activation energy for diffusion (E_D) and the heat of mixing due to sorption (ΔH_S). The diffusion of water molecules in the membrane is an activated process that is facilitated at a higher temperature, and thus E_D is typically positive. On the other hand, a higher temperature favors escape of water molecules from the membrane, and thus ΔH_S is usually negative. Therefore, E_P may be positive or negative depending on whether the temperature effect on diffusion or sorption is more dominant. As a first approximation, E_P is normally close to E_J minus the heat of evaporation of the permeant (ΔH_v) [126]. This was found to be indeed the case for pervaporative concentration of NaCl solutions, as shown in **Fig. 5.10B**, where the ΔH_v for water evaporation remained approximately constant over the concentration range [127,128]. Unfortunately, no experimental data or model predictions were found in the literature for the heat of evaporation of water from KAc solutions. KAc has a high solubility in water, and the solution thermodynamic behavior is complicated due to transition of salt-in-water to water-in-salt over a broad range of concentrations. Nonetheless, the data in **Fig. 5.10B** show that although the E_J and E_P for the two salt solutions are different, their (E_J - E_P) values are rather close.

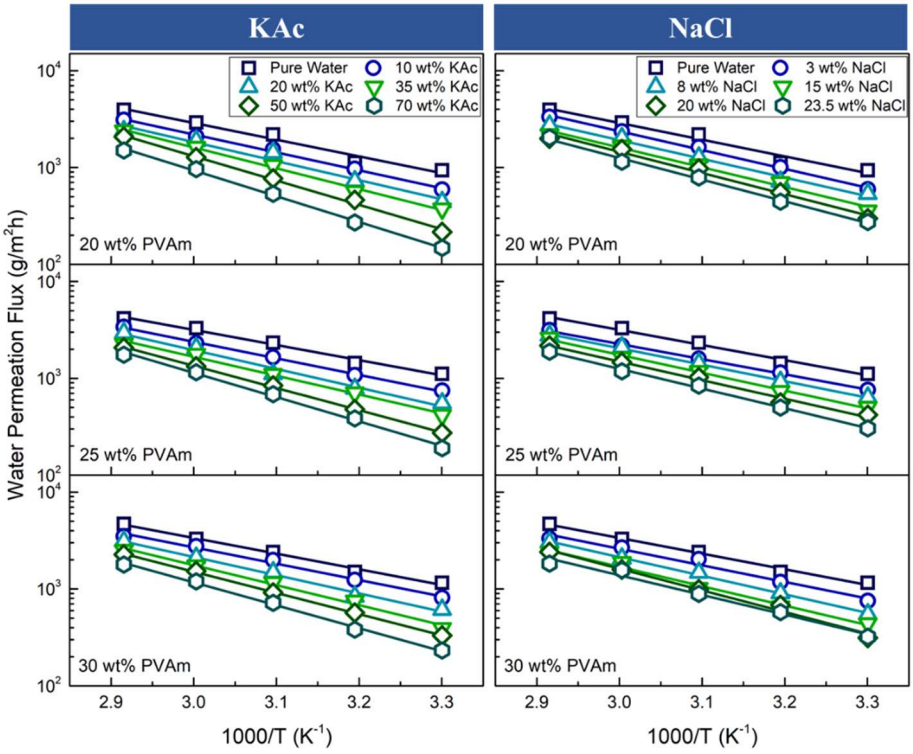

Fig.5.8. Effects of temperature on water flux at different feed salt concentrations for membranes fabricated with Protocol WMp at a PVAm content of 20, 25, and 30 wt% (on a solvent free basis) in dopamine/PVAm co-depositing solution. Total dopamine/PVAm content in the depositing solution was 2 g/L.

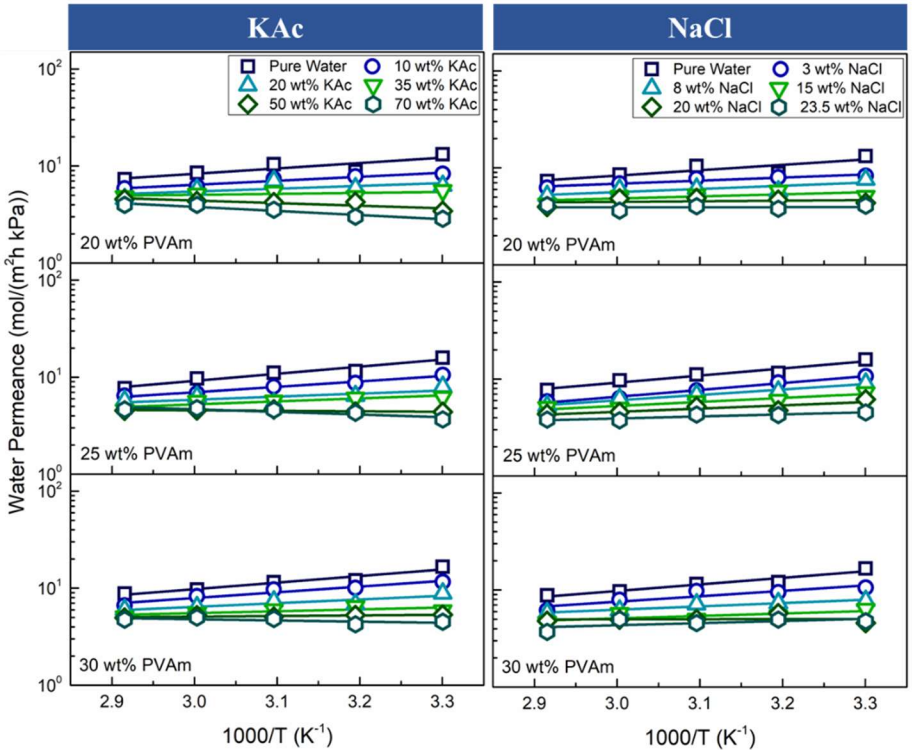

Fig.5.9. Effects of temperature on water permeance. Other conditions same as in Fig. 5.8.

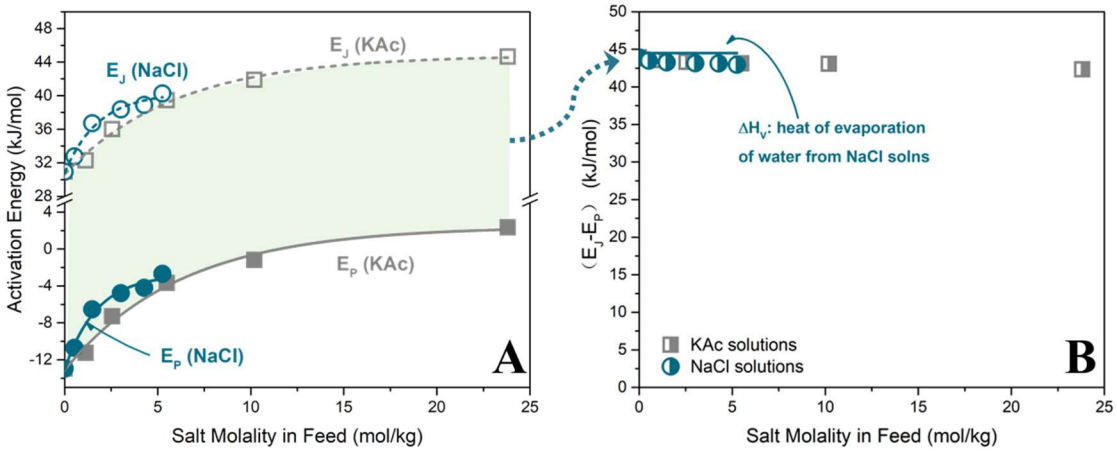

Fig. 5.10. (A) Activation energies E_J and E_P for water permeation vs molal salt concentration in feed. (B) A comparison of (E_J - E_P) and heat of evaporation of water from the salt solutions. Dopamine/PVAm mass ratio in co-depositing solution 70/30.

5.3.4. Membrane stabilities

Fig. 5.11 shows the membrane performance for pervaporative concentration of highly concentrated (70 wt%) KAc solution at 70℃ over a period of 200 h. The membrane exhibited a largely constant water permeation flux, at a high purity level with a conductivity below 50 μS/cm (corresponding to a salt retention rate higher than 99.99 wt%) over the entire test period, demonstrating its excellent stability in pervaporative concentration of KAc solutions. It may be noted that membranes fabricated with protocols WM and Wp were unsatisfactory, and liquid water leakage to the permeate side occurred during the course of the stability tests.

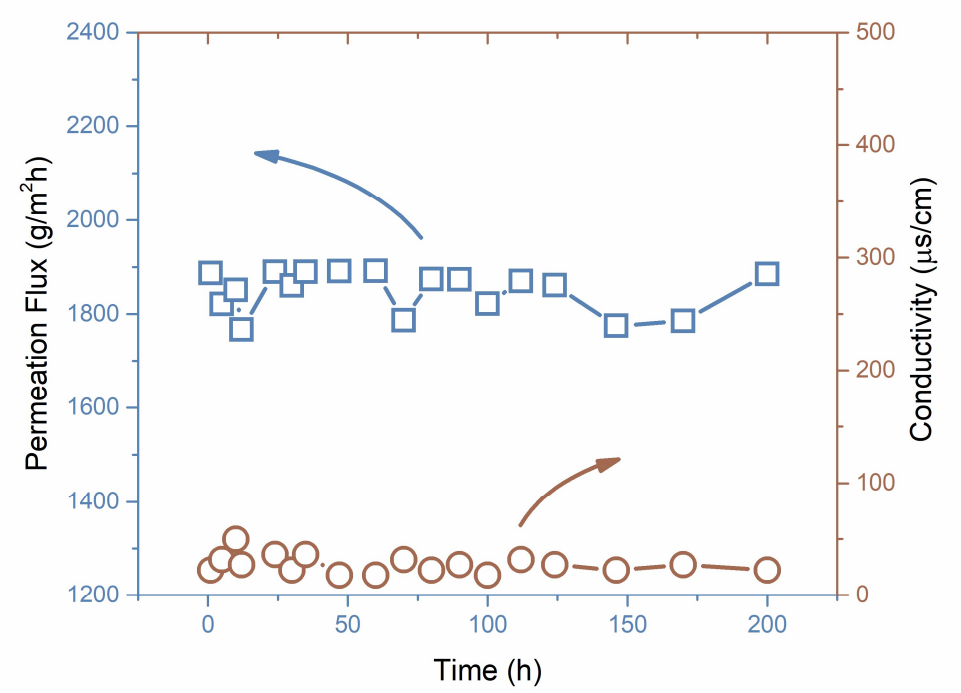

Fig.5.11. The membrane performance for pervaporative concentration of highly concentrated (70 wt%) KAc solution over a period of 200 h. Operating temperature 70℃.

5.4. Conclusions

Attempts were made to co-deposit PVAm/dopamine onto a PVDF hollow fiber substrate to form thin-film-composite hollow fiber membranes for concentration of KAc solutions with sweeping air pervaporation. A hydrophobic substrate was chosen to overcome the potential problems associated with liquid water crossover through the membrane when a hydrophilic microporous substrate was used where capillary condensation and pore wetting could occur gradually even after system shutdown. To facilitate deposition of dopamine/PVAm onto a hydrophobic substrate, methanol was used as a co-solvent for

improved surface wetting, and pre-coating of dopamine was used to form a hydrophilic binding layer that was better prepared for subsequent dopamine/PVAm deposition. The effectiveness of the approach to membrane formation was investigated, and the performance of the resulting membranes for pervaporative concentration of salt solutions was demonstrated. Though not fully optimized, it was shown that use of cosolvent water/methanol (90/10 in vol) in the depositing solution and precoating dopamine for 3 h prior to co-deposition of dopamine/PVAm were appropriate for membrane formation, and the membrane showed stable performance in concentrating KAc solutions at a high feed concentration (70 wt%) over a period of 200 h at an operating temperature of 70℃. A largely constant water flux of 1.7 - 1.9 kg/m^2h was achieved, with an essentially complete salt retention.

Chapter 6

A facile method to improve the dopamine deposition efficiency on hollow fiber membrane and the solution reusability

6.1 Introduction

In the previous chapters, PVAm was applied to co-deposit with dopamine to form a more robust coating with improved deposition kinetics. Moreover, a broader application area for this technique was developed by successfully applying it on a hydrophobic surface. However, some problems should be noticed. Even though the deposition time has been shortened to 12h, there is still enormous potential for further reduction. Moreover, the polymer solution can only be used for one deposition run, with most of the polymers being undeposited on the membrane and therefore, wasted. These problems limit the application of dopamine polymerization in membrane fabrication for actual industry from time and economic concerns.

Applying a more reactive oxidant to replace air oxygen has been demonstrated as a promising way to enhance dopamine polymerization kinetics, with reactive oxygen species (ROS) that are usually co-produced by Cu^{2+} and H_2O_2 being the most extensively studied[8,103,137]. Zhang et al. [8] found that by replacing air with ROS, the kinetics of dopamine polymerization were improved by more than 14 times. Moreover, the so-formed coating was also found to have a more uniform and compact structure and thus possess enhanced stability[8,29]. Therefore, it is proposed in this work to trigger the dopamine/PVAm co-deposition using ROS produced by Cu^{2+} /H_2O_2 to further improve the

deposition efficiency. Moreover, a facile strategy was applied in this work to make the H_2O_2 and $CuSO_4$ react and generate ROS near the membrane surface. By doing so, the deposition efficiency on the target surface was greatly improved, and the deposition solution became reusable. The so-prepared membrane was then applied to the pervaporative concentration of KAc and NaCl solutions, and the water permeation behaviors in the membrane at different feed concentrations and temperatures were investigated.

6.2 Experimental

6.2.1 Materials

The porous polyvinylidene fluoride (PVDF) hollow fiber membrane (mean pore size 0.3μm, inner diameter 0.7mm, outer diameter 1.3mm) was provided by Zhaojin Motian Membrane (China). Dopamine hydrochloride and Tris (hydroxylmethyl) aminomethane (Tris) were supplied by Sigma-Aldrich Canada. Polyvinylamine (PVAm) (Lupamin 1595, Mw 10,000) was purchased from BASF. Other reagents such as ethylenediaminetetraacetic acid disodium salt (EDTA-Na_2), copper (II) sulfate pentahydrate, sodium chloride and potassium acetate were all supplied by Sigma-Aldrich Canada. All of the reagents were used without further purification.

6.2.2 Preparation of the membrane

The hollow fiber membranes were firstly cut into segments with a uniform length of 40cm and then made into elements by bundling every four segments. The element has both ends wrapped with PTFE thin tubes, and the gap between the inner tube surface and the outer membrane surface was sealed using epoxy resin. The pre-deposition solution was made by dissolving 0.6g/L PVAm and a pre-determined amount of $CuSO_4$ in Tris buffer (15 mM)

with the methanol/water mixture at a volume ratio of 1:9 as the solvent. The pH of the pre-deposition solution was adjusted to 8.5-8.8 using hydrochloric acid. Then, the membrane element was immersed in the prepared solutions with only its outer surface in contact with the solution. 1.4 g/L of dopamine was added to the solution right after the H_2O_2 solution at a pre-determined concentration was injected into the cavity of the hollow fiber membrane, so that the freshly mixed dopamine could co-polymerize with the PVAm under the oxidation of ROS co-produced by $CuSO_4/H_2O_2$.After a deposition time of 9h, the membrane was rinsed in 0.1 g/L EDTA-Na_2 (pH: 5.45) solutions to take advantage of its complexation with heavy metal ions to remove any copper ions that were not stably attached to the coating. If any copper ions come off during the pervaporation process, they may contaminate the produced concentrated KAc solution.

6.2.3 Investigation of the weight gain

The deposition performance was investigated through the measurement of the weight gain of the substrate. The membrane was put into an oven at 70℃ for 20 mins to remove any retained moisture before weighing. The accumulated weight gain per m^2 was calculated based on the outer surface area of the substrate by setting the weight of pure dry substrate as the reference.

6.2.4 Measurement of membrane performance

The pervaporative concentration performance of the membrane was measured with the same setup in Chapter 5. The feed solution was stocked in a water tank, with the temperature controlled by a heating mantle and a thermo-regulator. The membrane element was in direct contact with the feed solution, with the contact area between the outer membrane surface and the feed solution kept at 46.53 cm^2 during the test. Dry air at a

flowing rate of 7L/min was used as a sweeping gas to sweep through the cavities of the membranes, and a cold trap was used to condense and collect water vapor. The uncondensed gas was released into the atmosphere after measurement of gas flow using a gas flowmeter. At a given temperature and feed composition, the permeation flux (J) can be obtained:

$$J = Q/A\Delta t \quad (6\text{-}1)$$

where Q is the weight of collected permeate during a period Δt, and A is the effective membrane area. To investigate the rejection performance of the membrane, a conductivity meter (WTW inoLab Cond Level 2) was used to measure the concentration of permeate (C_p). The following equation was employed to determine the salt rejection (R):

$$R = (C_f - C_p)/C_f \times 100\% \quad (6\text{-}2)$$

where C_f represents the concentration of the feed. During the pervaporation experiments, the quantity of feed solution will gradually decrease, resulting in an increase in the feed salt concentration. Thus, water with the same mass of collected permeate was added to the feed tank after each pervaporation experiment to compensate for the removed water. Each test was repeated three times, and the average data was reported.

6.3 Results and Discussion

6.3.1 The effect of H_2O_2 and $CuSO_4$ contents on deposition performance

In our work, the ROS co-produced by $CuSO_4$ /H_2O_2 played the role of the oxidant for the polymerization and deposition of dopamine/PVAm. Thus, it is of interest to look into how the concentration and ratio of $CuSO_4$ and H_2O_2 affect the deposition performance on the target membrane since they determine the ROS generation. The $CuSO_4$ solutions at 0.4, 0.8, 1.2 g/L, and H_2O_2 solutions at 0.1, 0.3, 0.5 g/L were tested, and the deposition amounts

at different conditions were shown in **Fig.6.1**. Note that the deposition time at all conditions was 9h. As seen, the $CuSO_4$ and H_2O_2 concentrations at 0.8 and 0.3 g/L, respectively, were optimum for the deposition of dopamine/PVAm among all tested situations. It shows that the higher concentrations of $CuSO_4$ and H_2O_2 are not necessarily the better condition for the deposition performance. In fact, several researchers have proved that the H_2O_2 at high content could inhibit the polymerization of dopamine[138–140]. Also, copper ions could chelate with dopamine by forming bonds with the amine and hydroxyl group in the dopamine structure. Excessive copper ions in the solution may occupy too much active groups on dopamine, limiting their adhesion to the target surface. The concentrations of $CuSO_4$ at 0.8 g/L and H_2O_2 at 0.3 g/L were used for the following works.

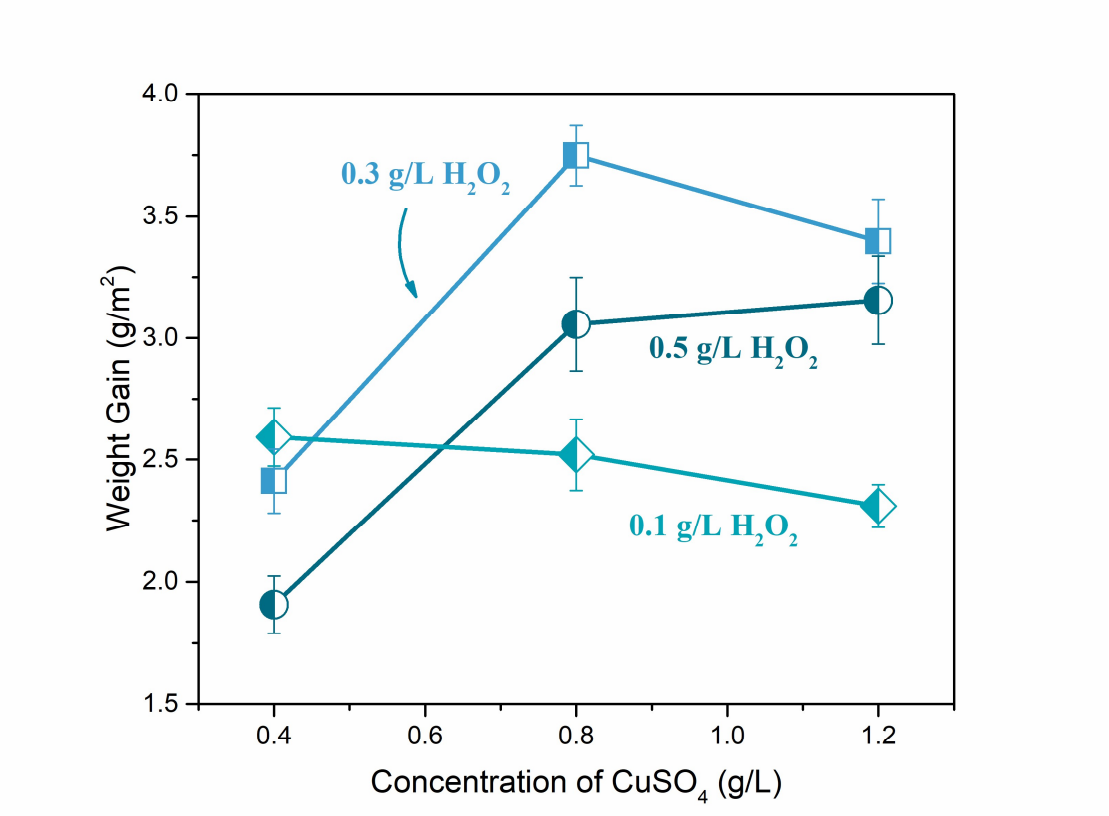

Fig.6.1 The effect of $CuSO_4$ and H_2O_2 concentrations on the weight gain of the substrate.

6.3.2 Reusability of the deposition solution

Instead of directly mixing into the bulk deposition solution, the H_2O_2 solution was injected into the inner surface of the hollow fiber membranes in this work. This modification greatly improved the deposition performance of dopamine/PVAm, including the deposition amount and the reusability of the deposition solution. **Fig.6.2** shows the deposition amounts on a series of substrates by reusing the deposition solution for multiple runs. To make the comparison, the conditions of injecting the H_2O_2 solution into the membrane and directly mixing the H_2O_2 into the bulk deposition solution were all tested. As seen, the solution with H_2O_2 directly mixed in bulk has a deposition amount of less than 1.5 g/L on the substrate for the first deposition and then decreased several folds in the following depositions. As for the modified fabrication method by applying H_2O_2 at the inner membrane surface, the deposition amount on the substrate is higher than 3.5 g/L for the first deposition run. Meanwhile, even after reusing for 6 runs, the modified method could still yield a deposition amount higher than 1.7 g/m^2. Note that this is even higher than the value obtained using the freshly prepared deposition solution with the H_2O_2 mixed in the solution bulk, indicating the impressive enhancement brought by our facile modification.

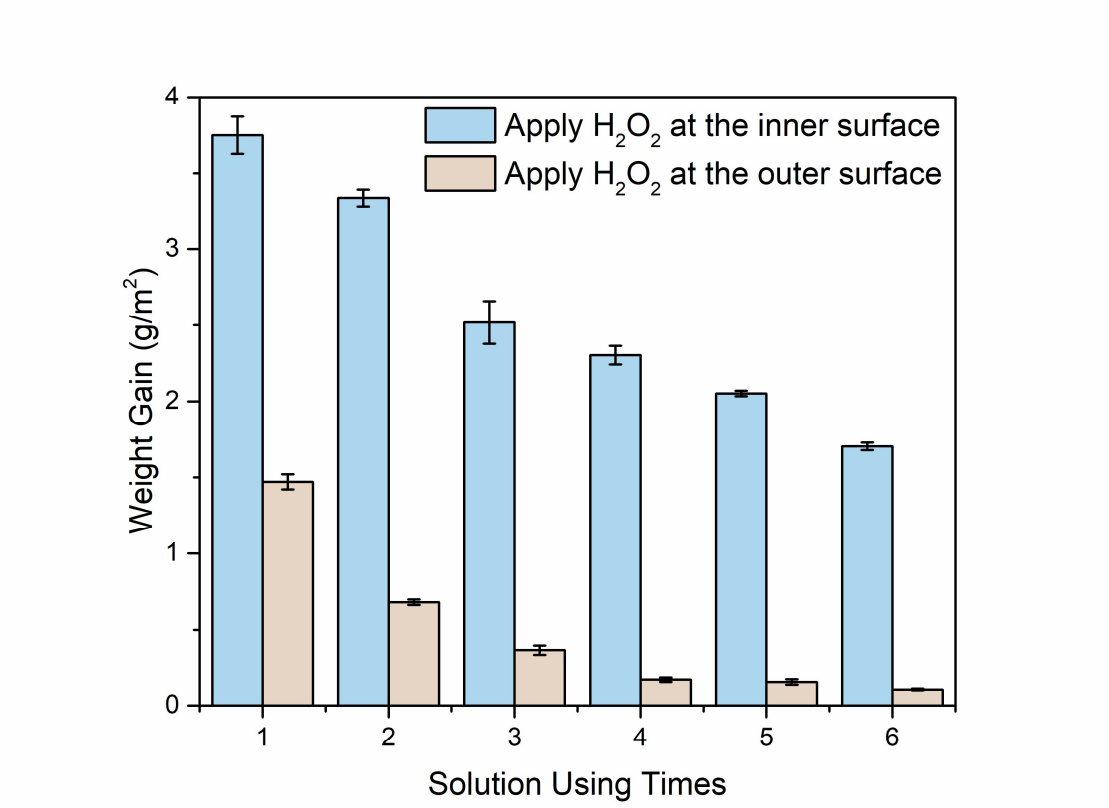

Fig.6.2 Reusability of the deposition solutions by applying H_2O_2 at the inner and outer membrane surfaces. The deposition time is 9h for each cycle.

A proposed explanation of how injecting H_2O_2 into the hollow fiber membrane improves the deposition performance was illustrated in **Fig.6.3**. When the H_2O_2 solution was injected into the membrane cavity, the solutions at both sides of the membrane contacted each other after penetrating the membrane pores. Therefore, the generation of ROS would mainly happen near the membrane surface, especially in the membrane pores. After that, the dopamine monomers started to polymerize into PDA under the oxidation of ROS. Since the ROS is concentrated around the membrane, a PDA layer could be quickly formed at the outer membrane surface. The formed PDA layer will, in turn, prohibit the ROS from releasing into the bulk solution via narrowing and/or blocking the open membrane pores. Therefore, most of the dopamine monomer floating in the solution bulk

remains unoxidized and are available to polymerize into PDA in the subsequent deposition runs.

In contrast, if the H_2O_2 was mixed in the solution directly, the ROS would be widely generated in the whole solution bulk. The PDA could hence be formed everywhere in the solution, including where far from the membrane surface. That being said, most of the formed PDA tend to float in the solution instead of adhering to the target surface. Moreover, these floating PDA kept combining with unoxidized dopamine monomers or other small PDA, preventing them from depositing on the target surface in the following runs.

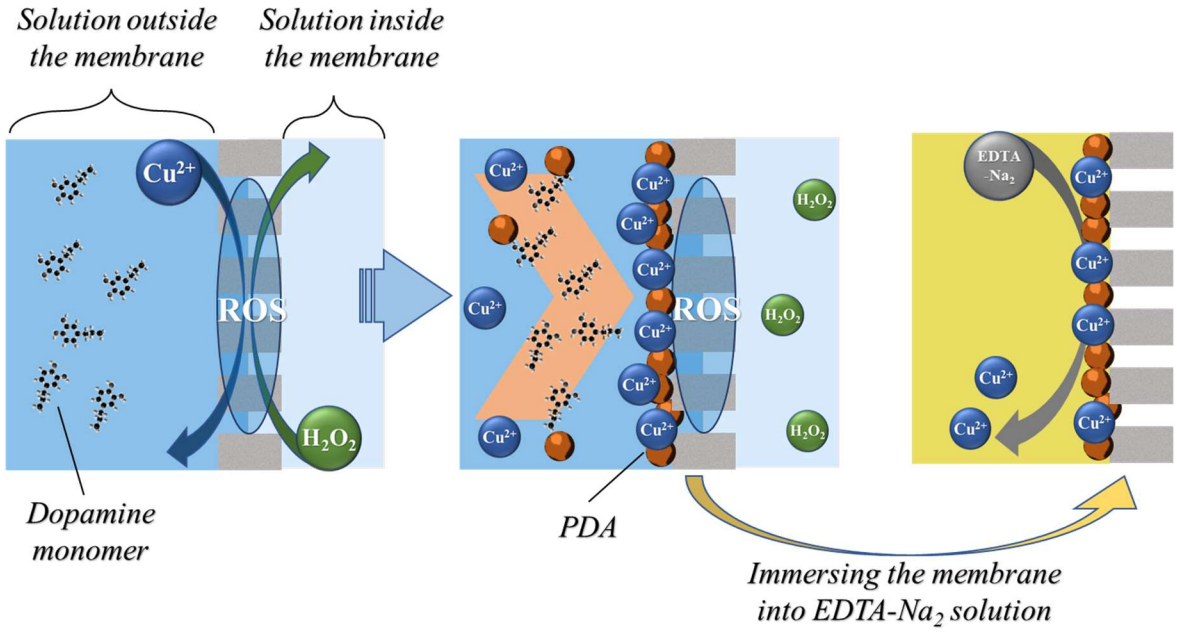

Fig.6.3 Illustration of the membrane fabrication process in this work.

6.3.3 Stability of the membranes in alkaline environment

As known, copper ions could chelate with dopamine or PDA through forming covalent bonds with the amine and hydroxyl groups in their structures. Thus, it is expected that some copper ions may remain in the formed PDA/PVAm layers, even after rinsing in EDTA-Na_2 solution. Thus, the incorporated copper ions were expected to improve the coating stability

via the formed covalent bonds. Also, plenty of previous research has demonstrated that the PDA formed under the oxidation of ROS possesses a smaller particle size, which could also benefit the coating stability[103,137,141,142]. To look into how the method in this work improves the stability of the resultant coating, membranes deposited with pure PDA, PDA/PVAm, and PDA/PVAm/Cu^{2+} were immersed in the 1 M NaOH solutions for as long as 12 h. The elution amounts of the deposited layers are presented in **Fig.6.4**. As seen, the incorporation of PVAm significantly improved the stability of the coating layer, which has also been approved in the previous chapters. Note that the addition of Cu^{2+} also slightly further improved the coating stability; however, since PVAm has essentially made the coating stable enough, the effect of Cu^{2+} was not significant.

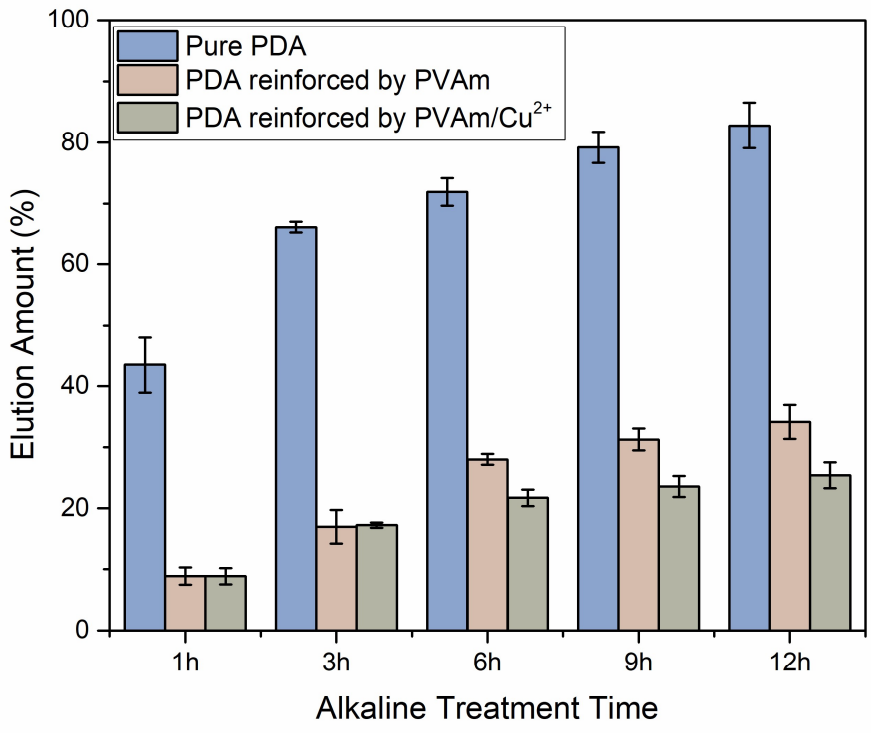

Fig.6.4 Resistance of different deposition layers to alkaline environment.

6.3.4 Pervaporative concentration of KAc and NaCl solutions

To evaluate the effects of operating temperature on the performance of pervaporative concentration for KAc solution, the temperature dependences of water permeation flux from the pervaporative concentration for KAc solutions with various concentrations using membranes with different PVAm contents were plotted in **Fig.6.5A**. As illustrated, the water permeation flux increases with the increase of operating temperature for all tested situations. This result is expectable since the rising temperature will not only increase the vapor pressure at the feed side, resulting in a higher driving force across the membrane, but also motivate the permeant water molecules and the membrane polymer chains. Moreover, a linear relationship between logarithmic water flux and reciprocal temperature was displayed, implying the temperature dependences of water permeation flux in this study fit an Arrhenius-type relation.

$$J = J_0 \exp\left(-E_J/RT\right) \quad (6\text{-}3)$$

where J_0 is the pre-exponential factor for the process, E_J is the activation energy for water permeation, R is the ideal gas constant, and T is the absolute temperature. It should be noted that the presented water permeation flux and so obtained activation energy, E_J, are not only a function of the intrinsic properties of the membranes, but also depend on the driving force in the pervaporation process. What's more, the so determined E_J is essentially an apparent activation energy for water permeation. Thus, the report of permeance value is encouraged as it has been demonstrated as a more favorable way to compare the pervaporation performances under different operating conditions[143]. The membrane permeance to water (P/l) can be calculated from water permeation flux (J) normalized by the mass transfer driving force:

$$(P/l) = J/\Delta P = J/(X\gamma p^{sat} - Yp^{p}) \quad (6\text{-}4)$$

where γ is the activity coefficient of water in the feed solution, X and Y are mole

fractions of water in the feed solution and permeate vapor, respectively, and p^{sat} and p^{p} are the saturated water vapor pressure on the feed side and the permeate side, respectively. The temperature dependence of the so calculated permeance data was shown in **Fig.6.5B**. As seen, the membrane water permeance at all test situations also fit an Arrhenius-type relation and the intrinsic activation energy, E_P, can be obtained through:

$$(P/l) = (P_0/l)\exp(-E_P/RT) \quad (6\text{-}5)$$

For comparison, the results of water permeation flux and water permeance using NaCl solutions with different concentrations as feed were also plotted in **Fig.6.5C** and **Fig.6.5D**, respectively. As shown in the figures, the pervaporative concentration of NaCl solution exhibits similar trends to that of KAc solution, and the temperature dependences of permeation flux and permeance also show an Arrhenius-type relation. It is worth mentioning that essentially complete salt rejection was achieved for all tested situations above.

To determine the effect of feed concentration on apparent and intrinsic activation energies for water permeation through the membrane, the E_J and E_P values were plotted in **Fig. 6.5E** versus the feed concentrations of KAc and NaCl solutions. In the figure, the results for membrane deposited with 30 wt% of PVAm were presented as representative. The feed concentration was shown in molarity to make the two different salt solutions comparable. As illustrated, both apparent and intrinsic activation energies increase with feed concentrations. This is because the rising feed concentration restricts the swelling of membranes and thus results in a more rigid membrane structure, and the activation energy (both E_J and E_P) which could reflect the energy barrier to water permeation in the membrane will consequently increase.

Even though the E_J and E_P values depend on several factors, it has been elucidated that the difference between them is usually close to the enthalpy change of evaporation of the permeant (ΔH_v)[126]. As indicated in **Fig.6.5F**, this relationship is well-applied to the

pervaporative concentration of NaCl solutions; moreover, the ΔH_v remained approximately constant for all concentrations. However, the heat of evaporation of water from KAc solutions is hard to obtain because of the lack of relevant thermodynamic models and the information in the literature. Therefore, the comparison of E_J-E_P and ΔH_v cannot be made for KAc solutions.

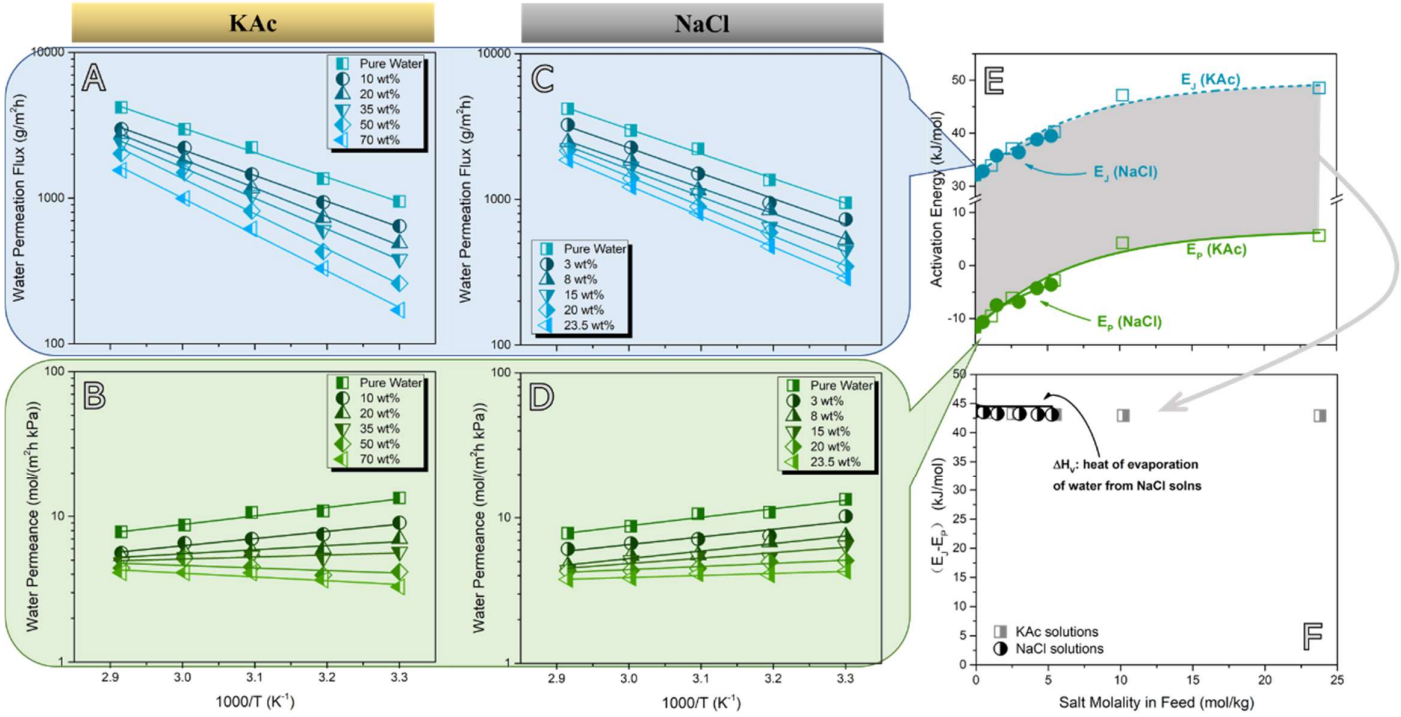

Fig.6.5 (A) Water permeation flux and (B) permeance of the membrane at different feed concentrations and temperatures using KAc solutions as feed. (C)(D) The case using NaCl solutions as feed. (E) E_J and E_P for water permeation vs salt concentration (molal) in feed. (F) A comparison of (E_J - E_P) and heat of evaporation of water from the salt solutions.

6.3.5 Stability of the membrane performance in long-term operation

To investigate the performance stability of the prepared membranes under the actual situation, the long-time pervaporative concentration of highly concentrated KAc solution was carried out, and the results were shown in **Fig.6.6**. 70 wt% KAc solution was used as feed, and an operating temperature of 70℃ was applied. As can be seen, the prepared membranes showed good stability over a test period of 200 hrs. Moreover, the rejection was essentially complete during the whole test period, demonstrating the reliable performance of the membrane in actual operation.

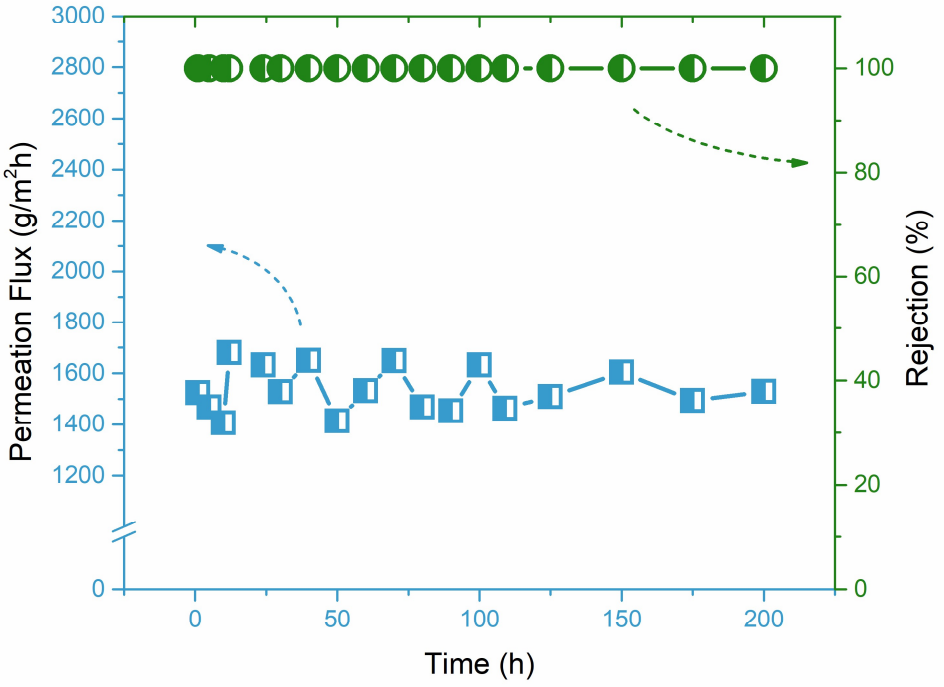

Fig.6.6 Demonstration of membrane stability for pervaporative removal of water from 70 wt% KAc solution at 70˚C.

6.4 Conclusion

In this work, a facile method was developed to help improve the co-deposition of PVAm

and dopamine on a hollow fiber substrate to fabricate a TFC membrane. The ROS co-produced by the $CuSO_4$ and H_2O_2 was applied as the oxidant for the polymerization of dopamine; however, unlike other works that mixed the Cu^{2+} and H_2O_2 in the bulk of the deposition solution, this work made them react specifically on the membrane. By doing so, the deposition efficiency of the dopamine/PVAm on the target hollow fiber membrane surface was dramatically improved, and the deposition solution also became reusable. Also, the resultant coating with incorporated Cu^{2+} showed improved resistance to alkaline, making the membrane more applicable for KAc concentration. As for the pervaporative concentration, the fabricated membrane showed essentially complete rejection in all tested conditions and exhibited a stable performance in a test period of 200h.

Chapter 7

General Conclusions, Original Contributions and Future Prospects

7.1 General Conclusions and Original Contributions

Dopamine-based TFC membranes were prepared in this work for sweeping gas pervaporative concentration of KAc solutions. The permeation behaviors and the stability of the membranes were investigated. The following general conclusions can be drawn from the research:

(1) TFC membranes comprising a PDA sublayer and PEI/PAA bilayers were prepared and studied for the pervaporative concentration of KAc solutions. It was found that the TFC membrane with only one PEI/PAA bilayer on top of the PDA sublayer was adequate for the pervaporative concentration of the salts. The resistance of the PEI/PAA bilayer was found to be largely the same when the number of the bilayers was sufficiently large, which indicated the bilayers were stable in the salt solutions under the tested conditions.

(2) PVAm was proposed for the first time as a co-depositant with dopamine to fabricate TFC membranes to take advantage of the covalent bonding between polydopamine and PVAm and the adhesive properties of PDA oligomers. It was found that incorporating PVAm could improve both the hydrophilicity and stability of the resultant membrane (with micro-porous PES membrane being the substrate). The optimal PVAm content in the depositing solution was 20-30 wt% (solvent-free basis) in terms of membrane stability and applicability.

(3) The co-deposition of PVAm/dopamine was then successfully applied onto a hollow fiber membrane with a hydrophobic surface by using methanol as a co-solvent and postponing the addition of PVAm. According to the deposition rate,

10 vol% of methanol as the co-solvent and postponing the addition of PVAm for 3h were suggested in this work. Overall, a broader target surface of this deposition technique was explored.

(4) The ROS co-produced by the $CuSO_4$ and H_2O_2 was applied as the oxidant to accelerate the co-deposition of PVAm/dopamine. A facile method was proposed to make the ROS generated specifically around the target substrate. The deposition efficiency on the target hollow fiber membrane surface was thus dramatically improved, and the deposition solution became reusable. Also, the resultant coating incorporated with Cu^{2+} showed improved resistance to alkaline, making the membrane more applicable for KAc concentration.

7.2 Recommendations for Future Work

(1) Codepositing with PVAm has been demonstrated as an effective compensation for the weak hydrophilicity of dopamine; however, the hydrophilicity of the PDA coating might be further enhanced by applying more techniques. Some small particles could adhere to the formed PDA-based layer, ascribed to the various functional groups existing on its surface. Zhang et al. [79]bound TiO_2 nanoparticles robustly onto the PDA by simply immersing a freshly made PDA-coated membrane into a TiO_2 suspension. The water contact angle of the resultant membrane surface decreased from 72° to 28° by adhering TiO_2 onto the PDA. Therefore, it is recommended that many other hydrophilic nanoparticles or microparticles (e.g., SiO_2, graphene oxide) be applied to further enhance the hydrophilicity of the resultant PDA layer in future works.

(2) Pervaporative concentration is favorable when handling feeds at high concentrations; however, its relatively low permeation rate when treating dilute feeds limits its application in the actual industry. Meanwhile, RO is a mature and widely applied technique for the concentration of salt waters. The main drawback

for RO is its high power consumption when treating highly concentrated feeds, ascribed to the requirement for overcoming the high osmosis pressure. Therefore, developing a hybrid system comprising RO and pervaporation is suggested to make the whole process more applicable to the actual industry. In the hybrid system, RO could be applied as the pre-treatment process to produce highly concentrated feeds for subsequent pervaporation.

(3) Up to now, the fabricated membranes in this work were only applied for the pervaporative concentration of salt solutions. Meanwhile, liquid-liquid separation is another field of interest for pervaporation. Since the selective layer is hydrophilic in this work, the membranes also have the potential to be applied to pervaporation dehydration of organic solvent since (1) water is more soluble onto the membrane surface, (2) water molecular is expected to show higher diffusivity in the membrane matrix because of the smaller size. Some typical organic solvents that were studied for pervaporation dehydration include ethylene glycol, isopropanol, and butanol. By doing so, a broader application field of the such membrane could be explored.

Bibliography

[1] H. Lee, S.M. Dellatore, W.M. Miller, P.B. Messersmith, Mussel-inspired surface chemistry for multifunctional coatings, Science. 318 (2007) 426–430.

[2] D. Wu, J. Martin, J. Du, Y. Zhang, D. Lawless, X. Feng, Thin film composite membranes comprising of polyamide and polydopamine for dehydration of ethylene glycol by pervaporation, J. Memb. Sci. 493 (2015) 622–635.

[3] S. Hong, Y.S. Na, S. Choi, I.T. Song, W.Y. Kim, H. Lee, Non-covalent self-assembly and covalent polymerization co-contribute to polydopamine formation, Adv. Funct. Mater. 22 (2012) 4711–4717.

[4] H. Wei, J. Ren, B.B. Han, L. Xu, L. Han, L. Jia, Stability of polydopamine and poly(DOPA) melanin-like films on the surface of polymer membranes under strongly acidic and alkaline conditions., Colloids Surf. B. Biointerfaces. 110 (2013) 10–15.

[5] H.C. Yang, M.B. Wu, Y.J. Li, Y.F. Chen, L.S. Wan, Z.K. Xu, Effects of polyethyleneimine molecular weight and proportion on the membrane hydrophilization by codepositing with dopamine, J. Appl. Polym. Sci. 133 (2016) 1–10.

[6] Z.-Y. Xi, Y.-Y. Xu, L.-P. Zhu, Y. Wang, B.-K. Zhu, A facile method of surface modification for hydrophobic polymer membranes based on the adhesive behavior of poly(DOPA) and poly(dopamine), J. Memb. Sci. 327 (2009) 244–253.

[7] H.C. Yang, K.J. Liao, H. Huang, Q.Y. Wu, L.S. Wan, Z.K. Xu, Mussel-inspired modification of a polymer membrane for ultra-high water permeability and oil-in-water emulsion separation, J. Mater. Chem. A. 2 (2014) 10225–10230.

[8] C. Zhang, Y. Ou, W.X. Lei, L.S. Wan, J. Ji, Z.K. Xu, $CuSO_4/H_2O_2$-induced rapid deposition of polydopamine coatings with high uniformity and enhanced stability, Angew. Chemie - Int. Ed. 55 (2016) 3054–3057.

[9] Y. Lv, S.J. Yang, Y. Du, H.C. Yang, Z.K. Xu, Co-deposition kinetics of polydopamine/polyethyleneimine coatings: Effects of solution composition and substrate surface, Langmuir. 34 (2018) 13123–13131.

[10] Y. Lv, H.C. Yang, H.Q. Liang, L.S. Wan, Z.K. Xu, Nanofiltration membranes via co-deposition of polydopamine/polyethylenimine followed by cross-linking, J. Memb. Sci. 476 (2015) 50–58.

[11] F. Van Ackern, L. Krasemann, B. Tieke, Ultrathin membranes for gas separation and pervaporation prepared upon electrostatic self-assembly of polyelectrolytes, Thin Solid Films. 327–329 (1998) 762–766.

[12] L. Krasemann, A. Toutianoush, B. Tieke, Self-assembled polyelectrolyte multilayer membranes with highly improved pervaporation separation of ethanol/water mixtures, J. Memb. Sci. 181 (2001) 221–228.

[13] A. Toutianoush, B. Tieke, Pervaporation separation of alcohol/water mixtures using self-assembled polyelectrolyte multilayer membranes of high charge density, Mater. Sci. Eng. C. 22 (2002) 459–463.

[14] A. Toutianoush, L. Krasemann, B. Tieke, Polyelectrolyte multilayer membranes for pervaporation separation of alcohol/water mixtures, Colloids Surfaces A Physicochem. Eng. Asp. 22 (2002) 881–889.

[15] L.A. Burzio, J.H. Waite, Cross-linking in adhesive quinoproteins: Studies with model decapeptides, Biochemistry. 39 (2000) 11147–11153.

[16] M.J. LaVoie, B.L. Ostaszewski, A. Weihofen, M.G. Schlossmacher, D.J. Selkoe, Dopamine covalently modifies and functionally inactivates parkin, Nat. Med. 11 (2005) 1214–1221.

[17] S.M. Kang, N.S. Hwang, J. Yeom, S.Y. Park, P.B. Messersmith, I.S. Choi, R. Langer, D.G. Anderson, H. Lee, One-step multipurpose surface functionalization by adhesive catecholamine, Adv. Funct. Mater. 22 (2012) 2949–2955.

[18] R. Zhang, Y. Su, X. Zhao, Y. Li, J. Zhao, Z. Jiang, A novel positively charged composite nanofiltration membrane prepared by bio-inspired adhesion of

polydopamine and surface grafting of poly(ethylene imine), J. Memb. Sci. 470 (2014) 9–17.

[19] I.R. Marques, G. Zin, L.T. Prando, C.C. Bretanha, M.C. Proner, E. Rigo, K. Rezzadori, C. da Costa, M. Di Luccio, Deposition of dodpamine and polyethyleneimine on polymeric membranes: Improvement of performance of ultrafiltration process, Macromol. Res. 28 (2020) 1091–1097.

[20] R. Pelton, Polyvinylamine: A tool for engineering interfaces, Langmuir. 30 (2014) 15373–15382.

[21] A. Wallqvist, Computer simulation of hydrophobic hydration forces on stacked plates at short range, J. Phys. Chem. 99 (1995) 2893–2899.

[22] C. Zhang, L. Gong, L. Xiang, Y. Du, W. Hu, H. Zeng, Z.K. Xu, Deposition and Adhesion of Polydopamine on the Surfaces of Varying Wettability, ACS Appl. Mater. Interfaces. 9 (2017) 30943–30950.

[23] S.H. Donaldson, A. Røyne, K. Kristiansen, M. V. Rapp, S. Das, M.A. Gebbie, D.W. Lee, P. Stock, M. Valtiner, J. Israelachvili, Developing a general interaction potential for hydrophobic and hydrophilic interactions, Langmuir. 31 (2015) 2051–2064.

[24] X.Q. Dou, D. Zhang, C. Feng, L. Jiang, Bioinspired Hierarchical Surface Structures with Tunable Wettability for Regulating Bacteria Adhesion, ACS Nano. 9 (2015) 10664–10672.

[25] Q. Yue, M. Wang, Z. Sun, C. Wang, C. Wang, Y. Deng, D. Zhao, A versatile ethanol-mediated polymerization of dopamine for efficient surface modification and the construction of functional core-shell nanostructures, J. Mater. Chem. B. 1 (2013) 6085–6093.

[26] H.S. Sundaram, X. Han, A.K. Nowinski, N.D. Brault, Y. Li, J.R. Ella-Menye, K.A. Amoaka, K.E. Cook, P. Marek, K. Senecal, S. Jiang, Achieving One-Step Surface Coating of Highly Hydrophilic Poly(Carboxybetaine Methacrylate) Polymers on Hydrophobic and Hydrophilic Surfaces, Adv. Mater. Interfaces. 1

(2014) 1–8.

[27] J. Jiang, L. Zhu, L. Zhu, B. Zhu, Y. Xu, Surface characteristics of a self-polymerized dopamine coating deposited on hydrophobic polymer films, Langmuir. 27 (2011) 14180–14187.

[28] Y. Luo, K. Kustin, I. Epstein, Mechanistic study of oscillations and bistability in the Cu-catalyzed reaction beween hydrogen peroxide and KSCN, J. Am. Chem. Soc. 54 (1989) 4541–4548.

[29] C. Zhang, Y. Lv, W.Z. Qiu, A. He, Z.K. Xu, Polydopamine Coatings with Nanopores for Versatile Molecular Separation, ACS Appl. Mater. Interfaces. 9 (2017) 14437–14444.

[30] H.B. Pols, G.H. Harmsen, Industrial wastewater treatment today and tomorrow, in: Water Sci. Technol., Pergamon Press Inc, 1994: pp. 109–117.

[31] K. El Kadi, I. Janajreh, Desalination by Freeze Crystallization: An Overview, Int. J. Therm. Environ. Eng. 15 (2017) 103–110.

[32] S.M. Rao, Reverse Osmosis, Resonance. 16 (2011) 1333–1336.

[33] A. Alkhudhiri, N. Darwish, N. Hilal, Membrane distillation: A comprehensive review, Desalination. 287 (2012) 2–18.

[34] E. Korngold, E. Korin, I. Ladizhensky, Water desalination by pervaporation with hollow fiber membranes, Desalination. 107 (1996) 121–129.

[35] M. Mujiburohman, X. Feng, Permselectivity, solubility and diffusivity of propyl propionate/water mixtures in poly(ether block amide) membranes, J. Memb. Sci. 300 (2007) 95–103.

[36] X. Feng, R.Y.M.M. Huang, Liquid Separation by Membrane Pervaporation: A Review, Ind. Eng. Chem. Res. 36 (1997) 1048–1066.

[37] P. Aptel, N. Challard, J. Cuny, J. Neel, Application of the pervaporation process to separate azeotropic mixtures, J. Memb. Sci. 1 (1976) 271–287.

[38] Y. jie Wu, Q. lin Huang, C. fa Xiao, K. kai Chen, X. feng Li, N. na Li, Study on the effects and properties of PVDF/FEP blend porous membrane, Desalination.

353 (2014) 118–124.

[39] A. Jonquières, R. Clément, P. Lochon, J. Néel, M. Dresch, B. Chrétien, Industrial state-of-the-art of pervaporation and vapour permeation in the western countries, J. Memb. Sci. 206 (2002) 87–117.

[40] R. Jiraratananon, A. Chanachai, R.Y.M. Huang, D. Uttapap, Pervaporation dehydration of ethanol-water mixtures with chitosan/hydroxyethylcellulose (CS/HEC) composite membranes I. Effect of operating conditions, J. Memb. Sci. 195 (2002) 143–151.

[41] D. Wu, A. Gao, H. Zhao, X. Feng, Pervaporative desalination of high-salinity water, Chem. Eng. Res. Des. 136 (2018) 154–164.

[42] L.D. Tijing, Y.C. Woo, J.-S. Choi, S. Lee, S.-H. Kim, H.K. Shon, Fouling and its control in membrane distillation—A review, J. Memb. Sci. 475 (2015) 215–244.

[43] T. Kataoka, T. Tsuru, S.I. Nakao, S. Kimura, Membrane transport properties of pervaporation and vapor permeation in ethanol-water system using polyacrylonitrile and cellulose acetate membranes, J. Chem. Eng. JAPAN. 24 (1991) 334–339.

[44] T. Tsuru, S. ichi Nakao, S. Kimura, T. Kataoka, Permeation equations developed for prediction of membrane performance in pervaporation, vapor permeation and reverse osmosis based on the solution-diffusion model, J. Chem. Eng. JAPAN. 24 (1991) 326–333.

[45] J.G. Wijmans, R.W. Baker, The solution-diffusion model: a review, J. Memb. Sci. 107 (1995) 1–21.

[46] R.W. Baker, MEMBRANE TECHNOLOGY, 2004.

[47] X. Lu, M. Elimelech, Fabrication of desalination membranes by interfacial polymerization: History, current efforts, and future directions, Chem. Soc. Rev. 50 (2021) 6290–6307.

[48] Y. Song, P. Sun, L.L. Henry, B. Sun, Mechanisms of structure and performance controlled thin film composite membrane formation via interfacial

polymerization process, J. Memb. Sci. 251 (2005) 67–79.

[49] F. Zhang, J. bing Fan, S. Wang, Interfacial Polymerization: From Chemistry to Functional Materials, Angew. Chemie - Int. Ed. 59 (2020) 21840–21856.

[50] Q.F. An, M.B.M.Y. Ang, Y.H. Huang, S.H. Huang, Y.H. Chiao, C.L. Lai, H.A. Tsai, W.S. Hung, C.C. Hu, Y.P. Wu, K.R. Lee, Microstructural characterization and evaluation of pervaporation performance of thin-film composite membranes fabricated through interfacial polymerization on hydrolyzed polyacrylonitrile substrate, J. Memb. Sci. 583 (2019) 31–39.

[51] M.J.T. Raaijmakers, N.E. Benes, Current trends in interfacial polymerization chemistry, Prog. Polym. Sci. 63 (2016) 86–142.

[52] G. Decher, J.D. Hong, Buildup of Ultrathin Multilayer Films by a Self-Assembly Process: II. Consecutive Adsorption of Anionic and Cationic Bipolar Amphiphiles and Polyelectrolytes on Charged Surfaces, Berichte Der Bunsengesellschaft Für Phys. Chemie. 95 (1991) 1430–1434.

[53] G. Decher, J. -D Hong, Buildup of ultrathin multilayer films by a self-assembly process, 1 consecutive adsorption of anionic and cationic bipolar amphiphiles on charged surfaces, Makromol. Chemie. Macromol. Symp. 46 (1991) 321–327.

[54] P.T. Hammond, Recent explorations in electrostatic multilayer thin film assembly, Curr. Opin. Colloid Interface Sci. 4 (1999) 430–442.

[55] R. Steitz, W. Jaeger, R. V. Klitzing, Influence of charge density and ionic strength on the multilayer formation of strong polyelectrolytes, Langmuir. 17 (2001) 4471–4474.

[56] R. Messina, Polyelectrolyte multilayering on a charged planar surface, Macromolecules. 37 (2004) 621–629.

[57] B.F. Abu-Sharkh, Structure and mechanism of formation of polyelectrolyte multilayers, Polymer (Guildf). 47 (2006) 3674–3680.

[58] Y. Xiang, S. Ping, Layer-by-layer self-assembly in the development of electrochemical energy conversion and storage devices from fuel cells to

supercapacitors, Chem. Soc. Rev. 5 (2012) 7291–7321.

[59] G. Decher, Fuzzy nanoassemblies: Toward layered polymeric multicomposites, Science. 277 (1997) 1232–1237.

[60] Z. Zhu, X. Feng, A. Penlidis, Self-assembled nano-structured polyelectrolyte composite membranes for pervaporation, Mater. Sci. Eng. C. 26 (2006) 1–8.

[61] Z. Zhu, X. Feng, A. Penlidis, Layer-by-layer self-assembled polyelectrolyte membranes for solvent dehydration by pervaporation, Mater. Sci. Eng. C. 27 (2007) 612–619.

[62] P. Zhang, J. Qian, Y. Yang, Q. An, X. Liu, Z. Gui, Polyelectrolyte layer-by-layer self-assembly enhanced by electric field and their multilayer membranes for separating isopropanol-water mixtures, J. Memb. Sci. 320 (2008) 73–77.

[63] G. Zhang, X. Gao, S. Ji, Z. Liu, Electric field-enhanced assembly of polyelectrolyte composite membranes, J. Memb. Sci. 307 (2008) 151–155.

[64] G. Zhang, L. Dai, L. Zhang, S. Ji, Effects of external electric field on film growth, morphology, and nanostructure of polyelectrolyte and nanohybrid multilayers onto insulating substrates, Langmuir. 27 (2011) 2093–2098.

[65] Y.H. Ko, Y.H. Kim, J. Park, K.T. Nam, J.H. Park, P.J. Yoo, Electric-field-assisted layer-by-layer assembly of weakly charged polyelectrolyte multilayers, Macromolecules. 44 (2011) 2866–2872.

[66] J.J. Richardson, M. Björnmalm, F. Caruso, Technology-driven layer-by-layer assembly of nanofilms, Science. 348 (2015) 62–67.

[67] J.J. Richardson, J. Cui, M. Björnmalm, J.A. Braunger, H. Ejima, F. Caruso, Innovation in Layer-by-Layer Assembly, Chem. Rev. 116 (2016) 14828–14867.

[68] R. Ouyang, J. Lei, H. Ju, Artificial receptor-functionalized nanoshell: facile preparation, fast separation and specific protein recognition, Nanotechnology. 21 (2010) 185502.

[69] W.-H. Zhou, S.-F. Tang, Q.-H. Yao, F.-R. Chen, H.-H. Yang, X.-R. Wang, A quartz crystal microbalance sensor based on mussel-inspired molecularly

imprinted polymer, Biosens. Bioelectron. 26 (2010) 585–589.

[70] S.H. Ku, J.S. Lee, C.B. Park, Spatial Control of Cell Adhesion and Patterning through Mussel-Inspired Surface Modification by Polydopamine, Langmuir. 26 (2010) 15104–15108.

[71] S. Ben-Valid, B. Botka, K. Kamarás, A. Zeng, S. Yitzchaik, Spectroscopic and electrochemical study of hybrids containing conductive polymers and carbon nanotubes, Carbon N. Y. 48 (2010) 2773–2781.

[72] M. Zhang, X. Zhang, X. He, L. Chen, Y. Zhang, Preparation and Characterization of Polydopamine-coated Silver Core/Shell Nanocables, Chem. Lett. 39 (2010) 552–553.

[73] W. Zhong, J. Hou, H.C. Yang, V. Chen, Superhydrophobic membranes via facile bio-inspired mineralization for vacuum membrane distillation, J. Memb. Sci. 540 (2017) 98–107.

[74] J. Wang, H. Guo, X. Shi, Z. Yao, W. Qing, F. Liu, C.Y. Tang, Fast polydopamine coating on reverse osmosis membrane: Process investigation and membrane performance study, J. Colloid Interface Sci. 535 (2019) 239–244.

[75] H. Guo, Z. Yao, J. Wang, Z. Yang, X. Ma, C.Y. Tang, Polydopamine coating on a thin film composite forward osmosis membrane for enhanced mass transport and antifouling performance, J. Memb. Sci. 551 (2018) 234–242.

[76] F. Yu, S. Chen, Y. Chen, H. Li, L. Yang, Y. Chen, Y. Yin, Experimental and theoretical analysis of polymerization reaction process on the polydopamine membranes and its corrosion protection properties for 304 Stainless Steel, J. Mol. Struct. 982 (2010) 152–161.

[77] D.R. Dreyer, D.J. Miller, B.D. Freeman, D.R. Paul, C.W. Bielawski, Elucidating the structure of poly(dopamine), Langmuir. 28 (2012) 6428–6435.

[78] E. Kaxiras, A. Tsolakidis, G. Zonios, S. Meng, Structural model of eumelanin, Phys. Rev. Lett. 97 (2006) 218102.

[79] R.-X.X. Zhang, L. Braeken, P. Luis, X.-L.L. Wang, B. Van der Bruggen, Novel

binding procedure of TiO2 nanoparticles to thin film composite membranes via self-polymerized polydopamine, J. Memb. Sci. 437 (2013) 179–188.

[80] L. Yao, C. He, S. Chen, W. Zhao, Y. Xie, S. Sun, S. Nie, C. Zhao, Codeposition of polydopamine and zwitterionic polymer on membrane surface with enhanced stability and antibiofouling property, Langmuir. 35 (2019) 1430–1439.

[81] S. Muchtar, M.Y. Wahab, L. Fang, S. Jeon, S. Rajabzadeh, R. Takagi, S. Mulyati, N. Arahman, M. Riza, H. Matsuyama, Polydopamine-coated poly(vinylidene fluoride) membranes with high ultraviolet resistance and antifouling properties for a photocatalytic membrane reactor, J. Appl. Polym. Sci. 136 (2018) 47312.

[82] F.K. Yang, B. Zhao, Adhesion properties of self-polymerized dopamine thin film, Open Surf. Sci. J. 3 (2014) 115–122.

[83] S. Beckford, M. Zou, Wear resistant PTFE thin film enabled by a polydopamine adhesive layer, Appl. Surf. Sci. 292 (2014) 350–356.

[84] X.L. Li, L.P. Zhu, J.H. Jiang, Z. Yi, B.K. Zhu, Y.Y. Xu, Hydrophilic nanofiltration membranes with self-polymerized and strongly-adhered polydopamine as separating layer, Chinese J. Polym. Sci. 30 (2012) 152–163.

[85] F. Pan, H. Jia, S. Qiao, Z. Jiang, J. Wang, B. Wang, Y. Zhong, Bioinspired fabrication of high performance composite membranes with ultrathin defect-free skin layer, J. Memb. Sci. 341 (2009) 279–285.

[86] B. Li, W. Liu, Z. Jiang, X. Dong, B. Wang, Y. Zhong, Ultrathin and Stable Active Layer of Dense Composite Membrane Enabled by Poly (dopamine), Langmuir. 25 (2009) 7368–7374.

[87] S. Kasemset, A. Lee, D.J. Miller, B.D. Freeman, M.M. Sharma, Effect of polydopamine deposition conditions on fouling resistance, physical properties, and permeation properties of reverse osmosis membranes in oil/water separation, J. Memb. Sci. 425 (2013) 208–216.

[88] Z.Y. Xi, Y.Y. Xu, L.P. Zhu, Y. Wang, B.K. Zhu, A facile method of surface modification for hydrophobic polymer membranes based on the adhesive

behavior of poly(DOPA) and poly(dopamine), J. Memb. Sci. 327 (2009) 244–253.

[89] F. Li, J. Meng, J. Ye, B. Yang, Q. Tian, C. Deng, Surface modification of PES ultrafiltration membrane by polydopamine coating and poly(ethylene glycol) grafting: Morphology, stability, and anti-fouling, Desalination. 344 (2014) 422–430.

[90] M. Zhou, J. Li, M. Zhang, H. Wang, Y. Lan, Y.N. Wu, F. Li, G. Li, A polydopamine layer as the nucleation center of MOF deposition on "inert" polymer surfaces to fabricate hierarchically structured porous films, Chem. Commun. 51 (2015) 2706–2709.

[91] Y. Bie, J. Yang, X. Liu, J. Wang, Y. Nuli, W. Lu, Polydopamine wrapping silicon cross-linked with polyacrylic acid as high-performance anode for lithium-ion batteries, ACS Appl. Mater. Interfaces. 8 (2016) 2899–2904.

[92] J. Zhang, T. Ren, G.P. Nayaka, P. Dong, J. Duan, X. Li, Y. Zhang, D. Wang, Design of polydopamine-encapsulation multiporous MnO cross-linked with polyacrylic acid binder for superior lithium ion battery anode, J. Alloys Compd. 783 (2019) 341–348.

[93] Y.L. Ji, M.B.M.Y. Ang, H.C. Hung, S.H. Huang, Q.F. An, K.R. Lee, J.Y. Lai, Bio-inspired deposition of polydopamine on PVDF followed by interfacial cross-linking with trimesoyl chloride as means of preparing composite membranes for isopropanol dehydration, J. Memb. Sci. 557 (2018) 58–66.

[94] Y. Zhang, B. Thingholm, K.N. Goldie, R. Ogaki, B. Städler, Assembly of poly(dopamine) films mixed with a nonionic polymer, Langmuir. 28 (2012) 17585–17592.

[95] Y. Liu, C.P. Chang, T. Sun, Dopamine-assisted deposition of dextran for nonfouling applications, Langmuir. 30 (2014) 3118–3126.

[96] W.Z. Qiu, H.C. Yang, Z.K. Xu, Dopamine-assisted co-deposition: An emerging and promising strategy for surface modification, Adv. Colloid Interface Sci. 256

(2018) 111–125.

[97] T.J. Kim, H. Vralstad, M. Sandru, M.B. Hägg, Separation performance of PVAm composite membrane for CO_2 capture at various pH levels, J. Memb. Sci. 428 (2013) 218–224.

[98] L. Deng, T.J. Kim, M.B. Hägg, Facilitated transport of CO_2 in novel PVAm/PVA blend membrane, J. Memb. Sci. 340 (2009) 154–163.

[99] P. Li, Z. Wang, W. Li, Y. Liu, J. Wang, S. Wang, High-performance multilayer composite membranes with mussel-inspired polydopamine as a versatile molecular bridge for CO_2 separation, ACS Appl. Mater. Interfaces. 7 (2015) 15481–15493.

[100] S.Y. Hu, Y. Zhang, D. Lawless, X. Feng, Composite membranes comprising of polyvinylamine-poly(vinyl alcohol) incorporated with carbon nanotubes for dehydration of ethylene glycol by pervaporation, J. Memb. Sci. 417–418 (2012) 34–44.

[101] S. Chaudhari, Y.S. Kwon, M.Y. Shon, S.E. Nam, Y.I. Park, Stability and pervaporation characteristics of PVA and its blend with PVAm membranes in a ternary feed mixture containing highly reactive epichlorohydrin, RSC Adv. 9 (2019) 5908–5917.

[102] S. Yu, M. Ma, J. Liu, J. Tao, M. Liu, C. Gao, Study on polyamide thin-film composite nanofiltration membrane by interfacial polymerization of polyvinylamine (PVAm) and isophthaloyl chloride (IPC), J. Memb. Sci. 379 (2011) 164–173.

[103] C. Zhang, H.N. Li, Y. Du, M.Q. Ma, Z.K. Xu, $CuSO_4/H_2O_2$-triggered polydopamine/poly(sulfobetaine methacrylate) coatings for antifouling membrane surfaces, Langmuir. 33 (2017) 1210–1216.

[104] L.D. Tijing, Y.C. Woo, J.S. Choi, S. Lee, S.H. Kim, H.K. Shon, Fouling and its control in membrane distillation-A review, J. Memb. Sci. 475 (2015) 215–244.

[105] M.C. García-Payo, M.A. Izquierdo-Gil, C. Fernández-Pineda, Wetting study of

hydrophobic membranes via liquid entry pressure measurements with aqueous alcohol solutions, J. Colloid Interface Sci. 230 (2000) 420–431.

[106] C.C. Ho, S.J. Ding, The pH-controlled nanoparticles size of polydopamine for anti-cancer drug delivery, J. Mater. Sci. Mater. Med. 24 (2013) 2381–2390.

[107] Z. Xie, D. Ng, M. Hoang, T. Duong, S. Gray, Separation of aqueous salt solution by pervaporation through hybrid organic-inorganic membrane: Effect of operating conditions, Desalination. 273 (2011) 220–225.

[108] E. Huth, S. Muthu, L. Ruff, J.A. Brant, Feasibility assessment of pervaporation for desalinating high-salinity brines, J. Water Reuse Desalin. 4 (2014) 109–124.

[109] Q. Wang, Y. Lu, N. Li, Preparation, characterization and performance of sulfonated poly(styrene-ethylene/butylene-styrene) block copolymer membranes for water desalination by pervaporation, Desalination. 390 (2016) 33–46.

[110] E. Halakoo, X. Feng, Layer-by-layer assembly of polyethyleneimine/graphene oxide membranes for desalination of high-salinity water via pervaporation, Sep. Purif. Technol. 234 (2019) 116077.

[111] I. Prihatiningtyas, G.A. Gebreslase, B. Van der Bruggen, Incorporation of Al2O3 into cellulose triacetate membranes to enhance the performance of pervaporation for desalination of hypersaline solutions, Desalination. 474 (2020) 114198.

[112] B. Liang, W. Zhan, G. Qi, S. Lin, Q. Nan, Y. Liu, B. Cao, K. Pan, High performance graphene oxide/polyacrylonitrile composite pervaporation membranes for desalination applications, J. Mater. Chem. A. 3 (2015) 5140–5147.

[113] A. Selim, A.J. Toth, E. Haaz, D. Fozer, A. Szanyi, N. Hegyesi, P. Mizsey, Preparation and characterization of PVA/GA/Laponite membranes to enhance pervaporation desalination performance, Sep. Purif. Technol. 221 (2019) 201–210.

[114] J. Zuo, Y. Wang, S.P. Sun, T.S. Chung, Molecular design of thin film composite

(TFC) hollow fiber membranes for isopropanol dehydration via pervaporation, J. Memb. Sci. 405 (2012) 123–133.

[115] G.M. Shi, T.S. Chung, Thin film composite membranes on ceramic for pervaporation dehydration of isopropanol, J. Memb. Sci. 448 (2013) 34–43.

[116] E. Halakoo, X. Feng, Self-assembled membranes from polyethylenimine and graphene oxide for pervaporation dehydration of ethylene glycol, J. Memb. Sci. 616 (2020) 118583.

[117] F. Li, J. Ye, L. Yang, C. Deng, Q. Tian, B. Yang, Surface modification of ultrafiltration membranes by grafting glycine-functionalized PVA based on polydopamine coatings, Appl. Surf. Sci. 345 (2015) 301–309.

[118] Y. Xu, H. Xu, Z. Zhu, H. Hou, J. Zuo, F. Cui, D. Liu, W. Wang, A mechanically durable, sustained corrosion-resistant photothermal nanofiber membrane for highly efficient solar distillation, J. Mater. Chem. A. 7 (2019) 22296–22306.

[119] Z. Li, K. Hu, X. Feng, Concentration of potassium acetate solutions via sweeping gas pervaporation using TFC membranes comprising of a PDA sublayer and PEI/PAA bilayers, Sep. Purif. Technol. 277 (2021) 119429.

[120] P.L. Stigliano, N. Pianta, S. Bonizzoni, M. Mauri, R. Simonutti, R. Lorenzi, B. Vigani, V. Berbenni, S. Rossi, P. Mustarelli, R. Ruffo, A physico-chemical investigation of highly concentrated potassium acetate solutions towards applications in electrochemistry, Phys. Chem. Chem. Phys. 23 (2021) 1139–1145.

[121] Z. Li, K. Hu, X. Feng, Concentration of potassium acetate solutions via sweeping gas pervaporation using TFC membranes comprising of a PDA sublayer and PEI/PAA bilayers, Sep. Purif. Technol. 277 (2021) 119429.

[122] D. Wu, A. Gao, H. Zhao, X. Feng, Pervaporative desalination of high-salinity water, Chem. Eng. Res. Des. 136 (2018) 154–164.

[123] X. Wu, S. Yang, S. Xu, X. Zhang, Solubility of potassium acetate in water, 2,2,2-trifluoroethanol, ethanol and their binary mixtures at 288.15–333.15 K, Chem. Res. Chinese Univ. 36 (2019) 921–926.

[124] P. Bharmoria, H. Gupta, V.P. Mohandas, P.K. Ghosh, A. Kumar, Temperature invariance of NaCl solubility in water: Inferences from salt-water cluster behavior of NaCl, KCl, and NH_4Cl, J. Phys. Chem. B. 116 (2012) 11712–11719.

[125] J. Xu, C. Gao, X. Feng, Thin-film-composite membranes comprising of self-assembled polyelectrolytes for separation of water from ethylene glycol by pervaporation, J. Memb. Sci. 352 (2010) 197–204.

[126] X. Feng, R.Y.M. Huang, Estimation of activation energy for permeation in pervaporation processes, J. Memb. Sci. 118 (1996) 127–131.

[127] R.G. Lunnon, The Latent Heat of Evaporation of Aqueous Salt Solutions, Proc. Phys. Soc. London. 25 (1912) 180–191.

[128] J.C.-S. Chou, Thermodynamic properties of aqueous sodium chloride solutions from 32 to 350 °F, Oklahoma State University, 1968.

[129] Y. He, L. Xu, X. Feng, Y. Zhao, L. Chen, Dopamine-induced nonionic polymer coatings for significantly enhancing separation and antifouling properties of polymer membranes: Codeposition versus sequential deposition, J. Memb. Sci. 539 (2017) 421–431.

[130] Z. Li, K. Hu, X. Feng, Co-depositing polyvinylamine and dopamine to enhance membrane performance for concentration of KAc solutions via sweeping air pervaporation, J. Memb. Sci. 656 (2022) 120664.

[131] J. Yan, L. Yang, M.F. Lin, J. Ma, X. Lu, P.S. Lee, Polydopamine spheres as active templates for convenient synthesis of various nanostructures, Small. 9 (2013) 596–603.

[132] X. Jiang, Y. Wang, M. Li, Selecting water-alcohol mixed solvent for synthesis of polydopamine nano-spheres using solubility parameter, Sci. Rep. 4 (2014) 1–6.

[133] I. You, H. Jeon, K. Lee, M. Do, Y.C. Seo, H.A. Lee, H. Lee, Polydopamine coating in organic solvent for material-independent immobilization of water-insoluble molecules and avoidance of substrate hydrolysis, J. Ind. Eng. Chem. 46 (2017) 379–385.

[134] H. Hu, J.C. Dyke, B.A. Bowman, C.C. Ko, W. You, Investigation of dopamine analogues: Synthesis, mechanistic understanding, and structure-property relationship, Langmuir. 32 (2016) 9873–9882.

[135] L.P. Zhu, J.Z. Yu, Y.Y. Xu, Z.Y. Xi, B.K. Zhu, Surface modification of PVDF porous membranes via poly(DOPA) coating and heparin immobilization, Colloids Surfaces B Biointerfaces. 69 (2009) 152–155.

[136] S. Hong, Y.S. Na, S. Choi, I.T. Song, W.Y. Kim, H. Lee, Non-covalent self-assembly and covalent polymerization co-contribute to polydopamine formation, Adv. Funct. Mater. 22 (2012) 4711–4717.

[137] J. Wang, J. Zhu, M.T. Tsehaye, J. Li, G. Dong, S. Yuan, X. Li, Y. Zhang, J. Liu, B. Van Der Bruggen, High flux electroneutral loose nanofiltration membranes based on rapid deposition of polydopamine/polyethyleneimine, J. Mater. Chem. A. 5 (2017) 14847–14857.

[138] T.G. Barclay, H.M. Hegab, S.R. Clarke, M. Ginic-Markovic, Versatile Surface Modification Using Polydopamine and Related Polycatecholamines: Chemistry, Structure, and Applications, Adv. Mater. Interfaces. 4 (2017) 120–125.

[139] Z. Wang, K. Wang, Y. Zhang, Y. Jiang, X. Lu, L. Fang, D. Gan, C. Lv, H. Zhang, S. Qu, Protein-Affinitive Polydopamine Nanoparticles as an Efficient Surface Modification Strategy for Versatile Porous Scaffolds Enhancing Tissue Regeneration, Part. Part. Syst. Charact. 33 (2016) 89–100.

[140] L. Tang, S. Mo, S.G. Liu, L.L. Liao, N.B. Li, H.Q. Luo, Synthesis of fluorescent polydopamine nanoparticles by Michael addition reaction as an analysis platform to detect iron ions and pyrophosphate efficiently and construction of an IMPLICATION logic gate, Sensors Actuators, B Chem. 255 (2018) 754–762.

[141] G. Li, B. Liu, L. Bai, Z. Shi, X. Tang, J. Wang, H. Liang, Y. Zhang, B. Van der Bruggen, Improving the performance of loose nanofiltration membranes by poly-dopamine/zwitterionic polymer coating with hydroxyl radical activation, Sep. Purif. Technol. 238 (2020) 116412.

[142] N. Gao, W. Fan, Z.K. Xu, Ceramic membrane with protein-resistant surface via dopamine/diglycolamine co-deposition, Sep. Purif. Technol. 234 (2020) 116135.

[143] R.W. Baker, J.G. Wijmans, Y. Huang, Permeability, permeance and selectivity: A preferred way of reporting pervaporation performance data, J. Memb. Sci. 348 (2010) 346–352.